

GABA_B Receptor Localization and Regulation

Inauguraldissertation

zur

Erlangung der Würde eines Doktors der Philosophie
vorgelegt der
Philosophisch-Naturwissenschaftlichen Fakultät
der Universität Basel

von

Nicole Guetg
aus Savognin (GR)

Basel, 2010

Genehmigt von der Philosophisch-Naturwissenschaftlichen Fakultät auf Antrag von

Prof. Dr. Bernhard Bettler

Prof. Dr. Markus Rüegg

Basel, den 23. Juni 2009

Prof. Dr. Eberhard Parlow

Dekan

Originaldokument gespeichert auf dem Dokumentenserver der Universität Basel edoc.unibas.ch



Dieses Werk ist unter dem Vertrag „Creative Commons Namensnennung-Keine kommerzielle Nutzung-Keine Bearbeitung 2.5 Schweiz“ lizenziert. Die vollständige Lizenz kann unter creativecommons.org/licences/by-nc-nd/2.5/ch eingesehen werden.



Namensnennung-Keine kommerzielle Nutzung-Keine Bearbeitung 2.5 Schweiz

Sie dürfen:



das Werk vervielfältigen, verbreiten und öffentlich zugänglich machen

Zu den folgenden Bedingungen:



Namensnennung. Sie müssen den Namen des Autors/Rechteinhabers in der von ihm festgelegten Weise nennen (wodurch aber nicht der Eindruck entstehen darf, Sie oder die Nutzung des Werkes durch Sie würden entlohnt).



Keine kommerzielle Nutzung. Dieses Werk darf nicht für kommerzielle Zwecke verwendet werden.



Keine Bearbeitung. Dieses Werk darf nicht bearbeitet oder in anderer Weise verändert werden.

- Im Falle einer Verbreitung müssen Sie anderen die Lizenzbedingungen, unter welche dieses Werk fällt, mitteilen. Am Einfachsten ist es, einen Link auf diese Seite einzubinden.
- Jede der vorgenannten Bedingungen kann aufgehoben werden, sofern Sie die Einwilligung des Rechteinhabers dazu erhalten.
- Diese Lizenz lässt die Urheberpersönlichkeitsrechte unberührt.

Die gesetzlichen Schranken des Urheberrechts bleiben hiervon unberührt.

Die Commons Deed ist eine Zusammenfassung des Lizenzvertrags in allgemeinverständlicher Sprache: <http://creativecommons.org/licenses/by-nc-nd/2.5/ch/legalcode.de>

Haftungsausschluss:

Die Commons Deed ist kein Lizenzvertrag. Sie ist lediglich ein Referenztext, der den zugrundeliegenden Lizenzvertrag übersichtlich und in allgemeinverständlicher Sprache wiedergibt. Die Deed selbst entfaltet keine juristische Wirkung und erscheint im eigentlichen Lizenzvertrag nicht. Creative Commons ist keine Rechtsanwalts-gesellschaft und leistet keine Rechtsberatung. Die Weitergabe und Verlinkung des Commons Deeds führt zu keinem Mandatsverhältnis.

Table of contents

1.	Summary	1
2.	Abbreviations	3
3.	Preface	5
4.	Background	6
4.1.	Synapses	6
4.2.	Ionotropic and metabotropic receptors	7
4.3.	Glutamate receptors	8
4.4.	The Ca ²⁺ /Calmodulin-dependent kinase II	9
4.5.	GABA receptors	9
4.6.	The GABA _B receptor	10
	<i>History</i>	
	<i>Structure</i>	
	<i>Physiological function</i>	
	<i>Localization</i>	
	<i>Regulation and trafficking</i>	
	<i>GABA_B receptors and neurological disorders</i>	
	<i>Future perspectives</i>	
5.	References	18
6.	Publications	27
6.1.	Compartment-dependent colocalization of Kir3.2-containing K ⁺ -channels and GABA _B receptors in hippocampal pyramidal cells	27
6.2.	The GABA _{B1a} isoform mediates heterosynaptic depression at hippocampal mossy fiber synapses	38
6.3.	A mouse model for visualization of GABA _B receptors	50
6.4.	NMDA receptor activation decreases surface GABA _B receptors by CaMKII-mediated phosphorylation of GABA _{B1} at serine 867	60
7.	Acknowledgements	104
8.	<i>Curriculum vitae</i>	105

1. Summary

GABA_B receptors are G-protein coupled receptors for gamma-amino butyric acid, the main inhibitory neurotransmitter in the brain. Functional GABA_B receptors are obligate heterodimers composed of GABA_{B1} and GABA_{B2} subunits. The GABA_{B1} subunit exists in two isoforms, GABA_{B1a} and GABA_{B1b}, that can be differentiated by a pair of sushi domains exclusively located on the ectodomain of GABA_{B1a}. As a consequence, two distinct receptor subtypes, GABA_{B(1a,2)}} and GABA_{B(1b,2)}}, are present in the brain. Depending on their subcellular localization, GABA_B receptors exert distinct regulatory effects on synaptic transmission. Presynaptically, GABA_B receptors inhibit Ca²⁺ influx by closing voltage-gated Ca²⁺-channels therefore regulating neurotransmitter release. Postsynaptically, GABA_B receptors activate inwardly rectifying Kir3-type K⁺-channels leading to hyperpolarisation of the postsynaptic membrane. Recently, it has become clear that GABA_{B(1a,2)}} and GABA_{B(1b,2)}} receptors convey individual functions, which are, at least in part, related to their distinct subcellular distribution.

The aim of this thesis was to gain further insight into the function of GABA_B receptors by characterizing their localization at the ultrastructural level in respect to effector channels and subtype composition. Moreover, it was of interest to study the dynamic regulation of GABA_B receptors in response to synaptic activity.

In the first part of this thesis, the localization of GABA_B receptors and Kir3-type effector channels was investigated in the CA1 region of the hippocampus. It could be demonstrated that postsynaptic GABA_B receptors colocalize with the Kir3.2 subunit of K⁺-channels in dendritic spines, but not in dendritic shafts of CA1 pyramidal cells (chapter 6.1.; Kulik et al., 2006).

The differential distribution of GABA_{B1} subunit isoforms at the mossy fiber-CA3 pyramidal neuron synapse was investigated in the second part of this work. Due to the lack of isoform specific antibodies, mice selectively expressing GABA_{B1a} or GABA_{B1b} were used. It could be shown that mainly the GABA_{B1a} subunit isoform contributes to the composition of presynaptic GABA_B receptors whereas GABA_{B1b} is the predominant GABA_{B1} subunit isoform on the postsynaptic side. Electrophysiological recordings were used to assess the

contribution of the two different GABA_{B1} subunit isoforms to functional pre- and postsynaptic receptors in response to pharmacological as well as physiological GABA_B receptor activation. The findings illustrate that the spatial segregation of GABA_{B1} subunit isoforms at mossy fiber terminals is sufficient to produce a strictly subtype-specific response (chapter 6.2.; Guetg et al., 2009).

In the third part of this work, a new mouse model containing a *GABA_{B1}-eGFP* transgene, allowing the visualization of GABA_B receptors, was generated. Crossing the *GABA_{B1}-eGFP* transgene into the GABA_{B1} deficient background allowed the study of GABA_B receptors tagged with a fluorescent protein under expression of endogenous promoter elements. Therefore these mice provide a useful tool to visualize the spatio-temporal distribution of GABA_B receptors *in vivo* and *in vitro* (chapter 6.3.; Casanova et al., 2009).

The dynamic regulation of surface GABA_B receptors induced by glutamate was investigated in primary hippocampal neurons and the results are presented in the last part of this thesis. Activation of NMDA receptors resulted in a decrease of surface GABA_B receptor levels. This decrease involved Ca²⁺-dependent activation of CaMKII. A CaMKII phosphorylation site within the cytoplasmic domain of the GABA_{B1} subunit was identified. Evidence that phosphorylation of this site is essential for the observed effect of NMDA receptor activation on GABA_B surface receptors is presented in this thesis. In conclusion, it could be demonstrated that GABA_B receptors are dynamically regulated and interact with other receptors and kinases. The results obtained, implicate that activity-dependent regulation of GABA_B receptors is potentially involved in the modulation of synaptic strength (chapter 6.4.).

2. Abbreviations

AMPA	α -amino-3-hydroxyle-5-methyl-4-isoxazole-propionate
AMPK	5'AMP-dependent protein kinase
APV	D-(-)-2-Amino-5-phosphonopentanoic acid
BAC	bacterial artificial chromosome
Ca ²⁺ /CaM	Ca ²⁺ /Calmodulin
CaMKII	Ca ²⁺ /Calmodulin-dependent kinase II
DIV	day <i>in vitro</i>
eGFP	enhanced green fluorescent protein
EPSC	excitatory postsynaptic current
ER	endoplasmic reticulum
ESI-MS/MS	electrospray-ionisation mass spectrometry
GABA	gamma-amino butyric acide
GABA _A	gamma-amino butyric acid type A
GABA _B	gamma-amino butyric acide type B
GABA _{B1} ^{-/-}	GABA _{B1} deficient
GABA _{B2} ^{-/-}	GABA _{B2} deficient
GABA _C	gamma-amino butyric acide type C
GDP	guanosine diphosphate
GHB	gamma-hydroxybutyrate
GPCR	G-protein coupled receptor
GTP	guanosine-5'-triphosphate
IPSC	inhibitory postsynaptic current
KN-93	N-[2-[[[3-(4-Chlorophenyl)-2-propenyl]methylamino]-methyl]phenyl]-N-(2-hydroxyethyl)-4-methoxy-benzenesulphonamide
LTD	long term depression
LTP	long term potentiation
mGluR	metabotropic glutamate receptor
MF	mossy fiber
NMDA	N-methyl-D-aspartate

PKA	cyclic AMP-dependent protein kinase
PSD	postsynaptic density
RP-HPLC	reverse-phase high-pressure liquid chromatography
WT	wild-type
1a ^{-/-}	GABA _{B1a} deficient
1b ^{-/-}	GABA _{B1b} deficient

3. Preface

This thesis is based on the following papers that are published or in preparation. Asterisks (*) indicate equal contributions by the authors.

I. Compartment-dependent colocalization of Kir3.2-containing K⁺ channels and GABA_B receptors in hippocampal pyramidal cells

Kulik A, Vida I, Fukazawa Y, Guetg N, Kasugai Y, Marker CL, Rigato F, Bettler B, Wickman K, Frotscher M, Shigemoto R

The Journal of Neuroscience 2006; 26:4289-97.

II. The GABA_{B1a} isoform mediates heterosynaptic depression at hippocampal mossy fiber synapses

Guetg N*, Seddik R*, Vigot R, Turecek R, Gassmann M, Vogt KE, Bräuner-Osborne H, Shigemoto R, Kretz O, Frotscher M, Kulik A, Bettler B

The Journal of Neuroscience 2009; 29:1414-23

III. A mouse model for visualization of GABA_B receptors

Casanova E*, Guetg N*, Vigot R, Seddik R, Julio-Pieper M, Hyland NP, Cryan JF, Gassmann M, and Bettler B

Genesis 2009; 47:595-602

IV. NMDA Receptor-Dependent GABA_B Receptor Internalization via CaMKII Phosphorylation of Serine 867 in GABA_{B1}

Guetg N*, Abdel Aziz S*, Holbro N, Turecek R, Rose T, Seddik R, Gassmann M, Moes S, Jenoe P, Oertner TG, Casanova E, and Bettler B

submitted

4. Background

The brain is a complex biological organ of great computational capability that constructs our sensory experiences, regulates our thoughts and emotions, and controls our actions.

(Eric R. Kandel)

4.1. Synapses

The human brain consists of billions of neurons communicating among each other to acquire, coordinate and disseminate information about the body and its environment. Communication between nerve cells is achieved through synapses, which transfer information by using electrical and chemical signals.

Electrical synapses are composed of specialized membrane channels localized in the pre- and postsynaptic plasma membrane, termed gap junctions. These membrane proteins are paired and aligned to form a pore connecting the pre- and postsynaptic cells. Through this relatively large pore a subset of substances including ions can simply diffuse. Action potential generation creates an altered ionic balance in the presynaptic side of an electrical synapse. As a result, ions diffuse through the pore which then changes the membrane potential of the associated postsynaptic cell (Sohl et al., 2005).

The second type of synapse is the chemical synapse. Presynaptic terminals contain membrane bound vesicles which are filled with neurotransmitters, the chemical components responsible for transmitting the signal between neurons. A change in membrane potential caused by an incoming action potential leads to the activation of voltage-gated Ca^{2+} -channels localized on the presynaptic terminal. The consequence is a rapid influx of Ca^{2+} ions. The increased presynaptic Ca^{2+} concentration leads to the fusion of the vesicles with the presynaptic membrane and the release of neurotransmitters in the synaptic cleft. Neurotransmitters diffuse through the synaptic cleft and bind to and activate receptors localized in the postsynaptic membrane. This leads to the opening of postsynaptic ion channels, and to changes in conductance and membrane potential of the postsynaptic cell (Becherer and Rettig, 2006; Di Maio, 2008).

The advantage of electrical synapses is the bidirectional nature of the transmission and its high speed. This facilitates the synchronization of signals over a population of neurons. In contrast, chemical synapses are slower but enable more specific and controlled way of transmitting signals.

4.2. Ionotropic and metabotropic receptors

Excitatory as well as inhibitory neurotransmitters act on two types of receptors; ionotropic and metabotropic receptors.

Ionotropic receptors mediate rapid communication between neurons. They are generally assembled from multiple subunits and form channels across the plasma membrane. Different subunit compositions result in different receptor characteristics and therefore specify and enlarge the range of functions associated with each receptor. An advantage of ionotropic receptors is the direct coupling of the neurotransmitter to the pore-forming channels. Upon neurotransmitter binding, a conformational change occurs allowing the flow of cations or anions across the membrane. The main class of excitatory ionotropic receptors are the glutamate receptors, consisting of the N-methyl-D-aspartate (NMDA) receptors, α -amino-3-hydroxyl-5-methyl-4-isoxazole-propionate (AMPA) receptors and kainate receptors. The main class of inhibitory ionotropic receptors are the gamma-amino butyric acid type A ($GABA_A$) and glycine receptors (Barrera and Edwardson, 2008; Lodge, 2009).

In contrast to ionotropic receptors, metabotropic receptors cannot serve themselves as channels for ion flow. They are G-protein coupled receptors (GPCRs). The classical GPCR signaling is mediated by coupling of receptors to heterotrimeric G-proteins and the subsequent regulation of numerous intracellular pathways. Upon agonist binding, the G-protein bound guanosine diphosphate (GDP) is exchanged for guanosine-5'-triphosphate (GTP) causing the heterotrimer dissociation into a $G\alpha$ subunit and a $G\beta\gamma$ -dimer, both of which independently activate or inhibit different effectors such as adenylyl cyclase, phospholipases and ion channels. Hydrolysis of GTP to GDP by GTPase activity terminates the signal. Three classes of glutamate induced metabotropic receptors (mGluRs) exist. They are classified by their sequence similarity, pharmacology and intracellular signaling

mechanism. The metabotropic receptor for GABA is the gamma-amino butyric acid type B (GABA_B) receptor which will be described in more detail in a following section (Bouvier, 2001; Prinster et al., 2005; Jacoby et al., 2006; Smrcka, 2008).

4.3. Glutamate receptors

L-glutamate (referred to as glutamate), the main excitatory neurotransmitter in the central nervous system, was first identified by Curtis and colleagues in the late fifties (Curtis et al., 1959). Glutamate released from a presynaptic neuron activates ionotropic as well as metabotropic glutamate receptors. Based on pharmacological and structural criteria, the ionotropic glutamate receptors are subdivided into three major classes; NMDA, AMPA and kainate receptors. In addition, glutamate can also activate the three classes of mGluRs (Collingridge and Lester, 1989). The ionotropic glutamate receptors are named according to their pharmacological agonists. One glutamate receptor, studied in this thesis, is the NMDA receptor and is therefore described in more detail.

Postsynaptic NMDA receptors are heterotetramers composed of NR1, NR2 (NR2A-D) and NR3 (A and B) subunits. Most functional NMDA receptors are formed by NR1 and NR2 subunits in which the NR1/NR2A heteromer represent the functional unit (Furukawa et al., 2005; Kohr, 2006). The NMDA receptor contains an extracellular binding site for glutamate and glycine and is blocked in a voltage-dependent way by the presence of a Mg²⁺ ion in the channel pore. (Lynch et al., 1983; Mayer et al., 1984; Nowak et al., 1984). Under physiological conditions, the Mg²⁺ block is removed by depolarization of the postsynaptic membrane induced by AMPA receptor activation. AMPA receptors primarily function as Na⁺ channels, with rapid activation kinetics. The NMDA receptor is permeable for Na⁺ and K⁺ ions; and unlike AMPA receptors, they are also permeable to Ca²⁺ and are characterized by their slow kinetics (Lynch et al., 1983). The binding of the obligate co-agonist glycine potentiates the channel conductance of NMDA receptors (Dingledine et al., 1990). However, it is still controversial if saturating levels of glycine are present under physiological conditions (Yang and Svensson, 2008; Li et al., 2009). The NMDA receptors are believed to be the main pathway for Ca²⁺ entry into dendritic spines during synaptic activity (Mainen et al., 1999; Kovalchuk et al., 2000). The Ca²⁺ influx following NMDA

receptor activation is crucial for NMDA receptor-dependent plasticity and can promote the activation of Ca²⁺/Calmodulin-dependent kinase II (CaMKII) (Malenka et al., 1989b; Malenka et al., 1989a; Malinow et al., 1989; Lisman et al., 2002).

4.4. The Ca²⁺/Calmodulin-dependent kinase II

CaMKII is one of the most abundant serine/threonine kinases in the brain and is activated by binding of Ca²⁺/Calmodulin (Ca²⁺/CaM) (Bennett et al., 1983; Kennedy et al., 1983). CaMKII is present predominantly in dendritic spines and is a component of the postsynaptic density (PSD). After binding of Ca²⁺/CaM, autophosphorylation turns the kinase into an active state (Miller and Kennedy, 1986; Ouyang et al., 1997). Dissociation of Ca²⁺/CaM exposes two previously hidden sites which are subsequently autophosphorylated preventing maximal kinase activity (Meador et al., 1993). Many papers have been published describing substrates and binding partners of CaMKII. CaMKII is involved in synaptic plasticity and memory formation. Several mouse models with altered CaMKII function have been generated over the years and all of them show impaired memory and learning functions (Elgersma et al., 2004). CaMKII has been shown to be a key molecule in long term potentiation (LTP), an experimental molecular model for memory formation. The Ca²⁺ influx following NMDA receptor activation promotes CaMKII-dependent phosphorylation of AMPA receptors and their recruitment to the PSD in spines (Malenka et al., 1989b; Malenka and Nicoll, 1999; Shen and Meyer, 1999). Today, the main focus of CaMKII research addresses the question of compartmentalization and translocation of CaMKII. Recent findings propose that CaMKII activity is restricted to single spines and therefore influences synaptic plasticity with a high degree of specificity (Lee et al., 2009).

4.5. GABA receptors

Gamma aminobutyric acid (GABA), first identified by Roberts and Frankel, is the main inhibitory neurotransmitter in the central nervous system, (Roberts and Frankel 1950).

Activation of GABA receptors generally results in hyperpolarisation of the membrane. Two classes of GABA receptors, differing in pharmacology and structure, the ionotropic GABA_A and metabotropic GABA_B receptors, have been identified in the central nervous system. In addition, a third class, the GABA_C activated receptors, has been described and is mainly found in the retina (Chebib, 2004). However some controversy remains whether these receptors constitute an independent class of receptors or if they are a subtype of GABA_A receptors.

Postsynaptic GABA_A receptors clamp the membrane at negative potentials by increasing chloride conductance (Payne et al., 2003). GABA_A receptors are heteropentamers composed of multiple subunits. Until now, sixteen different subunits (α_{1-6} , β_{1-3} , γ_{1-3} , δ , ϵ , π , θ) have been identified and provide structural heterogeneity. Most GABA_A receptors consist only of α -, β - and γ -subunits. The subunit composition determines the physiology and partially the localization of the receptor (Mohler et al., 1996). GABA_A receptors contain a benzodiazepine and barbiturate binding site making them an attractive drug target for treatment of numerous neurological disorders such as anxiety and epilepsy (Foster and Kemp, 2006). Benzodiazepine binding increases the frequency of channel opening whereas barbiturates prolong the duration of chloride channel open state. The fast inhibitory postsynaptic currents (IPSCs) mediated by the ionotropic GABA_A receptors can be distinguished from the slow IPSCs generated by metabotropic GABA_B receptors. This receptor type is described in more detail in the following section.

4.6. The GABA_B receptor

History

Twenty years after the identification of GABA in the brain, the first specific GABA_A antagonist, bicuculline, was described (Curtis et al., 1971). However, upon bicuculline application, some GABAergic effects remained, especially in the cerebral cortex. This was the first indication for the existence of multiple GABA receptor types. During the same time, the pharmaceutical industry brought the antispastic drug Lioresal (racemic baclofen) on the market. It was assumed that baclofen acts on non-classical, bicuculline-insensitive GABA receptors. Nevertheless, it took 10 years before GABA_B receptors were

first described (Bowery et al., 1979; Bowery et al., 1981; Hill and Bowery, 1981). First structural evidence came in 1984 with the finding that application of guanyl nucleotides reduces agonist affinity of GABA_B receptors (Hill et al., 1984). This was the proof that the GABA_B receptor is a G-protein coupled receptor. (Kerr and Ong, 1995)

Structure

Among G-protein coupled receptors, GABA_B receptors are unique in that they require two distinct subunits, GABA_{B1} and GABA_{B2}, to be functional (Jones et al., 1998; Kaupmann et al., 1998b; White et al., 1998; Kuner et al., 1999; Martin et al., 1999; Ng et al., 1999). Both subunits are seven-transmembrane domain proteins containing a long N-terminal domain and sharing a high degree of homology. However, within the GABA_B heteromer the individual subunits exert unique functions. The GABA_{B1} subunit binds GABA whereas the GABA_{B2} subunit is responsible for G-protein coupling (Malitschek et al., 1999; Galvez et al., 2000). Subsequent studies revealed that the GABA_{B1} subunit cannot translocate to the cell surface in the absence of the GABA_{B2} subunit and remains in the endoplasmic reticulum (ER) (Couve et al., 1998). The GABA_{B1} C-terminus contains a retention motif, RSRR, which can be masked by the GABA_{B2} subunit upon assembly in the ER (Margeta-Mitrovic et al., 2000; Pagano et al., 2001; Gassmann et al., 2005). As a consequence, the ER retention signal represents an important quality control mechanism that only allows correctly formed GABA_B heterodimers to integrate into the plasma membrane. Mice lacking the GABA_{B1} or GABA_{B2} protein do not show any remaining physiological GABA_B responses (Schuler et al., 2001; Gassmann et al., 2004). These data ultimately demonstrate that both receptor subunits, GABA_{B1} and GABA_{B2}, are required for the formation of functional GABA_B receptors.

Molecular diversity in the GABA_B system is based on the subunit isoforms GABA_{B1a} and GABA_{B1b}, which are encoded by the same gene but independently regulated at the transcriptional level (Steiger et al., 2004). The only structural difference between GABA_{B1a} and GABA_{B1b} are the two N-terminal sushi domains unique to GABA_{B1a} (Blein et al., 2004). No pharmacological difference in agonist binding has been described for the subunit isoforms *in vitro* in heterologous cells (Kaupmann et al., 1997). The differential distribution and the subsequent differential coupling to effector channels are discussed in more detail in the following chapters.

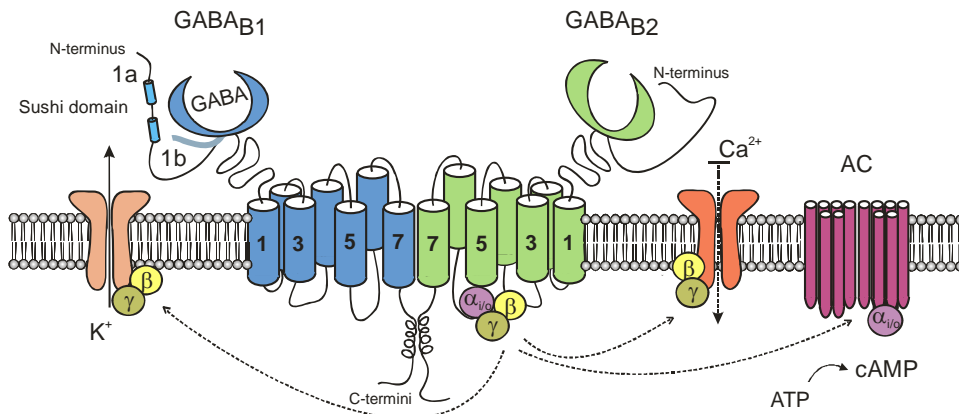


Figure 4.1. Structure and physiological role of GABA_B receptors. GABA_B receptors form obligate heterodimers composed of GABA_{B1} and GABA_{B2} subunits. The GABA_{B1} subunit contains the GABA binding site whereas the GABA_{B2} subunit couples to the G-protein. Two isoforms, GABA_{B1a} and GABA_{B1b}, exist, differing in the two sushi domains at the N-terminus. Upon activation of GABA_B receptors and the subsequent dissociation of the G-protein, the G_{i/o}α subunit inhibits adenylyl cyclase, whereas Gβγ-dimer translocates and binds to effector channels. Presynaptically, GABA_B receptor activation results in inhibition of voltage gated Ca²⁺-channels and therefore in the inhibition of neurotransmitter release. Postsynaptically, the coupling of the Gβγ-dimer to Kir3-type K⁺-channels results in accelerated K⁺ efflux and therefore in inhibition of the postsynaptic cell.

Physiological function

GABA_B receptors are metabotropic receptors and as such their physiological effects are mediated through G-protein activation. The GABA_B receptor predominantly couples to G_iα- and G_oα-type G-proteins (Campbell et al., 1993; Greif et al., 2000). After activation of the GABA_B receptor, the coupled G-protein dissociates into the Gα subunit and the Gβγ-dimer modulating signaling cascades and effector channels.

Presynaptically, GABA_B receptors control the release of GABA (autoreceptors) and other neurotransmitters (heteroreceptors), which is primarily mediated by the Gβγ-dimer (Bowery et al., 2002). Coupling of the Gβγ-dimer to the voltage-gated P/Q- (Ca_v2.1) and N-type (Ca_v2.2) Ca²⁺-channels decreases their conductance, thereby inhibiting

neurotransmitter release (Mintz and Bean, 1993; Santos et al., 1995; Herlitze et al., 1996; Ikeda, 1996; Lambert and Wilson, 1996; Poncer et al., 1997). In addition, the $G_{i/o}\alpha$ subunit reduces intracellular cAMP levels through inhibition of adenylyl cyclase. This restricts vesicle recruitment and priming (Xu and Wojcik, 1986; Knight and Bowery, 1996; Kaupmann et al., 1997; Sakaba and Neher, 2003).

Postsynaptically, the $G\beta\gamma$ -dimer couples to inwardly rectifying Kir3-type K^+ -channels (Luscher et al., 1997; Kaupmann et al., 1998a). The activation of K^+ -channels results in a K^+ efflux and therefore in cell hyperpolarization. $GABA_B$ receptors induce a slow inhibitory postsynaptic current (slow IPSC) which is distinct from the fast IPSC mediated by $GABA_A$ receptors (Otis et al., 1993).

In electrophysiological experiments, presynaptic $GABA_B$ heteroreceptor and autoreceptor activity is revealed from the inhibition of excitatory postsynaptic currents (EPSCs) and IPSCs, respectively. Postsynaptic $GABA_B$ receptor activity is detected directly by recording Kir3-type K^+ -currents.

Localization

In early postnatal development, $GABA_{B1}$ and $GABA_{B2}$ subunits are observed mainly in neurons and to a lower level in glial cells (Lopez-Bendito et al., 2004; Lujan and Shigemoto, 2006). In the adult, $GABA_B$ receptors are expressed in the entire brain (Benke et al., 1999; Bischoff et al., 1999), and pre- and postsynaptic localization have been described for various brain regions including cerebellum and ventrobasal thalamus (Kulik et al., 2002), as well as hippocampus (Kulik et al., 2003). In the hippocampus, the $GABA_B$ receptor was found on $GABA$ ergic and glutamatergic terminals mainly extrasynaptically and only rarely at the presynaptic membrane specialization. Postsynaptically, the $GABA_B$ receptors were mainly found in the perisynaptic and extrasynaptic region of the spines of CA1 pyramidal cells. As a consequence most $GABA_B$ receptors are located distant from release sites and probably require pooling of synaptically released $GABA$ to be activated.

Significant advances in our understanding of $GABA_B$ receptor heterogeneity, particularly in respect to receptor localization and function, came with the generation of $GABA_{B1a}$ and $GABA_{B1b}$ deficient mice (from here on referred as $1a^{-/-}$ and $1b^{-/-}$ respectively) (Vigot et al., 2006). It was expected that $GABA_{B1a}$ and $GABA_{B1b}$ subunit isoforms have different physiological roles. However, the lack of isoform-specific pharmacological compounds

and antibodies made this issue hard to address. Therefore, an alternative appealing approach was the generation of mice selectively expressing GABA_{B1a} or GABA_{B1b} subunit isoforms. By using these mutant mice, several groups studied the localization and physiological function of the two subunit isoforms in different brain regions (Perez-Garci et al., 2006; Shaban et al., 2006; Vigot et al., 2006; Ulrich et al., 2007).

Quantification of immunohistochemical experiments using electron microscopy revealed that, in the CA1 region of the hippocampus, GABA_{B1a} was predominantly localized presynaptically on glutamatergic synapses whereas GABA_{B1b} was more abundant postsynaptically. This distribution was confirmed with electrophysiological experiments showing that the inhibition of EPSCs was dramatically reduced in 1a^{-/-} mice compared to wild-type (WT) mice. This indicates that GABA_{B(1a,2)}} is the main receptor contributing to presynaptic receptor function at CA3-CA1 synapses. Interestingly, no differences in inhibition of IPSCs were observed for 1a^{-/-} and 1b^{-/-} compared to WT mice indicating equal contribution of GABA_{B1a} and GABA_{B1b} subunit isoforms on presynaptic GABAergic terminals. Postsynaptically, 1a^{-/-} mice show K⁺-currents similar to WT mice, whereas a 50% reduction was reported in 1b^{-/-} mice. This indicates that postsynaptic GABA_B responses are predominantly mediated by the GABA_{B1b} isoform (Vigot et al., 2006). In layer 5 neocortical pyramidal neurons inhibition of dendritic Ca²⁺ spikes was exclusively mediated by GABA_{B(1b,2)}} receptors whereas the presynaptic inhibition of GABA release was mediated through GABA_{B(1a,2)}} receptors (Perez-Garci et al., 2006). Studying the role of presynaptic GABA_B receptors during NMDA-independent presynaptic LTP in the lateral amygdala revealed that GABA_{B1a}, but not GABA_{B1b}, is the main heteroreceptor-forming subunit isoform at cortical afferents (Shaban et al., 2006). Similar functional segregation of GABA_{B(1a,2)}} and GABA_{B(1b,2)}} receptors was also observed in the thalamus (Ulrich et al., 2007).

In conclusion, these studies revealed that GABA_{B1a} and GABA_{B1b} differentially influence synaptic functions, primarily as a result of their distinct distribution. However, to clearly establish a regulatory significance for GABA_B receptor subtypes, it has to be demonstrated that they do not only generate differential effects in response to pharmacological but also in response to physiological activation.

Regulation and trafficking

Regulation and trafficking of GABA_B receptors are controversial topics in the field of GABA_B research. As described above, GABA_B receptors are assembled in the ER and it was assumed that they are transported as functional heterodimers. However, a recent publication proposes that GABA_{B1} and GABA_{B2} subunits are independently transported in dendritic intracellular compartments and assemble in the dendritic ER prior to insertion into the plasma membrane (Ramirez et al., 2009).

The presence of receptors at the cell surface determines their availability to neurotransmitters and consequently their activity. In recent years, a number of publications have discussed agonist-induced internalization, degradation and recycling of GABA_B receptors. GPCRs are known to desensitize as a result of agonist-induced internalization. However, it is generally believed that GABA_B receptors are stably expressed at the cell surface despite agonist-induced GABA_B receptor desensitization (Sickmann and Alzheimer, 2003; Cruz et al., 2004; Fairfax et al., 2004). Recently, it became clear that surface receptors undergo constitutive endocytosis and recycling in heterologous and in neuronal systems (Grampp et al., 2008; Vargas et al., 2008). Importantly, it was reported that glutamate regulates surface availability of GABA_B receptors in cortical neurons by promoting the degradation of endocytosed receptors (Vargas et al., 2008).

Similar to other GPCRs, the stability of GABA_B receptors at the membrane can be modulated by phosphorylation. Phosphorylation of serine 892 on the GABA_{B2} subunit (GABA_{B2}S982) through cyclic AMP-dependent protein kinase (PKA) increases GABA_B surface stability and as a consequence reduces the desensitization of postsynaptic GABA_B receptor responses (Couve et al., 2002). Similarly, phosphorylation of serine 783 on the GABA_{B2} subunit (GABA_{B2}S783) by 5'AMP-dependent protein kinase (AMPK) is reported to stabilize postsynaptic cell surface GABA_B receptors (Kuramoto et al., 2007). In addition, *in vitro* kinase assays, using GST-fusion proteins, identified serine 917 (GABA_{B1}S917) and serine 923 (GABA_{B1}S923) within the C-terminus of the GABA_{B1} subunits as AMPK phosphorylation sites. However, the physiological relevance for these phosphorylation sites has not been established yet (Kuramoto et al., 2007).

GABA_B receptors and neurological disorders

Neurological disorders such as bipolar disorders, anxiety, epilepsy and depression often result from an imbalance between excitation and inhibition. Therefore, ionotropic and metabotropic receptors are interesting therapeutic targets. A relatively wide range of drugs targeting GABA_A are on the market. In contrast, only two GABA_B receptor agonists are marketed. Gamma-hydroxybutyrate (GHB) (traded as Xyrem™) is used in narcolepsy treatment. Baclofen (traded as Lioresal™) is a muscle relaxant used in the treatment of spasticity. Unfortunately, baclofen treatment leads to adverse reactions such as drowsiness, nausea, muscle weakness, hallucinations and mental confusion. Only one additional compound is currently in phase II clinical studies; a GABA_B antagonist for potential for the treatment of Alzheimer's disease. (Bowery, 2006; Foster and Kemp, 2006)

Future perspectives

Despite the increasing knowledge gained since 1981 when Bowery *et al.* first described the GABA_B receptor, many questions remain unanswered. Recombinant GABA_B receptors do not fully reproduce the characteristic responses of native GABA_B receptors. It is therefore believed that the interaction of native GABA_B receptors with so far unknown proteins is crucial for their physiological function. One important field in GABA_B research in the near future will therefore be the identification of interacting proteins and their influence on GABA_B receptor regulation, localization, stabilization or desensitization. The sushi domains may represent a target for identifying interacting proteins and the subsequent description of functional properties.

Studies have shown that GABA_B receptors are not regulated in a way characteristic for classical GPCRs. Furthermore, not much is known about the modulation of GABA_B receptors in response to synaptic activity. Therefore, it is necessary to further investigate the regulation of GABA_B receptors in response to GABA and other neurotransmitters. Studying the regulatory mechanism of GABA_B receptors involves the discovery and description of new phosphorylation sites on both subunits, GABA_{B1} and GABA_{B2}. Furthermore, the functional interaction between GABA_B receptors and other inhibitory as well as excitatory neurotransmitter receptors at single synapses is important to be understood.

Drug development represents the most important topic to be developed. Enormous work has been done to describe the structure, localization and function of the GABA_B receptor. However, only two drugs have been marketed thus far and adverse reactions are known for baclofen treatment. It should be the final goal of GABA_B receptor research to develop useful drugs based on the knowledge obtained from basic research.

5. References

- Barrera NP, Edwardson JM (2008) The subunit arrangement and assembly of ionotropic receptors. *Trends Neurosci* 31:569-576.
- Becherer U, Rettig J (2006) Vesicle pools, docking, priming, and release. *Cell Tissue Res* 326:393-407.
- Benke D, Honer M, Michel C, Bettler B, Mohler H (1999) Gamma-aminobutyric acid type B receptor splice variant proteins GBR1a and GBR1b are both associated with GBR2 in situ and display differential regional and subcellular distribution. *J Biol Chem* 274:27323-27330.
- Bennett MK, Erondy NE, Kennedy MB (1983) Purification and characterization of a calmodulin-dependent protein kinase that is highly concentrated in brain. *J Biol Chem* 258:12735-12744.
- Bischoff S, Leonhard S, Reymann N, Schuler V, Shigemoto R, Kaupmann K, Bettler B (1999) Spatial distribution of GABA_BR1 receptor mRNA and binding sites in the rat brain. *J Comp Neurol* 412:1-16.
- Blein S, Ginham R, Uhrin D, Smith BO, Soares DC, Veltel S, McIlhinney RA, White JH, Barlow PN (2004) Structural analysis of the complement control protein (CCP) modules of GABA_B receptor 1a: only one of the two CCP modules is compactly folded. *J Biol Chem* 279:48292-48306.
- Bouvier M (2001) Oligomerization of G-protein-coupled transmitter receptors. *Nat Rev Neurosci* 2:274-286.
- Bowery NG (2006) GABA_B receptor: a site of therapeutic benefit. *Curr Opin Pharmacol* 6:37-43.
- Bowery NG, Doble A, Hill DR, Hudson AL, Shaw JS, Turnbull MJ (1979) Baclofen: a selective agonist for a novel type of GABA receptor. *Br J Pharmacol* 67:444P-445P.
- Bowery NG, Doble A, Hill DR, Hudson AL, Shaw JS, Turnbull MJ, Warrington R (1981) Bicuculline-insensitive GABA receptors on peripheral autonomic nerve terminals. *Eur J Pharmacol* 71:53-70.
- Bowery NG, Bettler B, Froestl W, Gallagher JP, Marshall F, Raiteri M, Bonner TI, Enna SJ (2002) International Union of Pharmacology. XXXIII. Mammalian gamma-aminobutyric acid_B receptors: structure and function. *Pharmacol Rev* 54:247-264.

- Campbell V, Berrow N, Dolphin AC (1993) GABA_B receptor modulation of Ca²⁺ currents in rat sensory neurones by the G protein G_o: antisense oligonucleotide studies. *J Physiol* 470:1-11.
- Casanova E, Guetg N, Vigot R, Seddik R, Julio-Pieper M, Hyland NP, Cryan JF, Gassmann M, and Bettler B (2009) A Mouse Model for Visualization of GABA_B receptors. *Genesis* (in press).
- Chebib M (2004) GABA_C receptor ion channels. *Clin Exp Pharmacol Physiol* 31:800-804.
- Collingridge GL, Lester RA (1989) Excitatory amino acid receptors in the vertebrate central nervous system. *Pharmacol Rev* 41:143-210.
- Couve A, Filippov AK, Connolly CN, Bettler B, Brown DA, Moss SJ (1998) Intracellular retention of recombinant GABA_B receptors. *J Biol Chem* 273:26361-26367.
- Couve A, Thomas P, Calver AR, Hirst WD, Pangalos MN, Walsh FS, Smart TG, Moss SJ (2002) Cyclic AMP-dependent protein kinase phosphorylation facilitates GABA_B receptor-effector coupling. *Nat Neurosci* 5:415-424.
- Cruz HG, Ivanova T, Lunn ML, Stoffel M, Slesinger PA, Luscher C (2004) Bi-directional effects of GABA_B receptor agonists on the mesolimbic dopamine system. *Nat Neurosci* 7:153-159.
- Curtis DR, Phillis JW, Watkins JC (1959) Chemical excitation of spinal neurones. *Nature* 183:611-612.
- Curtis DR, Duggan AW, Felix D, Johnston GA (1971) Bicuculline, an antagonist of GABA and synaptic inhibition in the spinal cord of the cat. *Brain Res* 32:69-96.
- Dascal N (1997) Signalling via the G protein-activated K⁺ channels. *Cell Signal* 9:551-573.
- Di Maio V (2008) Regulation of information passing by synaptic transmission: a short review. *Brain Res* 1225:26-38.
- Dingledine R, Kleckner NW, McBain CJ (1990) The glycine coagonist site of the NMDA receptor. *Adv Exp Med Biol* 268:17-26.
- Elgersma Y, Sweatt JD, Giese KP (2004) Mouse genetic approaches to investigating calcium/calmodulin-dependent protein kinase II function in plasticity and cognition. *J Neurosci* 24:8410-8415.
- Fairfax BP, Pitcher JA, Scott MG, Calver AR, Pangalos MN, Moss SJ, Couve A (2004) Phosphorylation and chronic agonist treatment atypically modulate GABA_B receptor cell surface stability. *J Biol Chem* 279:12565-12573.
- Foster AC, Kemp JA (2006) Glutamate- and GABA-based CNS therapeutics. *Curr Opin Pharmacol* 6:7-17.

- Furukawa H, Singh SK, Mancusso R, Gouaux E (2005) Subunit arrangement and function in NMDA receptors. *Nature* 438:185-192.
- Galvez T, Prezeau L, Milioti G, Franek M, Joly C, Froestl W, Bettler B, Bertrand HO, Blahos J, Pin JP (2000) Mapping the agonist-binding site of GABA_B type 1 subunit sheds light on the activation process of GABA_B receptors. *J Biol Chem* 275:41166-41174.
- Gassmann M, Haller C, Stoll Y, Aziz SA, Biermann B, Mosbacher J, Kaupmann K, Bettler B (2005) The RXR-type endoplasmic reticulum-retention/retrieval signal of GABA_{B1} requires distant spacing from the membrane to function. *Mol Pharmacol* 68:137-144.
- Gassmann M, Shaban H, Vigot R, Sansig G, Haller C, Barbieri S, Humeau Y, Schuler V, Muller M, Kinzel B, Klebs K, Schmutz M, Froestl W, Heid J, Kelly PH, Gentry C, Jatton AL, Van der Putten H, Mombereau C, Lecourtier L, Mosbacher J, Cryan JF, Fritschy JM, Luthi A, Kaupmann K, Bettler B (2004) Redistribution of GABA_{B(1)} protein and atypical GABA_B responses in GABA_{B(2)}-deficient mice. *J Neurosci* 24:6086-6097.
- Grampp T, Notz V, Broll I, Fischer N, Benke D (2008) Constitutive, agonist-accelerated, recycling and lysosomal degradation of GABA_B receptors in cortical neurons. *Mol Cell Neurosci* 39:628-637.
- Greif GJ, Sodickson DL, Bean BP, Neer EJ, Mende U (2000) Altered regulation of potassium and calcium channels by GABA_B and adenosine receptors in hippocampal neurons from mice lacking Galph_o. *J Neurophysiol* 83:1010-1018.
- Guetg N, Seddik R, Vigot R, Turecek R, Gassmann M, Vogt KE, Bräuner-Osborne H, Shigemoto R, Kretz O, Frotscher M, Kulik A, Bettler B (2009) The GABA_{B1a} isoform mediates heterosynaptic depression at hippocampal mossy fiber synapses. *J Neurosci* 29:1414-1423.
- Herlitze S, Garcia DE, Mackie K, Hille B, Scheuer T, Catterall WA (1996) Modulation of Ca²⁺ channels by G-protein beta gamma subunits. *Nature* 380:258-262.
- Hill DR, Bowery NG (1981) 3H-baclofen and 3H-GABA bind to bicuculline-insensitive GABA B sites in rat brain. *Nature* 290:149-152.
- Hill DR, Bowery NG, Hudson AL (1984) Inhibition of GABA_B receptor binding by guanyl nucleotides. *J Neurochem* 42:652-657.
- Ikeda SR (1996) Voltage-dependent modulation of N-type calcium channels by G-protein beta gamma subunits. *Nature* 380:255-258.

- Jacoby E, Bouhelal R, Gerspacher M, Seuwen K (2006) The 7 TM G-protein-coupled receptor target family. *ChemMedChem* 1:761-782.
- Jones KA, Borowsky B, Tamm JA, Craig DA, Durkin MM, Dai M, Yao WJ, Johnson M, Gunwaldsen C, Huang LY, Tang C, Shen Q, Salon JA, Morse K, Laz T, Smith KE, Nagarathnam D, Noble SA, Branchek TA, Gerald C (1998) GABA_B receptors function as a heteromeric assembly of the subunits GABA_BR1 and GABA_BR2. *Nature* 396:674-679.
- Kaupmann K, Huggel K, Heid J, Flor PJ, Bischoff S, Mickel SJ, McMaster G, Angst C, Bittiger H, Froestl W, Bettler B (1997) Expression cloning of GABA_B receptors uncovers similarity to metabotropic glutamate receptors. *Nature* 386:239-246.
- Kaupmann K, Schuler V, Mosbacher J, Bischoff S, Bittiger H, Heid J, Froestl W, Leonhard S, Pfaff T, Karschin A, Bettler B (1998a) Human gamma-aminobutyric acid type B receptors are differentially expressed and regulate inwardly rectifying K⁺ channels. *Proc Natl Acad Sci U S A* 95:14991-14996.
- Kaupmann K, Malitschek B, Schuler V, Heid J, Froestl W, Beck P, Mosbacher J, Bischoff S, Kulik A, Shigemoto R, Karschin A, Bettler B (1998b) GABA_B-receptor subtypes assemble into functional heteromeric complexes. *Nature* 396:683-687.
- Kennedy MB, Bennett MK, Erondy NE (1983) Biochemical and immunochemical evidence that the "major postsynaptic density protein" is a subunit of a calmodulin-dependent protein kinase. *Proc Natl Acad Sci U S A* 80:7357-7361.
- Kerr DI, Ong J (1995) GABA_B receptors. *Pharmacol Ther* 67:187-246.
- Knight AR, Bowery NG (1996) The pharmacology of adenylyl cyclase modulation by GABA_B receptors in rat brain slices. *Neuropharmacology* 35:703-712.
- Kohr G (2006) NMDA receptor function: subunit composition versus spatial distribution. *Cell Tissue Res* 326:439-446.
- Kovalchuk Y, Eilers J, Lisman J, Konnerth A (2000) NMDA receptor-mediated subthreshold Ca²⁺ signals in spines of hippocampal neurons. *J Neurosci* 20:1791-1799.
- Kulik A, Nakadate K, Nyiri G, Notomi T, Malitschek B, Bettler B, Shigemoto R (2002) Distinct localization of GABA_B receptors relative to synaptic sites in the rat cerebellum and ventrobasal thalamus. *Eur J Neurosci* 15:291-307.
- Kulik A, Vida I, Lujan R, Haas CA, Lopez-Bendito G, Shigemoto R, Frotscher M (2003) Subcellular localization of metabotropic GABA_B receptor subunits GABA_{B1a/b} and GABA_{B2} in the rat hippocampus. *J Neurosci* 23:11026-11035.

- Kulik A, Vida I, Fukazawa Y, Guetg N, Kasugai Y, Marker CL, Rigato F, Bettler B, Wickman K, Frotscher M, Shigemoto R (2006) Compartment-dependent colocalization of Kir3.2-containing K⁺ channels and GABA_B receptors in hippocampal pyramidal cells. *J Neurosci* 26:4289-4297.
- Kuner R, Kohr G, Grunewald S, Eisenhardt G, Bach A, Kornau HC (1999) Role of heteromer formation in GABA_B receptor function. *Science* 283:74-77.
- Kuramoto N, Wilkins ME, Fairfax BP, Revilla-Sanchez R, Terunuma M, Tamaki K, Iemata M, Warren N, Couve A, Calver A, Horvath Z, Freeman K, Carling D, Huang L, Gonzales C, Cooper E, Smart TG, Pangalos MN, Moss SJ (2007) Phospho-dependent functional modulation of GABA_B receptors by the metabolic sensor AMP-dependent protein kinase. *Neuron* 53:233-247.
- Lambert NA, Wilson WA (1996) High-threshold Ca²⁺ currents in rat hippocampal interneurons and their selective inhibition by activation of GABA_B receptors. *J Physiol* 492:115-127.
- Lee SJ, Escobedo-Lozoya Y, Szatmari EM, Yasuda R (2009) Activation of CaMKII in single dendritic spines during long-term potentiation. *Nature* 458:299-304.
- Li Y, Krupa B, Kang JS, Bolshakov V, Liu G (2009) Glycine site of NMDA receptor serves as a spatiotemporal detector of synaptic activity patterns. *J Neurophysiology* (in press).
- Lisman J, Schulman H, Cline H (2002) The molecular basis of CaMKII function in synaptic and behavioural memory. *Nat Rev Neurosci* 3:175-190.
- Lodge D (2009) The history of the pharmacology and cloning of ionotropic glutamate receptors and the development of idiosyncratic nomenclature. *Neuropharmacology* 56:6-21.
- Lopez-Bendito G, Shigemoto R, Kulik A, Vida I, Fairen A, Lujan R (2004) Distribution of metabotropic GABA receptor subunits GABA_{B1a/b} and GABA_{B2} in the rat hippocampus during prenatal and postnatal development. *Hippocampus* 14:836-848.
- Lujan R, Shigemoto R (2006) Localization of metabotropic GABA receptor subunits GABA_{B1} and GABA_{B2} relative to synaptic sites in the rat developing cerebellum. *Eur J Neurosci* 23:1479-1490.
- Luscher C, Jan LY, Stoffel M, Malenka RC, Nicoll RA (1997) G protein-coupled inwardly rectifying K⁺ channels (GIRKs) mediate postsynaptic but not presynaptic transmitter actions in hippocampal neurons. *Neuron* 19:687-695.
- Lynch G, Larson J, Kelso S, Barrionuevo G, Schottler F (1983) Intracellular injections of EGTA block induction of hippocampal long-term potentiation. *Nature* 305:719-721.

- Mainen ZF, Malinow R, Svoboda K (1999) Synaptic calcium transients in single spines indicate that NMDA receptors are not saturated. *Nature* 399:151-155.
- Malenka RC, Nicoll RA (1999) Long-term potentiation—a decade of progress? *Science* 285:1870-1874.
- Malenka RC, Kauer JA, Perkel DJ, Nicoll RA (1989a) The impact of postsynaptic calcium on synaptic transmission—its role in long-term potentiation. *Trends Neurosci* 12:444-450.
- Malenka RC, Kauer JA, Perkel DJ, Mauk MD, Kelly PT, Nicoll RA, Waxham MN (1989b) An essential role for postsynaptic calmodulin and protein kinase activity in long-term potentiation. *Nature* 340:554-557.
- Malinow R, Schulman H, Tsien RW (1989) Inhibition of postsynaptic PKC or CaMKII blocks induction but not expression of LTP. *Science* 245:862-866.
- Malitschek B, Schweizer C, Keir M, Heid J, Froestl W, Mosbacher J, Kuhn R, Henley J, Joly C, Pin JP, Kaupmann K, Bettler B (1999) The N-terminal domain of gamma-aminobutyric Acid_β receptors is sufficient to specify agonist and antagonist binding. *Mol Pharmacol* 56:448-454.
- Margeta-Mitrovic M, Jan YN, Jan LY (2000) A trafficking checkpoint controls GABA_β receptor heterodimerization. *Neuron* 27:97-106.
- Martin SC, Russek SJ, Farb DH (1999) Molecular identification of the human GABA_βR2: cell surface expression and coupling to adenylyl cyclase in the absence of GABA_βR1. *Mol Cell Neurosci* 13:180-191.
- Mayer ML, Westbrook GL, Guthrie PB (1984) Voltage-dependent block by Mg²⁺ of NMDA responses in spinal cord neurones. *Nature* 309:261-263.
- Meador WE, Means AR, Quirocho FA (1993) Modulation of calmodulin plasticity in molecular recognition on the basis of x-ray structures. *Science* 262:1718-1721.
- Miller SG, Kennedy MB (1986) Regulation of brain type II Ca²⁺/calmodulin-dependent protein kinase by autophosphorylation: a Ca²⁺-triggered molecular switch. *Cell* 44:861-870.
- Mintz IM, Bean BP (1993) GABA_β receptor inhibition of P-type Ca²⁺ channels in central neurons. *Neuron* 10:889-898.
- Mohler H, Fritschy JM, Luscher B, Rudolph U, Benson J, Benke D (1996) The GABA_A receptors. From subunits to diverse functions. *Ion channels* 4:89-113.
- Ng GY, Clark J, Coulombe N, Ethier N, Hebert TE, Sullivan R, Kargman S, Chateaufneuf A, Tsukamoto N, McDonald T, Whiting P, Mezey E, Johnson MP, Liu Q, Kolakowski LF, Jr.,

- Evans JF, Bonner TI, O'Neill GP (1999) Identification of a GABA_B receptor subunit, gb2, required for functional GABA_B receptor activity. *J Biol Chem* 274:7607-7610.
- Nowak L, Bregestovski P, Ascher P, Herbet A, Prochiantz A (1984) Magnesium gates glutamate-activated channels in mouse central neurones. *Nature* 307:462-465.
- Otis TS, De Koninck Y, Mody I (1993) Characterization of synaptically elicited GABA_B responses using patch-clamp recordings in rat hippocampal slices. *J Physiol* 463:391-407.
- Ouyang Y, Kantor D, Harris KM, Schuman EM, Kennedy MB (1997) Visualization of the distribution of autophosphorylated calcium/calmodulin-dependent protein kinase II after tetanic stimulation in the CA1 area of the hippocampus. *J Neurosci* 17:5416-5427.
- Pagano A, Rovelli G, Mosbacher J, Lohmann T, Duthey B, Stauffer D, Ristig D, Schuler V, Meigel I, Lampert C, Stein T, Prezeau L, Blahos J, Pin J, Froestl W, Kuhn R, Heid J, Kaupmann K, Bettler B (2001) C-terminal interaction is essential for surface trafficking but not for heteromeric assembly of GABA_B receptors. *J Neurosci* 21:1189-1202.
- Payne JA, Rivera C, Voipio J, Kaila K (2003) Cation-chloride co-transporters in neuronal communication, development and trauma. *Trends Neurosci* 26:199-206.
- Perez-Garci E, Gassmann M, Bettler B, Larkum ME (2006) The GABA_{B1b} isoform mediates long-lasting inhibition of dendritic Ca²⁺ spikes in layer 5 somatosensory pyramidal neurons. *Neuron* 50:603-616.
- Poncer JC, McKinney RA, Gahwiler BH, Thompson SM (1997) Either N- or P-type calcium channels mediate GABA release at distinct hippocampal inhibitory synapses. *Neuron* 18:463-472.
- Prinster SC, Hague C, Hall RA (2005) Heterodimerization of G protein-coupled receptors: specificity and functional significance. *Pharmacol Rev* 57:289-298.
- Ramirez OA, Vidal RL, Tello JA, Vargas KJ, Kindler S, Hartel S, Couve A (2009) Dendritic Assembly of Heteromeric gamma-Aminobutyric Acid Type B Receptor Subunits in Hippocampal Neurons. *J Biol Chem* 284:13077-13085.
- Sakaba T, Neher E (2003) Direct modulation of synaptic vesicle priming by GABA_B receptor activation at a glutamatergic synapse. *Nature* 424:775-778.
- Santos AE, Carvalho CM, Macedo TA, Carvalho AP (1995) Regulation of intracellular [Ca²⁺] and GABA release by presynaptic GABA_B receptors in rat cerebrocortical synaptosomes. *Neurochem Int* 27:397-406.

- Schuler V, Luscher C, Blanchet C, Klix N, Sansig G, Klebs K, Schmutz M, Heid J, Gentry C, Urban L, Fox A, Spooren W, Jatou AL, Vigouret J, Pozza M, Kelly PH, Mosbacher J, Froestl W, Kaslin E, Korn R, Bischoff S, Kaupmann K, van der Putten H, Bettler B (2001) Epilepsy, hyperalgesia, impaired memory, and loss of pre- and postsynaptic GABA_B responses in mice lacking GABA_{B(1)}. *Neuron* 31:47-58.
- Shaban H, Humeau Y, Herry C, Cassasus G, Shigemoto R, Ciochi S, Barbieri S, van der Putten H, Kaupmann K, Bettler B, Luthi A (2006) Generalization of amygdala LTP and conditioned fear in the absence of presynaptic inhibition. *Nat Neurosci* 9:1028-1035.
- Shen K, Meyer T (1999) Dynamic control of CaMKII translocation and localization in hippocampal neurons by NMDA receptor stimulation. *Science* 284:162-166.
- Sickmann T, Alzheimer C (2003) Short-term desensitization of G-protein-activated, inwardly rectifying K⁺ (GIRK) currents in pyramidal neurons of rat neocortex. *J Neurophysiol* 90:2494-2503.
- Smrcka AV (2008) G protein betagamma subunits: central mediators of G protein-coupled receptor signaling. *Cell Mol Life Sci* 65:2191-2214.
- Sohl G, Maxeiner S, Willecke K (2005) Expression and functions of neuronal gap junctions. *Nat Rev Neurosci* 6:191-200.
- Steiger JL, Bandyopadhyay S, Farb DH, Russek SJ (2004) cAMP response element-binding protein, activating transcription factor-4, and upstream stimulatory factor differentially control hippocampal GABA_BR1a and GABA_BR1b subunit gene expression through alternative promoters. *J Neurosci* 24:6115-6126.
- Ulrich D, Besseyrias V, Bettler B (2007) Functional mapping of GABA_B-receptor subtypes in the thalamus. *J Neurophysiol* 98:3791-3795.
- Vargas KJ, Terunuma M, Tello JA, Pangalos MN, Moss SJ, Couve A (2008) The availability of surface GABA_B receptors is independent of gamma-aminobutyric acid but controlled by glutamate in central neurons. *J Biol Chem* 283:24641-24648.
- Vigot R, Barbieri S, Brauner-Osborne H, Turecek R, Shigemoto R, Zhang YP, Lujan R, Jacobson LH, Biermann B, Fritschy JM, Vacher CM, Muller M, Sansig G, Guetg N, Cryan JF, Kaupmann K, Gassmann M, Oertner TG, Bettler B (2006) Differential compartmentalization and distinct functions of GABA_B receptor variants. *Neuron* 50:589-601.

- White JH, Wise A, Main MJ, Green A, Fraser NJ, Disney GH, Barnes AA, Emson P, Foord SM, Marshall FH (1998) Heterodimerization is required for the formation of a functional GABA_B receptor. *Nature* 396:679-682.
- Xu J, Wojcik WJ (1986) Gamma aminobutyric acid B receptor-mediated inhibition of adenylate cyclase in cultured cerebellar granule cells: blockade by islet-activating protein. *J Pharmacol Exp Ther* 239:568-573.
- Yang CR, Svensson KA (2008) Allosteric modulation of NMDA receptor via elevation of brain glycine and D-serine: the therapeutic potentials for schizophrenia. *Pharmacol Ther* 120:317-332.

6. Publications

6.1. **Compartment-dependent colocalization of Kir3.2-containing K⁺ channels and GABA_B receptors in hippocampal pyramidal cells**

Kulik A, Vida I, Fukazawa Y, Guetg N, Kasugai Y, Marker CL, Rigato F, Bettler B, Wickman K, Frotscher M, Shigemoto R

The Journal of Neuroscience 2006; 26:4289-97

The inwardly rectifying Kir3-type K⁺-channels are the postsynaptic G-protein activated effector channels of GABA_B receptors (Luscher et al., 1997). The Kir3-type channels are comprised of four subunits: Kir3.1, Kir3.2, Kir3.3 and Kir3.4 (Dascal, 1997). Kir3.1 and Kir3.2 are the prevalent subunits in the brain. This study investigates the spatial distribution and correlation of GABA_B receptors and Kir3.2 in the rat hippocampus by using preembedding electron microscopy and SDS-digested freeze-fracture replica immunolabeling.

Within this work, it was demonstrated that immunoreactivities for GABA_{B1} and Kir3.2 are similarly distributed in the hippocampus. In the CA1 area of the rat hippocampus, Kir3.2-channels were enriched peri- and extrasynaptically and were observed only rarely in the synaptic membrane specialization. Quantitative analysis revealed that at asymmetrical synapses (putative glutamatergic synapses) both GABA_{B1} and Kir3.2 were enriched perisynaptically and that their distribution was overlapping. In contrast, at symmetrical synapses (putative GABAergic synapses) Kir3.2 and GABA_{B1} immunoparticles were distributed equally over the extrasynaptic space.

Furthermore, the spatial relationship between Kir3.2 and GABA_{B1} immunoreactivity was investigated. Interestingly, a different relative distance between Kir3.2 and GABA_{B1} was observed in dendritic spines and dendritic shafts of CA1 pyramidal neurons. In 70% of the dendritic spines containing Kir3.2 and GABA_{B1}, the distance between immunogold particles representing GABA_{B1} and Kir3.2 was less than 50nm. In contrast, the mean distance between GABA_{B1} and Kir3.2 immunogold particles in the dendritic shaft was

significantly increased. A similar distribution was observed in dendritic spines and shafts of CA3 pyramidal neurons.

These data indicate that at least in the dendritic spines GABA_B receptors and K⁺-channels are clustered allowing efficient Gβγ-mediated effector coupling. Furthermore, it can be proposed that K⁺-channels, localized in the dendritic shaft of pyramidal cells, may be predominantly activated by other GPCRs than GABA_B. It is possible that this differential distribution of Kir3.2–GABA_{B1} clusters provides an effective tool to control the postsynaptic inhibition of the neurons both temporally and spatially.

Statement of personal contribution:

- Contribution to the acquisition and analysis of data

Compartment-Dependent Colocalization of Kir3.2-Containing K⁺ Channels and GABA_B Receptors in Hippocampal Pyramidal Cells

Ákos Kulik,^{1,2} Imre Vida,¹ Yugo Fukazawa,^{2,5} Nicole Guetg,^{1,3} Yu Kasugai,² Cheryl L. Marker,⁴ Franck Rigato,¹ Bernhard Bettler,³ Kevin Wickman,⁴ Michael Frotscher,¹ and Ryuichi Shigemoto^{2,5,6}

¹Institute of Anatomy and Cell Biology, Department of Neuroanatomy, University of Freiburg, 79104 Freiburg, Germany, ²Division of Cerebral Structure, National Institute for Physiological Sciences, Myodaiji, Okazaki 444-8787, Japan, ³Pharmazentrum, Department of Clinical–Biological Sciences, University of Basel, 4056 Basel, Switzerland, ⁴Department of Pharmacology, University of Minnesota, Minneapolis, Minnesota 55455, ⁵Department of Physiological Sciences, The Graduate University of Advanced Studies (Sokendai), Myodaiji, Okazaki 444-8787, Japan, and ⁶SORST Japan Science and Technology Corporation, Kawaguchi 332-0012, Japan

G-protein-coupled inwardly rectifying K⁺ channels (Kir3 channels) coupled to metabotropic GABA_B receptors are essential for the control of neuronal excitation. To determine the distribution of Kir3 channels and their spatial relationship to GABA_B receptors on hippocampal pyramidal cells, we used a high-resolution immunocytochemical approach. Immunoreactivity for the Kir3.2 subunit was most abundant postsynaptically and localized to the extrasynaptic plasma membrane of dendritic shafts and spines of principal cells. Quantitative analysis of immunogold particles for Kir3.2 revealed an enrichment of the protein around putative glutamatergic synapses on dendritic spines, similar to that of GABA_{B1}. Consistent with this observation, a high degree of coclustering of Kir3.2 and GABA_{B1} was revealed around excitatory synapses by the highly sensitive SDS-digested freeze–fracture replica immunolabeling. In contrast, in dendritic shafts receptors and channels were found to be mainly segregated. These results suggest that Kir3.2-containing K⁺ channels on dendritic spines preferentially mediate the effect of GABA, whereas channels on dendritic shafts are likely to be activated by other neurotransmitters as well. Thus, Kir3 channels, localized to different subcellular compartments of hippocampal principal cells, appear to be differentially involved in synaptic integration in pyramidal cell dendrites.

Key words: GABA_{B1}; Kir3; G-protein-coupled receptors; electron microscopy; immunocytochemistry; spillover

Introduction

Inwardly rectifying potassium channels play a crucial role in the control of neuronal excitation by mediating slow inhibitory synaptic responses and contributing to the resting membrane potential (Hille, 1992; Chen and Johnston, 2005). A subfamily of inwardly rectifying channels (Kir3) is directly coupled to G-proteins and mediates the effect of metabotropic receptors in a membrane-delimited manner (Wickman et al., 1994; Huang et al., 1995; Wickman and Clapham, 1995; Schreibmayer et al., 1996; Dascal, 1997; Yamada et al., 1998; Stanfield et al., 2002; Bichet et al., 2003). Kir3 channels serve as a common effector for various neurotransmitters including the major inhibitory transmitter GABA acting on type B receptors (GABA_BRs) (Andrade et

al., 1986; Mihara et al., 1987; North et al., 1987; Trussell and Jackson, 1987; Lüscher et al., 1997; Sharon et al., 1997; Kaupmann et al., 1998; Torrecilla et al., 2002; Chen and Johnston, 2005; Koyrakh et al., 2005; Marker et al., 2005).

The mammalian Kir3 channel subfamily comprises four subunits designated Kir3.1, Kir3.2, Kir3.3, and Kir3.4 (Dascal, 1997). The functional channels exist as homotetrameric or heterotetrameric complexes (Inanobe et al., 1995; Kofuji et al., 1995; Krapivinsky et al., 1995; Slesinger et al., 1996; Spauschus et al., 1996; Wischmeyer et al., 1997). In the CNS, channels are thought to be mainly composed of the Kir3.1 and Kir3.2 subunits (Duprat et al., 1995; Lesage et al., 1995; Leaney, 2003). Recent evidence further suggests that the Kir3.2 subunit is an essential part of the functional channel, determining its assembly and surface localization (Inanobe et al., 1999; Ma et al., 2002). Indeed, lack of Kir3.2 leads to reduced Kir3.1 expression (Liao et al., 1996; Signorini et al., 1997) and to loss of slow inhibitory postsynaptic responses in hippocampal pyramidal cells (Lüscher et al., 1997).

Neurons in the hippocampal formation express high levels of Kir3 subunit transcripts (Dixon et al., 1995; Kobayashi et al., 1995; Karschin et al., 1996; Liao et al., 1996). Although a large body of electrophysiological and pharmacological data are available on the function of these channels (Gähwiler and Brown,

Received Sept. 30, 2005; revised Feb. 27, 2006; accepted Feb. 27, 2006.

This work was supported by Deutsche Forschungsgemeinschaft, Sonderforschungsbereiche 505 (A.K., I.V., M.F.), the Swiss Science Foundation (B.B.), Neurex (B.B., M.F.), and National Institutes of Health Grants MH61933 and DA011806 (K.W.). We are grateful to Prof. Peter Jonas for his helpful comments on this manuscript. We thank Dr. Andrea Lörincz, Sanae Hara, Emi Kamiya, Anikó Schneider, and Sigrun Nestel for their support with tissue preparation for the SDS-FRL and electron microscopy.

Correspondence should be addressed to Ákos Kulik, Institute of Anatomy and Cell Biology, Department of Neuroanatomy, University of Freiburg, Albertstrasse 17, 79104 Freiburg, Germany. E-mail: Akos.Kulik@anat.uni-freiburg.de.

DOI:10.1523/JNEUROSCI.4178-05.2006

Copyright © 2006 Society for Neuroscience 0270-6474/06/264289-09\$15.00/0

1985; Andrade et al., 1986; Andrade and Nicoll, 1987; Nicoll, 1988; Sodickson and Bean, 1996; Lüscher et al., 1997; Takigawa and Alzheimer, 2002, 2003; Leaney, 2003; Chen and Johnston, 2005), the localization of Kir3 in various subcellular compartments of principal cell remains mostly unknown. Previous immunohistochemical studies showed high levels of Kir3 channels in the dendrites of pyramidal cells (Ponce et al., 1996; Drake et al., 1997), suggesting a subcellular distribution similar to that of GABA_B receptors (Kulik et al., 2003). To investigate the spatial relationship of the channel and receptor, we studied the subcellular localization of the Kir3.2 subunit and determined the compartment-dependent colocalization of Kir3.2 and GABA_{B1} in pyramidal cells by using high-resolution immunocytochemical techniques. Interestingly, we found that Kir3.2 and GABA_{B1} are mostly segregated on dendritic shafts, contacted by inhibitory GABAergic boutons, whereas the two proteins are highly colocalized on dendritic spines adjacent to the excitatory synapses.

Materials and Methods

Antibodies and controls

Antibodies. An affinity-purified polyclonal antibody specific for the C-terminal domain of the Kir3.2 subunit (Lesage et al., 1994; Isomoto et al., 1996) was purchased from Alomone Labs (Jerusalem, Israel). This antibody recognizes the Kir3.2a and Kir3.2c splicing isoforms. It additionally recognizes the Kir3.2d isoform, which is predominantly expressed in testis (Inanobe et al., 1999). To localize GABA_B receptors composed of GABA_{B1} and GABA_{B2} subunits (Kaupmann et al., 1998), two affinity-purified polyclonal antibodies recognizing both *a* and *b* splice variants of the GABA_{B1} subunit were used. The first antibody (B17) was raised in rabbits, and its characteristics and specificity have been described previously (Kulik et al., 2002, 2003). The second antibody (B62) was raised in guinea pigs against a GST fusion protein containing amino acid residues 857–960 of the GABA_{B1} protein (Kaupmann et al., 1997). Its specificity was confirmed by immunoblot analysis: it gave rise to two immunoreactive bands with molecular masses of 130 and 100 kDa corresponding to GABA_{B1a} and GABA_{B1b} proteins (supplemental Fig. 1A, available at www.jneurosci.org as supplemental material). The B62 antibody yielded an immunoreactive pattern in the hippocampus (supplemental Fig. 1B, available at www.jneurosci.org as supplemental material) similar to that obtained with the well characterized B17 antibody. To identify the postsynaptic density of excitatory synapses, a monoclonal anti-postsynaptic density-95 (PSD-95) antibody was also used (Upstate Biotechnology, Lake Placid, NY). To determine the spatial relationship of GABA_B receptors and the K⁺–Cl[–] cotransporter 2 (KCC2) an antibody against the cotransporter (Upstate Biotechnology) was used.

Controls. The specificity of the immunolabeling for Kir3.2 and GABA_{B1} in these experiments was controlled by (1) staining of sections obtained from either Kir3.2- (Torrecilla et al., 2002) or GABA_{B1}-deficient mice (Schuler et al., 2001), and (2) in case of double- and triple-labeling experiments, omitting one of the primary antibodies. No immunolabeling was detected on sections and replicas derived from Kir3.2- or GABA_{B1}-deficient mice (supplemental Fig. 1C, available at www.jneurosci.org as supplemental material) stained with the respective primary antibodies in preembedding and replica experiments, further confirming specificity of the antibodies. When one of the primary antibodies was omitted, but secondary antibodies were included, no immunolabeling was detected for the respective protein excluding the possibility of cross-reactivity of the primary and secondary antibodies.

Immunoblot analysis

Immunoblot analysis was performed as described previously (Shigemoto et al., 1997). The crude membrane preparations from adult rat forebrain were separated by 7.5% SDS-PAGE and transferred onto polyvinylidene difluoride (Bio-Rad, Hercules, CA) membrane. The membrane was blocked with Block-Ace (Dainippon Pharmaceutical, Suita, Japan) and then reacted with the affinity-purified GABA_{B1} (B62) antibody (0.5 μg/ml). An alkaline phosphatase-labeled secondary antibody (1:5000; Chemicon, Temecula, CA) was used to visualize protein bands.

Immunocytochemistry

A total of 19 adult male Wistar rats (Charles River, Freiburg, Germany), 7 adult wild-type mice, 5 Kir3.2-deficient mice, and 6 GABA_{B1}-deficient mice were used in the present study. Care and handling of the animals before and during the experiments followed European Union regulations and was approved by the animal care and use committees of the authors' institutions.

Preembedding immunocytochemistry

Immunohistochemical labeling for light and electron microscopy was performed as described previously (Kulik et al., 2002). For light microscopy, animals (*n* = 5 rats; *n* = 3 wild-type mice; *n* = 2 Kir3.2-deficient mice; *n* = 3 GABA_{B1}-deficient mice) were deeply anesthetized with Narkodorm-n (pentobarbital; 180 mg/kg, i.p.) (Alvetra, Neumünster, Germany) and perfused transcardially with 4% paraformaldehyde (Merck, Darmstadt, Germany), 15% saturated picric acid, and 0.05% glutaraldehyde (Polyscience, Warrington, PA) made up in 0.1 M phosphate buffer (PB). Tissue blocks were cryoprotected and freeze-thawed, and sections were cut (40 μm). Sections were incubated with 0.6 μg/ml primary antibody for Kir3.2 in 25 mM PBS containing 3% normal goat serum (NGS) (Vector Laboratories, Burlingame, CA) and 0.1% Triton X-100. After washes in PBS, the sections were incubated with biotinylated goat anti-rabbit IgG antibody (1:100; Vector Laboratories), then reacted with avidin–biotin peroxidase complex (ABC kit; 1:100; Vector Laboratories), and finally incubated with 0.025% 3,3'-diaminobenzidine tetrahydrochloride (Sigma, St. Louis, MO) and 0.003% hydrogen peroxide. For electron microscopy, animals (*n* = 8 rats; *n* = 2 wild-type mice; *n* = 1 Kir3.2-deficient mouse; *n* = 1 GABA_{B1}-deficient mouse) were perfused with the same fixative as described for light microscopy. Sections (50 μm) were incubated in a blocking solution followed by the primary antibodies (2.0–3.0 μg/ml) diluted in Tris-buffered saline (TBS) containing 3% NGS. After washing, the sections were incubated with 1.4 nm gold-coupled goat anti-rabbit or goat anti-guinea pig secondary antibodies (Fab fragment; 1:100; Nanogold; Nanoprobes, Stony Brook, NY), and then reacted with HQ Silver kit (Nanoprobes). After treatment with OsO₄, the sections were stained with uranyl acetate, dehydrated, and flat-embedded in epoxy resin (Durcupan; ACM; Fluka; Sigma).

Three-dimensional reconstruction and quantification of Kir3.2 and GABA_{B1} immunoreactivity

The three-dimensional (3D) reconstruction of CA1 pyramidal cell dendritic spines and shafts immunoreactive for either the Kir3.2 or GABA_{B1} subunits was performed from serial ultrathin sections obtained from preembedding material as described previously (Kulik et al., 2002). Samples were taken from the very surface (<3 μm) of blocks containing strata oriens, radiatum, or lacunosum-moleculare of CA1. For each immunoparticle (located within 25 nm from the membrane), the distances to the closest edge of asymmetrical and symmetrical synapses were measured along the surface of the 3D reconstructed profiles.

SDS-digested freeze–fracture replica immunolabeling

Animals (*n* = 6 rats; *n* = 2 wild-type mice; *n* = 2 Kir3.2-deficient mice; *n* = 2 GABA_{B1}-deficient mice) were deeply anesthetized with sodium pentobarbital (50 mg/kg, i.p.), and the hearts were surgically exposed for perfusion fixation. First, the vascular system was flushed by circulating 25 mM PBS for 1 min. This was followed by transcardial perfusion with a fixative containing 2% paraformaldehyde and 15% saturated picric acid made up in 0.1 M PB. Sagittal sections from the CA1 or the CA3 area were cut on a micro slicer at a thickness of 90 μm. The slices were cryoprotected in a solution containing 30% glycerol made up in 0.1 M PB overnight at 4°C, and then were frozen by a high-pressure freezing machine (HPM 101; BAL-TEC, Balzers, Lichtenstein). Frozen samples were inserted into a double replica table and then fractured into two pieces at –115°C. Fractured faces were replicated by deposition of carbon (2–3 nm thickness), platinum (2 nm), and carbon (20 nm) in a freeze–fracture replica machine (BAF 060; BAL-TEC). They were digested in a solution containing 2.5% SDS and 20% sucrose made up in 15 mM Tris buffer, pH 8.3, at 105°C for 15 min followed by their incubation in the same solution overnight at room temperature. The replicas were washed in 25 mM TBS containing 0.05% bovine serum albumin (BSA) (Nacalai Tesque, Kyoto,

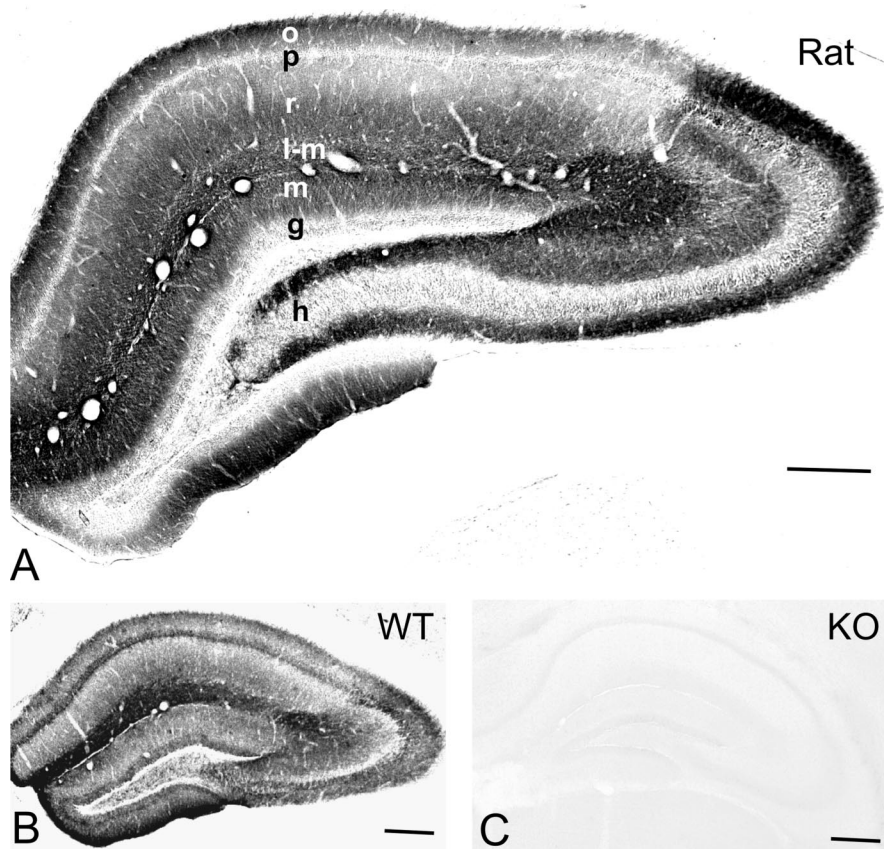


Figure 1. Distribution of immunoreactivity for the Kir3.2 subunit in the hippocampus. *A, B*, The immunostaining was moderate to strong in dendritic layers of the CA area and dentate gyrus in the rat (*A*) and wild-type (WT) mouse (*B*). In the CA1, the immunolabeling for the protein was strong and homogeneous in the stratum lacunosum-moleculare, whereas the strata oriens and radiatum showed uneven immunostaining with moderate intensity of immunoreactivity in the proximal half and high intensity in the distal half of these layers. In CA3, the immunoreactivity for Kir3.2 was strong in the strata oriens, radiatum, and lacunosum-moleculare. In the dentate gyrus, strong immunostaining was detected in the hilus and moderate in the molecular layer. *C*, No immunoreactivity for Kir3.2 was found in the hippocampus of the Kir3.2-deficient (KO) mice. Scale bars, 200 μ m. o, Stratum oriens; p, stratum pyramidale; r, stratum radiatum; l-m, stratum lacunosum-moleculare; m, stratum moleculare; g, stratum granulosum; h, hilus.

Japan) and incubated in a blocking solution containing 5% BSA in 25 mM TBS for 1 h. Subsequently, the replicas were incubated in the primary antibody for Kir3.2 or, in double- and triple-immunolabeling experiments, with mixtures of primary antibodies (20–25 μ g/ml) for Kir3.2 and GABA_{B1} or Kir3.2, GABA_{B1}, and PSD-95 diluted in TBS containing 5% BSA overnight at room temperature. In control experiments, replicas were incubated in a mixture of primary antibodies for KCC2, GABA_{B1}, and PSD-95 diluted in the same solution as described above. After several washes, the replicas were reacted with a mixture of gold-coupled goat anti-rabbit (for Kir3.2 or KCC2), goat anti-guinea pig (for GABA_{B1}), and goat anti-mouse (for PSD-95) secondary antibodies (1:30; BioCell Research Laboratories, Cardiff, UK) made up in 25 mM TBS containing 5% BSA overnight at room temperature. They were then washed and picked up on 100-mesh grids. For quantitative analysis, samples were taken from layers of CA1 and CA3 double-immunolabeled for the Kir3.2 and GABA_{B1} subunits. Clusters of immunoparticles for Kir3.2 and GABA_{B1} were determined by outlining the areas covered by immunogold particles (three particles or more within a distance of 50 nm) on dendritic shafts and on dendritic spines of pyramidal cells. Distances between the center of clusters of Kir3.2 and the closest clusters of GABA_{B1} were measured along the surface of the profiles. The relative frequency for the cluster pairs was determined by binning the data set at 50 nm. Values are expressed as mean \pm SEM, and for statistical comparison the nonparametric double-sided nonpaired Wilcoxon–Mann–Whitney test was used.

Results

Kir3.2 immunoreactivity in dendritic layers of the hippocampus

The use of the Kir3.2 affinity-purified antibody revealed a specific pattern of immunostaining in the rat (Fig. 1*A*) and wild-type mouse hippocampus (Fig. 1*B*). The immunoreactivity for the protein was widely distributed in the hippocampus with moderate to strong staining in dendritic layers. In CA1, the immunolabeling for Kir3.2 was homogeneously strong in the stratum lacunosum-moleculare, whereas the strata radiatum and oriens showed an uneven immunostaining with moderate intensity in the proximal half and high intensity in the distal half of these layers. In CA3, the immunoreactivity was strongest in strata oriens, radiatum, and lacunosum-moleculare, whereas in the stratum lucidum it was moderate. In the dentate gyrus, strong immunostaining for the subunit was detected in the hilus and moderate in the molecular layer. In the pyramidal and granule cell layers, weak labeling was observed. No immunoreactivity for Kir3.2 was detected in the white matter. In sections obtained from Kir3.2-deficient mice, the specific immunolabeling pattern was completely abolished (Fig. 1*C*).

Kir3.2 is preferentially localized to extrasynaptic membrane of dendrites

To determine the subcellular localization of Kir3.2 responsible for the immunostaining in dendritic layers, we used preembedding immunogold labeling. For electron-microscopic investigation, tissue blocks were taken from the CA1 area. Immunoreactivity for the Kir3.2 subunit was primarily found in postsynaptic elements, namely, on dendritic shafts and spines of putative pyramidal cells (Fig. 2). Clusters of immunogold particles were localized to the extrasynaptic plasma membrane of dendritic shafts (Fig. 2*A, B, F, G, I*) establishing symmetrical (putative GABAergic) synapses with presynaptic boutons (Fig. 2*B, G*). Strong immunolabeling was also found on the extrasynaptic membrane of dendritic spines (Fig. 2*A, C–F, H, I*). Immunoparticles also appeared occasionally at the edge (Fig. 2*D, F*) and over the postsynaptic membrane specialization of asymmetrical, putative glutamatergic synapses on dendritic spines (Fig. 2*C*). This predominantly extrasynaptic localization of the channel is in good agreement with the finding of Nehring et al. (2000), who showed that the Kir3.2 subunit is unable to form a complex with PSD-95 at postsynaptic sites. In addition to pyramidal cells, immunoreactivity for Kir3.2 was also seen on the extrasynaptic plasma membrane of putative interneuron dendrites (Fig. 2*J*), identified by the lack of dendritic spines and the presence of asymmetrical synapses. In contrast to the strong dendritic labeling, very little immunolabeling was seen in somata of pyramidal cells under our experimental conditions. Presynaptically, weak immunoreactivity for Kir3.2 was occasionally detected in axon terminals making

asymmetrical synapses with dendritic spines in strata oriens and radiatum (Fig. 2*C,E*). Immunoparticles were localized either to the extrasynaptic plasma membrane (Fig. 2*C*) or to the presynaptic membrane specialization of boutons (Fig. 2*E*). The specificity of the labeling in preembedding material was confirmed by the absence of labeling in Kir3.2-deficient animals.

Enrichment of Kir3.2 around excitatory synapses on dendritic spines

The pattern of the subcellular distribution of Kir3.2, particularly the strong labeling on dendritic spines of hippocampal pyramidal cells, is very similar to that of GABA_B receptors (Kulik et al., 2003). To compare the distribution of the Kir3.2 and GABA_{B1} on dendrites of pyramidal cells in relation to putative GABAergic and glutamatergic synapses, three-dimensional (3D) reconstructions were made from serial ultrathin sections and the distances of the immunoparticles from the edge of symmetrical and asymmetrical synaptic specializations were measured. This approach revealed that, on dendritic shafts, the channel and the receptor showed no association to symmetrical, putative GABAergic synapses (Fig. 3*A*) (209 particles on eight dendrites for Kir3.2 and 241 particles on seven dendrites for GABA_{B1}). In contrast, on dendritic spines, both Kir3.2 and GABA_{B1} were found to be preferentially localized around asymmetrical synapses. The distribution for Kir3.2 showed a peak between 0 and 240 nm from the synapses (Fig. 3*B*) (313 particles on 66 spines). Similarly, for GABA_{B1} the peak of the distribution was located between 60 and 240 nm (Fig. 3*B*) (325 particles on 49 spines), consistent with previous data obtained from CA1 and CA3 areas (Kulik et al., 2003). For both proteins ~60% of the immunoparticles were located within a distance of 240 nm from the edge of asymmetrical synapses indicating an enrichment of the molecules in the vicinity of putative glutamatergic synapses on dendritic spines.

Preferential colocalization of Kir3.2 and GABA_{B1} on dendritic spines of CA1 pyramidal cells

To directly investigate the colocalization of Kir3.2 and GABA_{B1} in subcellular compartments of CA1 pyramidal cells, we performed double- and triple-labeling immunocytochemistry by using the highly sensitive SDS-digested freeze–fracture replica immunolabeling technique (Hagiwara et al., 2005; Tanaka et al., 2005). Consistent with the results of preembedding experiments, strong immunolabeling for Kir3.2 was found postsynaptically. Clusters of immunoparticles were observed on the protoplasmic face of the membrane of dendritic shafts and spines of putative pyramidal cells (Fig. 4*A*). Double immunolabeling for Kir3.2 and GABA_{B1} further revealed that, on dendritic shafts, the channels and receptors were mainly segregated (Fig. 4*B*), whereas on dendritic spines, a high degree of coclustering of the immunogold

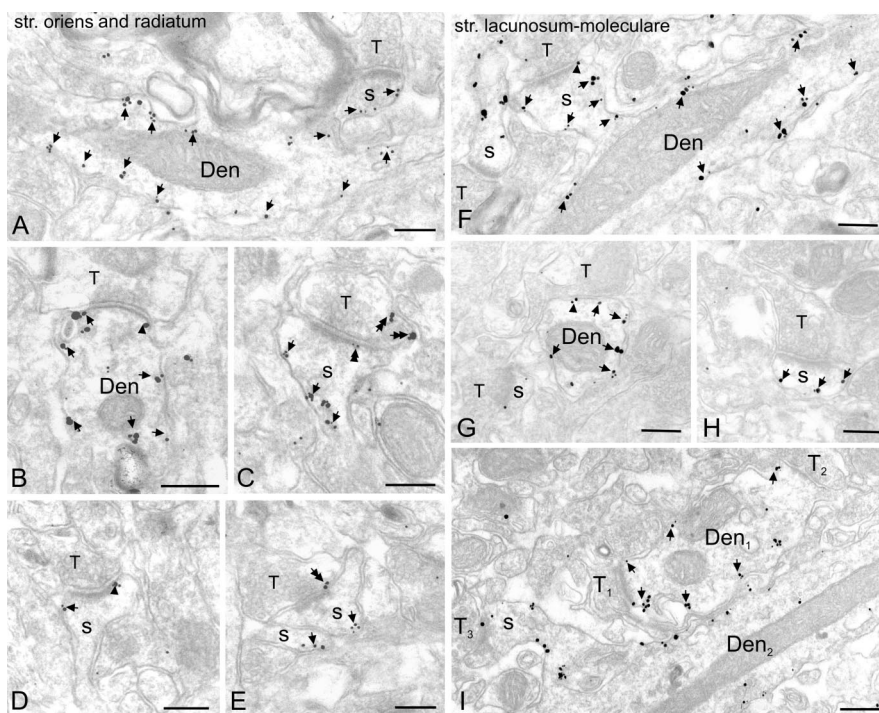


Figure 2. Preferential postsynaptic localization of Kir3.2 in dendritic layers of the CA1 area. Electron micrographs show immunoreactivity for the Kir3.2 subunit in the strata oriens (*A, C*), radiatum (*B, D, E*), and lacunosum-moleculare (*F–I*) as detected by the preembedding immunogold method. *A, B, F, G, I*, Clusters of immunogold particles were seen along the extrasynaptic plasma membrane (arrows) of dendritic shafts (Den) of pyramidal cells contacted by terminals (T) of presumed GABAergic cells. Labeling was occasionally found at the edge of symmetrical synaptic specializations (arrowheads in *B, G*). *A, C–F, H, I*, Immunoparticles were abundant on the extrasynaptic plasma membrane (arrows) of dendritic spines of pyramidal cells (s). They also appeared occasionally over the postsynaptic specialization (double arrowhead in *C*) at synapses between axon terminals (T) of putative pyramidal cells and dendritic spines and at the edge of asymmetrical synapses (arrowheads in *D, F*). *C, E*, Presynaptically, immunogold particles (double arrows) were localized to the extrasynaptic plasma membrane and to the presynaptic membrane specialization of axon terminals (T) establishing asymmetrical synapses. *I*, Immunolabeling was also visible in dendritic shafts of presumed interneurons (Den₁) establishing asymmetrical synapses with presynaptic boutons (T₁, T₂). Note that the dendritic spine (s), contacted by an axon terminal (T₃), and the dendritic shaft (Den₂) of a pyramidal cell are also labeled. Scale bars, 0.2 μ m.

particles for the two proteins was observed (Fig. 4*C*). To quantify the spatial relationship of the channel and receptor subunits, the distances between clusters of Kir3.2 and the closest clusters of GABA_{B1} were measured on dendritic shafts and spines (Fig. 4*D*). This analysis revealed that, on dendritic shafts, only 84 of 302 clusters (28%) were within 100 nm, whereas on dendritic spines 86 of 90 clusters (96%) were within this distance (Fig. 4*D*). The location of the Kir3.2–GABA_{B1} complexes relative to excitatory synaptic sites, demarcated by the presence of PSD-95, an essential component of the excitatory postsynaptic specialization, was investigated in triple-immunolabeling experiments. The Kir3.2–GABA_{B1} coclusters were found on the extrasynaptic membrane close to the location of PSD-95 immunoreactivity on dendritic spines (Fig. 4*E, F*). Weak Kir3.2 and GABA_{B1} immunolabeling was found in putative excitatory terminals, but no coclustering of the proteins was observed. Thus, our results demonstrate that, on dendritic shafts, where mostly GABAergic synapses are located, the Kir3.2-containing inwardly rectifying K⁺ channels and GABA_B receptors are mainly segregated, whereas on dendritic spines, adjacent to glutamatergic synapses, the two proteins show a close association.

To assess the functional relevance of the observed association, we investigated the spatial relationship of molecules on dendritic spines that are functionally unrelated to GABA_B receptors. To this end, we have performed immunogold labeling for KCC2,

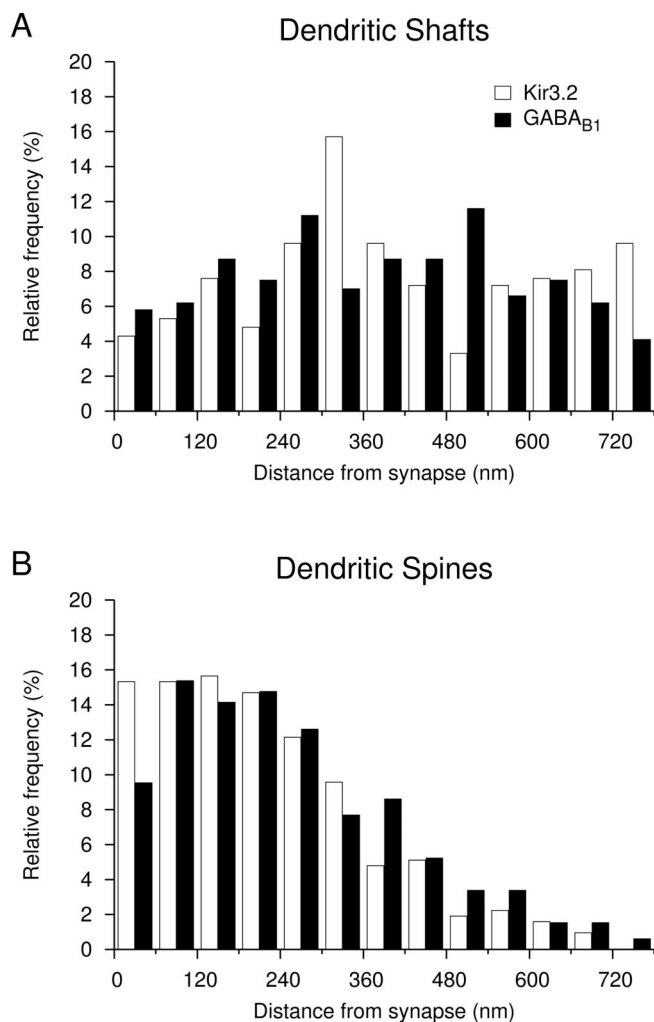


Figure 3. Distribution of immunoparticles for the Kir3.2 and GABA_{B1} subunits relative to symmetrical and asymmetrical synapses on dendrites of CA1 pyramidal cells as assessed by preembedding immunogold labeling. **A**, Histogram showing the spatial distribution of immunoparticles for Kir3.2 (open bars; $n = 209$) and GABA_{B1} (filled bars; $n = 241$) around symmetrical synapses on dendritic shafts. Distances of immunogold particles were measured from the closest edge of the synapses along the surface of dendritic shafts reconstructed from serial ultrathin sections. Values were allocated to 60-nm-wide bins and expressed as relative frequencies. **B**, Histogram showing the spatial distribution of immunoparticles for Kir3.2 ($n = 313$) and GABA_{B1} ($n = 325$) around asymmetrical synapses on dendritic spines. These data show that there is no association of Kir3.2 and GABA_{B1} to symmetrical, putative GABAergic synapses on dendritic shafts, but there is an enrichment of both proteins in the vicinity of asymmetrical, putative glutamatergic synapses on dendritic spines.

GABA_{B1}, and PSD-95. This experiment revealed that, although immunoreactivity for KCC2 is abundantly localized to the dendritic spines (Gulyás et al., 2001), the cotransporter and the receptor were found to be mainly segregated (Fig. 4G) in this compartment.

Colocalization of Kir3.2 and GABA_{B1} on CA3 pyramidal cells

Finally, we investigated the distribution and colocalization of Kir3.2 and GABA_{B1} in the CA3 region. Samples were taken from the stratum oriens and processed for Kir3.2, GABA_{B1}, and PSD-95 immunolabeling using the replica technique. Similarly to the CA1 area, clusters of immunogold particles for Kir3.2 were found on dendritic shafts (Fig. 5A) and spines (Fig. 5B). The mean number of particles per cluster on the dendritic shafts of the CA3 area was, however, higher (6.4 ± 0.2 particles/cluster; 162

clusters) compared with the CA1 area (4.2 ± 0.2 particles/cluster; 93 clusters; $p < 0.01$) in a good agreement with the difference in the staining intensity observed at the light-microscopic level (Fig. 1A). Despite this difference in cluster size, the colocalization pattern of Kir3.2 and GABA_{B1} was similar to that of the CA1 area. On dendritic shafts, the channel and receptor were mainly segregated (Fig. 5A), whereas on dendritic spines, the proteins showed a high level of colocalization (Fig. 5B).

Discussion

The present study describes the subcellular localization of the Kir3.2 subunit of the G-protein-coupled inwardly rectifying K⁺ channel and its spatial relationship to GABA_B receptor in the adult rat hippocampus. Kir3 channel proteins were primarily found postsynaptically and localized to dendritic shafts and dendritic spines of pyramidal cells. Double immunolabeling for Kir3.2 and GABA_{B1} using the replica technique revealed that, on dendritic shafts, the two proteins were mostly segregated, whereas on dendritic spines, around putative glutamatergic synapses, a high degree of coclustering of the ion channel and receptor subunits was observed. Immunolabeling for KCC2, a protein with no known functional association with GABA_B receptors, showed that the transporter and the receptor were mainly segregated on dendritic spines. Thus, the observed close spatial relationship of Kir3.2 and GABA_{B1} likely reflects their functional interaction in this subcellular compartment.

Kir3.2 is preferentially localized to dendritic shafts and spines in hippocampal pyramidal cells

The Kir3.2 is the most abundant subunit of the Kir3 channel in the hippocampus as shown by previous *in situ* hybridization (Kobayashi et al., 1995; Karschin et al., 1996; Liao et al., 1996) and immunocytochemical studies (Liao et al., 1996; Signorini et al., 1997; Inanobe et al., 1999; Koyrakh et al., 2005). It has been further suggested that this subunit plays an essential role in the assembly and surface localization of functional channels (Inanobe et al., 1999; Ma et al., 2002). Accordingly, our results, obtained by using an antibody recognizing the Kir3.2a and Kir3.2c isoforms, but not the ubiquitously expressed Kir3.2b splice variant (Isomoto et al., 1996), show that the Kir3.2 protein was widely distributed in the hippocampus and the immunolabeling was particularly strong in dendritic layers.

At the ultrastructural level, the majority of the Kir3.2 subunits were observed on the extrasynaptic membrane of dendritic shafts and spines and was hardly detectable on somata of pyramidal cells. These immunocytochemical data thus underlie the dominant postsynaptic role of Kir3 channels observed in previous electrophysiological studies (Andrade et al., 1986; Lüscher et al., 1997; Kurachi and Ishii, 2003). Furthermore, the dendritic localization of the subunit corresponds well to the fact that Kir3-mediated currents are significantly larger in dendrites than in somata of hippocampal neurons (Newberry and Nicoll, 1985; Inanobe et al., 1999; Takigawa and Alzheimer, 1999; Chen and Johnston, 2005). This preferential dendritic localization offers an optimal position, on the one hand, for the modulation of the channels by various G-protein-coupled receptors residing in the dendritic compartments (Dournaud et al., 1996; Kia et al., 1996; Lujan et al., 1997; Shigemoto et al., 1997; Kulik et al., 2003). On the other hand, dendritic channels can be efficiently involved in the integration of synaptic inputs. Kir3 channels were shown to contribute to the resting membrane potential on dendrites (Chen and Johnston, 2005) and can thereby modulate the amplification of synaptic potentials by voltage-gated channels (Johnston et al.,

1996). Kir3 channels associated with glutamatergic synapses can counteract excitatory postsynaptic responses by hyperpolarization and by shunting the excitatory synaptic currents (Takigawa and Alzheimer, 2003). Furthermore, after activation by GABA_B receptors, these channels can also act as a brake on NMDA receptor responses by favoring their Mg²⁺ block and resulting in reduced synaptic plasticity (Otmakhova and Lisman, 2004). Conversely, activation of NMDA receptors results in the potentiation of the GABA_B- and Kir3-mediated slow inhibitory synaptic response (Huang et al., 2005) that parallels with the long-term potentiation of excitatory transmission.

In addition to the strong postsynaptic labeling, a low but consistent presynaptic immunoreactivity for Kir3.2 was detected. Similar results were obtained for three subunits, Kir3.1, Kir3.2, and Kir3.3, in various brain regions in previous immunocytochemical studies (Liao et al., 1996; Morishige et al., 1996; Ponce et al., 1996; Drake et al., 1997; Grosse et al., 2003). Although the function of the presynaptic Kir3 channels remains unknown (Lüscher et al., 1997), their proximity to the axonal active zones strongly suggests an involvement in the regulation of neurotransmitter release.

Predominant colocalization of Kir3.2 with GABA_{B1} on dendritic spines of pyramidal cells

The coupling between Kir3 channels and receptors is mediated by G-proteins in a membrane-delimited manner (Pfaffinger et al., 1985; Dascal, 1997; Yamada et al., 1998). Theoretical considerations suggest that the distance between receptor and effector should be small (e.g., <500 nm) (Karschin, 1999) to enable their interaction. Moreover, it was hypothesized that preformed receptor–ion channel complexes could exist ensuring reliable and efficient coupling. The rapid activation of Kir3 channels by GABA_B receptors in response to synaptically released GABA would support this latter hypothesis (Otis et al., 1993). To address the spatial relationship of Kir3.2 and the GABA_B receptors, we used the highly sensitive SDS-digested freeze–fracture replica immunolabeling method, which provides a means for visualizing the distribution of molecules over the surface of the plasma membrane (Hagiwara et al., 2005). The results of this approach revealed that, on dendritic shafts of the pyramidal cells, contacted by GABAergic boutons, ion channels and receptors were mainly segregated, whereas on dendritic spines, contacted by excitatory terminals, a high degree of colustering of the proteins was detected.

The observed distribution of the ion channels and GABA_B

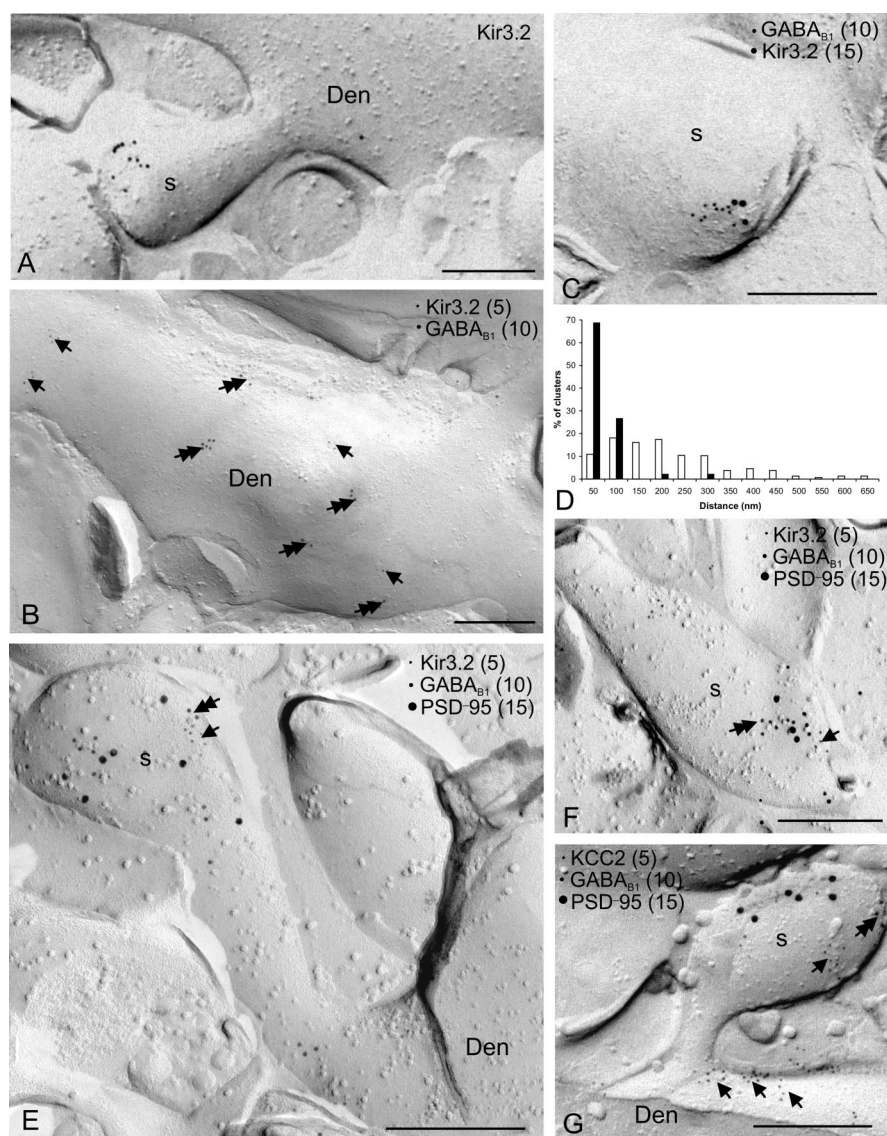


Figure 4. Colocalization of Kir3.2 and GABA_{B1} on dendritic spines of CA1 pyramidal cells. Localization of the Kir3.2 subunit and its colocalization with the GABA_{B1} subunit is demonstrated by the SDS-digested freeze–fracture replica labeling technique. **A**, Immunoparticles for Kir3.2 were found on dendritic spines (s) of principal cells. **B**, Double immunogold labeling for Kir3.2 (5 nm particles; arrows) and GABA_{B1} (10 nm; double arrows) revealed that the two proteins were mainly segregated on dendritic shafts of pyramidal cells (Den). **C**, Double labeling for Kir3.2 (15 nm) and GABA_{B1} (10 nm) showed that the two proteins colocalized on dendritic spines of pyramidal cells (s). **D**, Histogram showing the spatial relationship between clusters of Kir3.2 and GABA_{B1} on dendritic shafts ($n = 302$ clusters; open bars) and on dendritic spines ($n = 90$ clusters; filled bars). Distances were measured between the center of Kir3.2 clusters and the closest GABA_{B1} cluster. Values were allocated to 50-nm-wide bins and expressed as relative frequencies. **E**, **F**, Triple immunolabeling for Kir3.2 (5 nm), GABA_{B1} (10 nm), and PSD-95 (15 nm) demonstrated the colustering of the Kir3.2 (arrows) and GABA_{B1} (double arrows) subunits around the site of the location of the PSD-95, indicating a close localization of Kir3.2–GABA_{B1} to glutamatergic synapses on dendritic spines of pyramidal cell. **G**, The spatial relationship of GABA_B (double arrows) receptors and the functionally unrelated KCC2 (arrows) was also investigated on dendritic spines. Two proteins were found to be preferentially segregated in this subcellular compartment. Scale bars, 0.2 μ m.

receptors on dendritic shafts raises the question how segregated channels are activated. First, the Kir3.2-containing channels may colocalize with and couple to other G-protein-coupled receptors (e.g., adenosine A1, 5-HT_{1A}, D₂) (Andrade et al., 1986; Nicoll, 1988; Liao et al., 1996; Ehrenguber et al., 1997; Lüscher et al., 1997; Takigawa and Alzheimer, 1999). This possibility is supported by the results of electrophysiological experiments in which the GABA_B receptor agonist baclofen evoked Kir3 currents only in a subset of isolated patches of pyramidal cell dendrites, whereas agonists of other metabotropic receptors could elicit

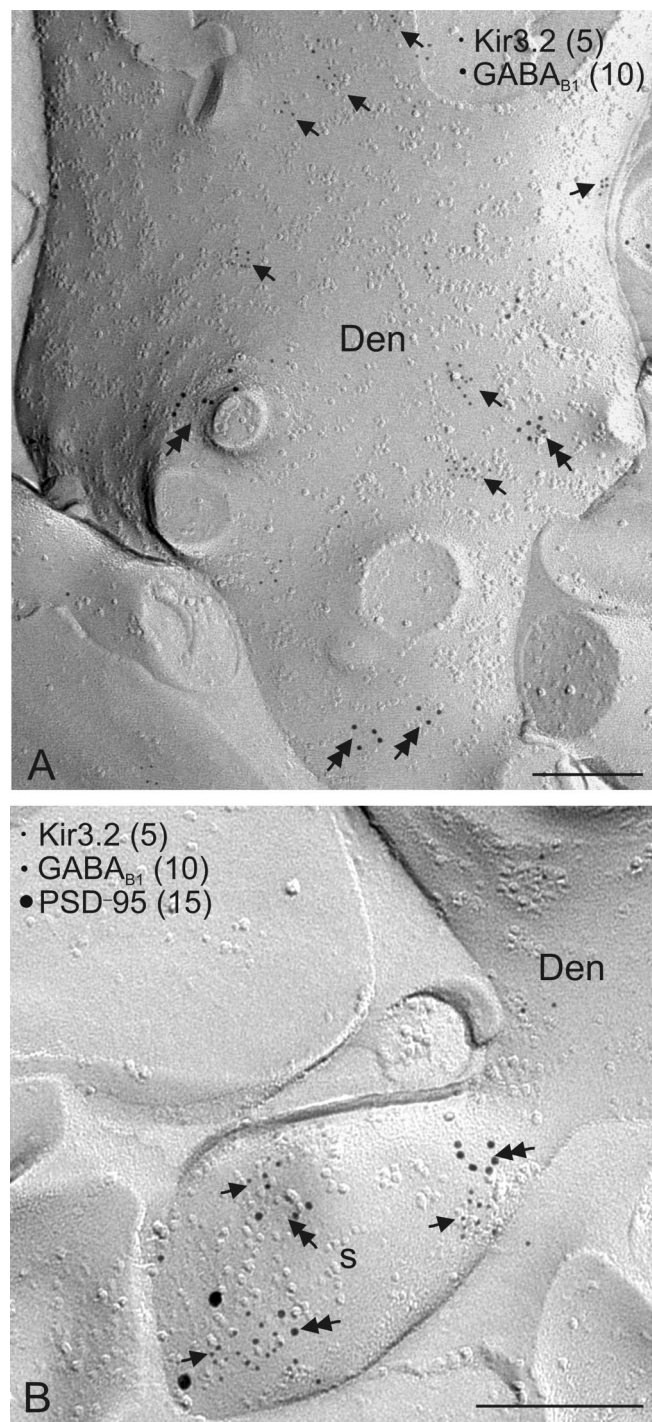


Figure 5. Colocalization of Kir3.2 and GABA_B1 on CA3 pyramidal cells as assessed by the SDS-digested freeze–fracture replica labeling technique. The spatial relationship of Kir3.2 and GABA_B1 was investigated as described in Figure 4. **A, B**, The proteins were found to be mainly segregated on dendritic shafts of pyramidal cells (Den), whereas the channel and the receptor were colocalized on dendritic spines (s) around glutamatergic synapses. Scale bars, 0.2 μ m.

currents in nonresponsive ones (Takigawa and Alzheimer, 1999; Chen and Johnston, 2005). Second, these channels may also be activated by GABA_B receptors. Despite the segregation of Kir3.2 and GABA_B1, the mean distance between molecules may be sufficient for functional interaction (Karschin, 1999), although, in this scenario, the coupling is expected to be less efficient and less reliable. Finally, constitutively active dendritic Kir3 channels

have been observed in CA1 pyramidal cells (Chen and Johnston, 2005). Although the identity and the subunit composition of these ion channels are unclear, they may correspond to a segregated channel population.

It was proposed that GABA_B receptor localization to dendritic spines is important for the modulation of metabotropic glutamate receptors (Hirono et al., 2001; Tabata et al., 2004). However, the intimate spatial relationship of GABA_B receptors and Kir3 channels on dendritic spines around excitatory synapses, observed in this study, is suggestive of a functional coupling of the two proteins and may reflect the existence of preformed complexes. This scenario is further supported by the observation that the functionally unrelated KCC2 and GABA_B1 were mainly found to be segregated in this subcellular compartment. In turn, the high level of colocalization of Kir3.2 and GABA_B1 indicates that the ion channels strategically located to interact with individual glutamatergic synapses are primarily under the control of the inhibitory transmitter GABA spilling over from GABAergic synapses (Isaacson et al., 1993; Kulik et al., 2003; Cryan and Kaupmann, 2005).

In summary, the present study shows that the Kir3.2-containing K⁺ channels are preferentially located on the extrasynaptic membrane of hippocampal pyramidal cells and can be divided into two major populations with different roles in synaptic integration. Kir3 channels on dendritic shafts can mediate the effect of various transmitter systems including subcortical projections that show behavior state-dependent activity (Pace-Schott and Hobson, 2002). In contrast, Kir3 channels on dendritic spines appear to preferentially mediate the effect of GABA released from local feedback and feedforward inhibitory circuits via GABA_B receptors. Thus, this channel population can provide a spatially and temporally well defined control to excitatory transmission by the GABAergic system.

References

- Andrade R, Nicoll RA (1987) Pharmacologically distinct actions of serotonin on single pyramidal neurons of the rat hippocampus recorded in vitro. *J Physiol (Lond)* 394:99–124.
- Andrade R, Malenka RC, Nicoll RA (1986) A G protein couples serotonin and GABA_B receptors to the same channels in hippocampus. *Science* 234:1261–1265.
- Bichet D, Haass FA, Jan LY (2003) Merging functional studies with structures of inward rectifier K⁺ channels. *Nat Rev Neurosci* 4:957–967.
- Chen X, Johnston D (2005) Constitutively active G-protein-gated inwardly rectifying K⁺ channels in dendrites of hippocampal CA1 pyramidal neurons. *J Neurosci* 25:3787–3792.
- Cryan JF, Kaupmann K (2005) Don't worry "B" happy!: a role for GABA_B receptors in anxiety and depression. *Trends Pharmacol Sci* 26:36–43.
- Dascal N (1997) Signalling via the G protein-activated K⁺ channels. *Cell Signal* 9:551–573.
- Dixon AK, Gubituz AK, Ashford ML, Richardson PJ, Freeman TC (1995) Distribution of mRNA encoding the inwardly rectifying K⁺ channel, BIR1 in rat tissues. *FEBS Lett* 374:135–140.
- Dournaud P, Gu YZ, Schonbrunn A, Mazella J, Tannenbaum GS, Beaudet A (1996) Localization of the somatostatin receptor SST2A in the rat brain using a specific anti-peptide antibody. *J Neurosci* 16:4468–4478.
- Drake CT, Bausch SB, Milner TA, Chavkin C (1997) GIRK1 immunoreactivity is present predominantly in dendrites, dendritic spines, and somata in the CA1 region of the hippocampus. *Proc Natl Acad Sci USA* 94:1007–1012.
- Duprat F, Lesage F, Guillemare E, Fink M, Hugnot J-P, Bigay J, Lazdunski M, Romey G, Barhanin J (1995) Heterologous multimeric assembly is essential for K⁺ channel activity of neuronal and cardiac G-protein-activated inward rectifiers. *Biochem Biophys Res Commun* 212:657–663.
- Ehrengruber MU, Doupnik CA, Xu Y, Garvey J, Jasek MC, Lester HA, Davidson N (1997) Activation of heteromeric G protein-gated inward rectifier K⁺ channels overexpressed by adenovirus gene transfer inhibits the ex-

- citability of hippocampal neurons. *Proc Natl Acad Sci USA* 94:7070–7075.
- Gähwiler BH, Brown DA (1985) GABA_B-receptor-activated K⁺ current in voltage-clamped CA3 pyramidal cells in hippocampal cultures. *Proc Natl Acad Sci USA* 82:1558–1562.
- Grosse G, Eulitz D, Thiele T, Pahner I, Schröter S, Takamori S, Grosse J, Wickman K, Tapp R, Weh RW, Ottersen OP, Ahnert-Hilger G (2003) Axonal sorting of Kir3.3 defines a GABA-containing neuron in the CA3 region of rodent hippocampus. *Mol Cell Neurosci* 24:709–724.
- Gulyás AI, Sik A, Payne JA, Kaila K, Freund TF (2001) The KCl cotransporter, KCC2, is highly expressed in the vicinity of excitatory synapses in the rat hippocampus. *Eur J Neurosci* 13:2205–2217.
- Hagiwara A, Fukazawa Y, Deguchi-Tawarada M, Ohtsuka T, Shigemoto R (2005) Differential distribution of release-related proteins in the hippocampal CA3 area as revealed by freeze-fracture replica labeling. *J Comp Neurol* 489:195–216.
- Hille B (1992) *Ionic channels of excitable membranes*. Sunderland, MA: Sinauer.
- Hirono M, Yoshioka T, Konishi S (2001) GABA_B receptor activation enhances mGluR-mediated responses at cerebellar excitatory synapses. *Nat Neurosci* 4:1207–1216.
- Huang C-L, Slesinger P, Casey P, Jan YN, Jan LY (1995) Evidence that direct binding of G_{βγ} to the GIRK1 G protein-gated inwardly rectifying K⁺ channel is important for channel activation. *Neuron* 15:1133–1143.
- Huang CS, Shi S-H, Ule J, Ruggiu M, Barker LA, Darnell RB, Jan YN, Jan LY (2005) Common molecular pathways mediate long-term potentiation of synaptic excitation and slow synaptic inhibition. *Cell* 123:105–118.
- Inanobe A, Ito H, Ito M, Hosoya Y, Kurachi Y (1995) Immunological and physical characterization of the brain G protein-gated muscarinic potassium channel. *Biochem Biophys Res Commun* 217:1238–1244.
- Inanobe A, Yoshimoto Y, Horio Y, Morishige K-I, Hibino H, Matsumoto S, Tokunaga Y, Maeda T, Hata Y, Takai Y, Kurachi Y (1999) Characterization of G-protein-gated K⁺ channels composed of Kir3.2 subunits in dopaminergic neurons of the substantia nigra. *J Neurosci* 19:1006–1013.
- Isaacson JS, Solis JM, Nicoll RA (1993) Local and diffuse synaptic actions of GABA in the hippocampus. *Neuron* 10:165–175.
- Isomoto S, Kondo C, Takahashi N, Matsumoto S, Yamada M, Takumi T, Horio Y, Kurachi Y (1996) A novel ubiquitously distributed isoform of GIRK2 (GIRK2B) enhances GIRK1 expression of the G-protein-gated K⁺ current in *Xenopus* oocytes. *Biochem Biophys Res Commun* 218:286–291.
- Johnston D, Magee JC, Colbert CM, Christie BR (1996) Active properties of neuronal dendrites. *Annu Rev Neurosci* 19:165–186.
- Karschin A (1999) G protein regulation of inwardly rectifying K⁺ channels. *News Physiol Sci* 14:215–220.
- Karschin C, Dismann E, Stühmer W, Karschin A (1996) IRK1–3 and GIRK1–4 inwardly rectifying K⁺ channel mRNAs are differentially expressed in the adult rat brain. *J Neurosci* 16:3559–3570.
- Kaupmann K, Huggel K, Heid J, Flor PJ, Bischoff S, Mickel SJ, McMaster G, Angst C, Bittiger H, Froestl W, Bettler B (1997) Expression cloning of GABA_B receptors uncovers similarity to metabotropic glutamate receptors. *Nature* 386:239–246.
- Kaupmann K, Schuler V, Mosbacher J, Bischoff S, Bittiger H, Heid J, Froestl W, Leonhard S, Pfaff T, Karschin A, Bettler B (1998) Human γ-aminobutyric acid type B receptors are differentially expressed and regulate inwardly rectifying K⁺ channels. *Proc Natl Acad Sci USA* 95:14991–14996.
- Kia HK, Miquel MC, Brisorgueil MJ, Daval G, Riad M, El Mestikawy S, Hamon M, Verge D (1996) Immunocytochemical localization of serotonin 1A receptors in the central nervous system. *J Comp Neurol* 365:289–305.
- Kobayashi T, Ikeda K, Ichikawa T, Abe S, Togashi S, Kumanishi T (1995) Molecular cloning of a mouse G-protein-activated K⁺ channel (mGIRK1) and distinct distribution of three GIRK (GIRK1, 2 and 3) mRNAs in mouse brain. *Biochem Biophys Res Commun* 208:1166–1173.
- Kofuji P, Davidson N, Lester HA (1995) Evidence that neuronal G-protein-gated inwardly rectifying K⁺ channels are activated by G_{βγ} subunits and function as heteromultimers. *Proc Natl Acad Sci USA* 92:6542–6546.
- Koyrakh L, Lujan R, Colon J, Karschin C, Kurachi Y, Karschin A, Wickman K (2005) Molecular and cellular diversity of neuronal G-protein-gated potassium channels. *J Neurosci* 25:11468–11478.
- Krapivinsky G, Gordon EA, Wickman K, Velimirovic B, Krapivinsky L, Clapham DE (1995) The G-protein-gated atrial K⁺ channel I_{KACH} is a heteromultimer of two inwardly rectifying K⁺-channel proteins. *Nature* 374:135–141.
- Kulik A, Nakadate K, Nyiri G, Notomi T, Malitschek B, Bettler B, Shigemoto R (2002) Distinct localization of GABA_B receptors relative to synaptic sites in the rat cerebellum and ventrobasal thalamus. *Eur J Neurosci* 15:291–307.
- Kulik A, Vida I, Lujan R, Haas CA, López-Bendito G, Shigemoto R, Frotscher M (2003) Subcellular localization of metabotropic GABA_B receptor subunits GABA_{B1a/b} and GABA_{B2} in the rat hippocampus. *J Neurosci* 23:11026–11035.
- Kurachi Y, Ishii M (2003) Cell signalling control of the G protein-gated potassium channel and its subcellular localization. *J Physiol (Lond)* 554:285–294.
- Leaney JL (2003) Contribution of Kir3.1, Kir3.2A and Kir3.2C subunits to native G protein-gated inwardly rectifying potassium currents in cultured hippocampal neurons. *Eur J Neurosci* 18:2110–2118.
- Lesage F, Duprat F, Fink M, Guillemare E, Coppola T, Lazdunski M, Hugnot J-P (1994) Cloning provides evidence for a family of inward rectifier and G-protein coupled K⁺ channels in the brain. *FEBS Lett* 353:37–42.
- Lesage F, Guillemare E, Fink M, Duprat F, Heurteaux C, Fosset M, Roemy G, Barhanin J, Lazdunski M (1995) Molecular properties of neuronal G-protein-activated inwardly rectifying K⁺ channels. *J Biol Chem* 270:28660–28667.
- Liao YJ, Jan YN, Jan LY (1996) Heteromultimerization of G-protein-gated inwardly rectifying K⁺ channel proteins GIRK1 and GIRK2 and their altered expression in *weaver* brain. *J Neurosci* 16:7137–7150.
- Lujan R, Roberts JDB, Shigemoto R, Somogyi P (1997) Differential plasma membrane distribution of metabotropic glutamate receptors mGluR1a, mGluR2, and mGluR5, relative to neurotransmitter release sites. *J Chem Neuroanat* 13:219–241.
- Lüscher C, Jan LY, Stöffel M, Malenka RC, Nicoll RA (1997) G protein-coupled inwardly rectifying K⁺ channels (GIRKs) mediate postsynaptic but not presynaptic transmitter actions in hippocampal neurons. *Neuron* 19:687–695.
- Ma D, Zerangue N, Raab-Graham K, Fried SR, Jan YN, Jan LY (2002) Diverse trafficking patterns due to multiple traffic motifs in G protein-activated inwardly rectifying potassium channels from brain and heart. *Neuron* 33:715–729.
- Marker CL, Lujan R, Loh HH, Wickman K (2005) Spinal G-protein-gated potassium channels contribute in a dose-dependent manner to the analgesic effect of μ- and δ- but not κ-opioids. *J Neurosci* 25:3551–3559.
- Mihara S, North RA, Surprenant A (1987) Somatostatin increases an inwardly rectifying potassium conductance in guinea pig submucous plexus neurons. *J Physiol (Lond)* 390:335–355.
- Morishige KI, Inanobe A, Takahashi N, Yoshimoto Y, Kurachi H, Miyake A, Tokunaga Y, Maeda T, Kurachi Y (1996) G protein-gated K⁺ channel (GIRK1) protein is expressed presynaptically in the paraventricular nucleus of the hypothalamus. *Biochem Biophys Res Commun* 220:300–305.
- Nehring RB, Wischmeyer E, Döring F, Veh RW, Sheng M, Karschin A (2000) Neuronal inwardly rectifying K⁺ channels differentially couple to PDZ proteins of the PSD-95/SAP90 family. *J Neurosci* 20:156–162.
- Newberry NR, Nicoll RA (1985) Comparison of the action of baclofen with gamma-aminobutyric acid on rat hippocampal pyramidal cells in vitro. *J Physiol (Lond)* 360:161–185.
- Nicoll RA (1988) The coupling of neurotransmitter receptors to ion channels in the brain. *Science* 241:545–551.
- North RA, Williams JT, Surprenant A, Christie MJ (1987) μ and δ receptors belong to a family of receptors that are coupled to potassium channels. *Proc Natl Acad Sci USA* 84:5487–5491.
- Otis TS, De Koninck Y, Mody I (1993) Characterization of synaptically elicited GABA_B responses using patch-clamp recordings in rat hippocampal slices. *J Physiol (Lond)* 463:391–407.
- Otmakhova NA, Lisman JE (2004) Contribution of I_h and GABA_B to synaptically induced afterhyperpolarizations in CA1: a brake on the NMDA response. *J Neurophysiol* 92:2027–2039.
- Pace-Schott EF, Hobson JA (2002) The neurobiology of sleep: genetics, cellular physiology and subcortical networks. *Nat Rev Neurosci* 3:591–605.
- Pfaffinger PJ, Martin JM, Hunter D, Nathanson NM, Hille B (1985) GTP-binding proteins couple cardiac muscarinic receptors to a K⁺ channel. *Nature* 317:536–538.

- Ponce A, Bueno E, Kentros C, de Miera EV-S, Chow A, Hillman D, Chen S, Zhu L, Wu MB, Rudy B, Thornhill WB (1996) G-protein-gated inward rectifier K⁺ channel proteins (GIRK1) are present in the soma and dendrites as well as in nerve terminals of specific neurons in the brain. *J Neurosci* 16:1990–2001.
- Schreibmayer W, Dessauer CW, Vorobiov D, Gilman AG, Lester HA, Davidson N, Dascal N (1996) Inhibition of an inwardly rectifying K⁺ channels by G-protein α -subunits. *Nature* 380:624–627.
- Schuler V, Lüscher C, Blanchet C, Klix N, Sansig G, Klebs K, Schmutz M, Heid J, Gentry C, Urban L, Fox A, Spooren W, Jatton AL, Vigouret J, Pozza M, Kelly PH, Mosbacher J, Froestl W, Kaslin E, Korn R, et al. (2001) Epilepsy, hyperalgesia, impaired memory, and loss of pre- and postsynaptic GABA(B) responses in mice lacking GABA(B1). *Neuron* 31:47–58.
- Sharon D, Vorobiov D, Dascal N (1997) Positive and negative coupling of the metabotropic glutamate receptors to a G protein-activated K⁺ channel, GIRK, in *Xenopus* oocytes. *J Gen Physiol* 109:477–490.
- Shigemoto R, Kinoshita A, Wada E, Nomura S, Ohishi H, Takada M, Flor PJ, Neki A, Nakanishi S, Mizuno N (1997) Differential presynaptic localization of metabotropic glutamate receptor subtypes in the rat hippocampus. *J Neurosci* 17:7503–7522.
- Signorini S, Liao YJ, Duncan SA, Jan LY, Stöffel M (1997) Normal cerebellar development but susceptibility to seizures in mice lacking G protein-coupled, inwardly rectifying K⁺ channel GIRK2. *Proc Natl Acad Sci (USA)* 94:923–927.
- Slesinger PA, Patil N, Liao J, Jan YN, Jan LY, Cox DR (1996) Functional effects of the mouse *weaver* mutation on G protein-gated inwardly rectifying K⁺ channels. *Neuron* 16:321–331.
- Sodickson DL, Bean BP (1996) GABA_B receptor-activated inwardly rectifying potassium current in dissociated hippocampal CA3 neurons. *J Neurosci* 16:6374–6385.
- Spaschus A, Lentjes K-U, Wischmeyer E, Dissmann E, Karschin C, Karschin A (1996) A G-protein-activated inwardly rectifying K⁺ channel (GIRK4) from human hippocampus associates with other GIRK channels. *J Neurosci* 16:930–938.
- Stanfield PR, Nakajima S, Nakajima Y (2002) Constitutively active and G-protein coupled inward rectifier K⁺ channels: Kir2.0 and Kir3.0. *Rev Physiol Biochem Pharmacol* 145:47–179.
- Tabata T, Araishi K, Hashimoto K, Hashimoto Y, van der Putten H, Bettler B, Kano M (2004) Ca²⁺ activity at GABA_B receptors constitutively promotes metabotropic glutamate signalling in the absence of GABA. *Proc Natl Acad Sci USA* 101:16952–16957.
- Tagigawa T, Alzheimer C (1999) G protein-activated inwardly rectifying K⁺ (GIRK) currents in dendrites of rat neocortical pyramidal cells. *J Physiol (Lond)* 517:385–390.
- Tagigawa T, Alzheimer C (2002) Phasic and tonic attenuation of EPSPs by inward rectifier K⁺ channels in rat hippocampal pyramidal cells. *J Physiol (Lond)* 539:67–75.
- Tagigawa T, Alzheimer C (2003) Interplay between activation of GIRK current and deactivation of I_h modifies temporal integration of excitatory input in CA1 pyramidal cells. *J Neurophysiol* 89:2238–2244.
- Tanaka J-I, Matsuzaki M, Tarusawa E, Momiyama A, Molnar E, Kasai H, Shigemoto R (2005) Number and density of AMPA receptors in single synapses in immature cerebellum. *J Neurosci* 25:799–807.
- Torreccilla M, Marker CL, Cintora SC, Stöffel M, Williams JT, Wickman K (2002) G-protein-gated potassium channels containing Kir3.2 and Kir3.3 subunits mediate the acute inhibitory effects of opioids on locus ceruleus neurons. *J Neurosci* 22:4328–4334.
- Trussell LO, Jackson MB (1987) Dependence of an adenosine-activated potassium current on a GTP-binding protein in mammalian central neurons. *J Neurosci* 7:3306–3316.
- Wickman K, Clapham DE (1995) Ion channel regulation by G proteins. *Physiol Rev* 75:865–885.
- Wickman KD, Iniguez-Lluhl JA, Davenport PA, Taussig R, Krapivinsky GB, Linder ME, Gilman AG, Clapham DE (1994) Recombinant G-protein $\beta\gamma$ -subunits activate the muscarinic-gated atrial potassium channel. *Nature* 368:255–257.
- Wischmeyer E, Döring F, Wischmeyer E, Spaschus A, Thomzig A, Veh R, Karschin A (1997) Subunit interactions in the assembly of neuronal Kir3.0 inwardly rectifying K⁺ channels. *Mol Cell Neurosci* 9:194–206.
- Yamada M, Inanobe A, Kurachi Y (1998) G protein regulation of potassium ion channels. *Pharmacol Rev* 50:723–757.

6.2. The GABA_{B1a} isoform mediates heterosynaptic depression at hippocampal mossy fiber synapses

Guetg N*, Seddik R*, Vigot R, Turecek R, Gassmann M, Vogt KE, Bräuner-Osborne H, Shigemoto R, Kretz O, Frotscher M, Kulik A, Bettler B

The Journal of Neuroscience 2009; 29:1414-23

*Authors contributed equally to this work.

GABA_B receptors are composed of GABA_{B1a} and GABA_{B1b} subunit isoforms forming functional receptors together with the GABA_{B2} subunit. In this publication, the differential subcellular localization of GABA_B receptor subtypes in the CA3 region of the hippocampus was investigated. It was of particular interest to understand to what extent GABA_{B(1a,2)} and GABA_{B(1b,2)} receptors inhibit glutamate release in response to physiological activation. Because of the lack of isoform specific antibodies, mice deficient for either GABA_{B1a} (1a^{-/-} mice) or GABA_{B1b} (1b^{-/-} mice) were used. Using preembedding electron microscopy, it was first demonstrated that the GABA_B receptor is present pre- and postsynaptically at mossy fiber (MF)–CA3 pyramidal neuron synapses. While GABA_{B(1a,2)} is the predominant receptor localized on glutamatergic MF terminals, GABA_{B(1b,2)} is more abundant in spines and dendritic shafts of pyramidal neurons. This is in agreement with findings at other glutamatergic synapses (Vigot et al., 2006; Ulrich et al., 2007). Furthermore, the subsynaptic distribution of GABA_{B1} isoforms at the MF-CA3 pyramidal neuron synapse was studied. In 1a^{-/-} mice, significantly lower levels of immunogold particles were found to be localized over the presynaptic membrane specialization compared to wild-type (WT) mice. Postsynaptically, an accumulation of immunoparticles in vicinity of the postsynaptic density was observed. However, no difference in the spatial distribution between WT, 1a^{-/-} and 1b^{-/-} mice was found.

Using electrophysiological whole-cell patch-clamp recordings, the contribution of GABA_{B1a} and GABA_{B1b} to functional pre- and postsynaptic GABA_B receptors at the MF-CA3 pyramidal neuron synapse was assessed. In a first series of experiments GABA_B receptors

were activated pharmacologically with saturating concentrations of baclofen. In $1a^{-/-}$ mice, the inhibition of EPSCs mediated by presynaptic $GABA_{B(1b,2)}$ receptors was reduced by 50% compared to WT mice. In contrast, presynaptic $GABA_B$ receptors were fully functional in $1b^{-/-}$ mice. Postsynaptically, pharmacological activation of $GABA_B$ receptors elicited similar outward K^+ -currents in $1a^{-/-}$ and $1b^{-/-}$ mice. These currents were reduced compared to WT mice. Surprisingly, the pharmacological activation of pre- as well as postsynaptic $GABA_B$ receptors at MF-CA3 pyramidal neuron synapses did not however entirely reproduce the spatial segregation observed in the ultrastructural analysis.

The physiological activation of $GABA_B$ receptors at the MF-CA3 pyramidal neuron synapse was studied next. For this purpose, heterosynaptic depression in WT, $1a^{-/-}$ and $1b^{-/-}$ mice was examined. The results obtained indicate, that only $GABA_{B(1a,2)}$ receptors are responsible for presynaptic inhibition of glutamate release in response to endogenously released GABA from neighboring interneurons. The spatial segregation of $GABA_{B1}$ subunit isoforms at mossy fiber terminals is therefore sufficient to produce a strictly subtype-specific response. In addition, postsynaptic $GABA_B$ receptor activation by endogenously released GABA was investigated. Late IPSC were only detectable in WT mice but not in $1a^{-/-}$ and $1b^{-/-}$ mice respectively. This implies that both $GABA_{B(1a,2)}$ and $GABA_{B(1b,2)}$ contribute to postsynaptic responses under physiological conditions.

Statement of personal contribution:

- Ultrastructural experiments and corresponding quantification
- Western blot analysis
- Contribution to the preparation of the manuscript
- Design of figures

The GABA_{B1a} Isoform Mediates Heterosynaptic Depression at Hippocampal Mossy Fiber Synapses

Nicole Guetg,^{1,3*} Riad Seddik,^{1*} Réjan Vigot,¹ Rostislav Turecek,¹ Martin Gassmann,¹ Kaspar E. Vogt,² Hans Bräuner-Osborne,^{1,4} Ryuichi Shigemoto,^{5,6,7} Oliver Kretz,³ Michael Frotscher,³ Ákos Kulik,³ and Bernhard Bettler¹

¹Department of Biomedicine, Institute of Physiology, Pharmazentrum, and ²Division of Pharmacology and Neurobiology, Biozentrum, University of Basel, 4056 Basel, Switzerland, ³Institute of Anatomy and Cell Biology, Department of Neuroanatomy, University of Freiburg, 79104 Freiburg, Germany, ⁴Department of Medicinal Chemistry, Faculty of Pharmaceutical Sciences, University of Copenhagen, 2100 Copenhagen, Denmark, ⁵Division of Cerebral Structure, National Institute for Physiological Sciences, and ⁶Department of Physiological Sciences, The Graduate University of Advanced Studies (Sokendai), Myodaiji, Okazaki 444-8787, Japan, and ⁷Solution Oriented Research for Science and Technology, Japan Science and Technology Corporation, Kawaguchi 332-0012, Japan

GABA_B receptor subtypes are based on the subunit isoforms GABA_{B1a} and GABA_{B1b}, which associate with GABA_{B2} subunits to form pharmacologically indistinguishable GABA_{B(1a,2)} and GABA_{B(1b,2)} receptors. Studies with mice selectively expressing GABA_{B1a} or GABA_{B1b} subunits revealed that GABA_{B(1a,2)} receptors are more abundant than GABA_{B(1b,2)} receptors at glutamatergic terminals. Accordingly, it was found that GABA_{B(1a,2)} receptors are more efficient than GABA_{B(1b,2)} receptors in inhibiting glutamate release when maximally activated by exogenous application of the agonist baclofen. Here, we used a combination of genetic, ultrastructural and electrophysiological approaches to analyze to what extent GABA_{B(1a,2)} and GABA_{B(1b,2)} receptors inhibit glutamate release in response to physiological activation. We first show that at hippocampal mossy fiber (MF)-CA3 pyramidal neuron synapses more GABA_{B1a} than GABA_{B1b} protein is present at presynaptic sites, consistent with the findings at other glutamatergic synapses. In the presence of baclofen at concentrations $\geq 1 \mu\text{M}$, both GABA_{B(1a,2)} and GABA_{B(1b,2)} receptors contribute to presynaptic inhibition of glutamate release. However, at lower concentrations of baclofen, selectively GABA_{B(1a,2)} receptors contribute to presynaptic inhibition. Remarkably, exclusively GABA_{B(1a,2)} receptors inhibit glutamate release in response to synaptically released GABA. Specifically, we demonstrate that selectively GABA_{B(1a,2)} receptors mediate heterosynaptic depression of MF transmission, a physiological phenomenon involving transsynaptic inhibition of glutamate release via presynaptic GABA_B receptors. Our data demonstrate that the difference in GABA_{B1a} and GABA_{B1b} protein levels at MF terminals is sufficient to produce a strictly GABA_{B1a}-specific effect under physiological conditions. This consolidates that the differential subcellular localization of the GABA_{B1a} and GABA_{B1b} proteins is of regulatory relevance.

Key words: GABA(B); GABA-B; metabotropic; hippocampus; presynaptic inhibition; heteroreceptor

Introduction

GABA_B receptors are the G-protein coupled receptors for γ -aminobutyric acid (GABA), the main inhibitory neurotransmitter in the CNS. They have been implicated in a variety of disorders, including cognitive impairments, anxiety, depression and epilepsy (Calver et al., 2002; Bettler et al., 2004). Presynaptic GABA_B receptors inhibit neurotransmitter release via the inhibition of Ca²⁺ channels and second-messenger-mediated effects

downstream of Ca²⁺ entry (Scanziani et al., 1992; Jarolimek and Misgeld, 1997; Yamada et al., 1999; Sakaba and Neher, 2003). They are commonly divided into autoreceptors and heteroreceptors depending on whether they control the release of GABA or other neurotransmitters, respectively. Postsynaptic GABA_B receptors activate Kir3-type K⁺ channels, which induces slow inhibitory potentials and mediates shunting inhibition (Lüscher et al., 1997). The physiological functions of GABA_B receptors have been mostly inferred from electrophysiological experiments in which the receptors were pharmacologically activated by exogenous application of the agonist baclofen. Physiological activation of GABA_B receptors usually requires strong stimulus intensities, suggesting that pooling of synaptically released GABA is required to activate them (Isaacson et al., 1993; Scanziani, 2000). This agrees with ultrastructural data demonstrating that most GABA_B receptors are located distant from release sites (López-Bendito et al., 2004; Lacey et al., 2005; Kulik et al., 2006). A tonic activation of GABA_B receptors through ambient GABA was also observed, which may partly explain their predominantly extrasynaptic lo-

Received Aug. 5, 2008; revised Dec. 2, 2008; accepted Dec. 31, 2008.

This work was supported by Neurex (B.B., M.F.), the Swiss Science Foundation (3100A0-117816; B.B.), and the Deutsche Forschungsgemeinschaft Sonderforschungsbereich 505/780 (A.K., M.F.). We thank A. Schneider, S. Nestel, and B. Joch for technical assistance, V. Besseyrias for breeding and genotyping of mice, and J. Tiao and D. Ulrich for comments on this manuscript.

The authors declare no competing financial interests.

*N.G. and R.S. contributed equally to this work.

Correspondence should be addressed to either of the following: Bernhard Bettler, Department of Biomedicine, Institute of Physiology, Pharmazentrum, University of Basel, CH-4056 Basel, Switzerland, E-mail: bernhard.bettler@unibas.ch; or Ákos Kulik, Institute of Anatomy and Cell Biology, Department of Neuroanatomy, University of Freiburg, Albertstrasse 17, D-79104 Freiburg, Germany, E-mail: akos.kulik@anat.uni-freiburg.de.

DOI:10.1523/JNEUROSCI.3697-08.2009

Copyright © 2009 Society for Neuroscience 0270-6474/09/291414-10\$15.00/0

calization as well (Lei and McBain, 2003; Price et al., 2005; Liu et al., 2006).

GABA_B receptors are heteromers composed of GABA_{B1} and GABA_{B2} subunits (Calver et al., 2002; Bettler et al., 2004). The only molecular distinction in the GABA_B receptor system is based on the subunit isoforms GABA_{B1a} and GABA_{B1b}, which differ in their ectodomains by a pair of “sushi domains” that are unique to GABA_{B1a} (Hawrot et al., 1998). Heteromeric GABA_{B(1a,2)} and GABA_{B(1b,2)} receptors do not exhibit pharmacological differences and couple to the same effector systems in transfected cells. To address the reason for the existence of two receptor subtypes we generated GABA_{B1a}^{-/-} (1a^{-/-}) and GABA_{B1b}^{-/-} (1b^{-/-}) mice, which express either one or the other GABA_{B1} subunit isoform. Pharmacological studies with these mice suggest that GABA_{B1a} and GABA_{B1b} differentially influence synaptic functions, primarily as a result of their distinct distributions to axonal and dendritic compartments (Ulrich and Bettler, 2007). In principle, since GABA_{B1a} and GABA_{B1b} subunits are independently regulated at the transcriptional level (Steiger et al., 2004), this allows for dynamically adjustable GABA_B signaling at axonal and dendritic effectors. However, to clearly establish a regulatory significance for GABA_B receptor subtypes, it needs to be demonstrated that they not only yield differential effects in response to pharmacological activation, but also in response to physiological activation (Huang, 2006). A physiological phenomenon proposed to rely on the endogenous activation of GABA_B heteroreceptors is heterosynaptic depression (Isaacson et al., 1993; Vogt and Nicoll, 1999; Chandler et al., 2003). Here, we studied heterosynaptic depression at MF-CA3 pyramidal neuron synapses to address to what extent the two GABA_B receptor subtypes inhibit glutamate release in response to activation by synaptically released GABA.

Materials and Methods

Mutant mouse strains. The generation of 1a^{-/-} and 1b^{-/-} mice was described previously (Vigot et al., 2006). For control experiments we additionally used GABA_{B1}-deficient (1^{-/-}) mice that completely lack GABA_{B1} protein (Schuler et al., 2001). Homozygous mutant mice and wild-type (WT) littermate mice were obtained by breeding heterozygous mice on a pure inbred BALB/c genetic background. All animal experiments were subjected to institutional review and approved by the veterinary office of Basel-Stadt.

Pre-embedding immunocytochemistry and quantitative analysis. Pre-embedding GABA_{B1} immunogold labeling and electron microscopy was done as described, using affinity-purified guinea pig polyclonal antiserum B62 raised against the C-terminal 103 amino acid residues of GABA_{B1a} and GABA_{B1b} (Kulik et al., 2006). Light microscopy confirmed that the B62 antiserum immunostains WT, 1a^{-/-}, and 1b^{-/-} hippocampal sections, but not 1^{-/-} sections (data not shown). Pre-embedding electron microscopy showed a reduction of the immunogold particle density by 86% in 1^{-/-} hippocampal sections compared with WT sections, which agrees well with earlier control experiments where the reduction of immunogold particles in 1^{-/-} sections was 88% (Vigot et al., 2006). Immunogold particles that nonspecifically labeled 1^{-/-} sections were approximately equally distributed over presynaptic and postsynaptic membranes, as described (Vigot et al., 2006). Pre-embedding electron microscopy of WT, 1a^{-/-}, and 1b^{-/-} mice (8–12 weeks old, *n* = 3 per genotype) included the analysis of 10 different MF boutons per mouse. MF boutons were identified by their large size (3–6 μm in diameter), the dense packing with synaptic vesicles and their contacts with at least 2 spines. For each MF bouton we examined at least 4 consecutive sections. Only immunogold particles at the plasma membrane (closer than 20 nm) of morphologically identifiable large MF boutons and their postsynaptic structures were analyzed. The postsynaptic distribution of GABA_{B1} protein relative to asymmetrical, putative glutamatergic synapses was determined by measuring the distance between

each immunogold particle and the edge of the nearest synapse along the surface of spines. Immunogold particles were allocated to 60 nm wide bins, followed by calculating the relative abundance in each bin. The experimenter was blind to the genotype of the mice.

Immunoblot quantification. The ratio of GABA_{B1a} to GABA_{B1b} protein in the CA3 region of the hippocampus was determined by immunoblot analysis using rabbit polyclonal GABA_{B1} antiserum Ab174.1 raised against the C-terminal domain of GABA_{B1a} and GABA_{B1b} (Vigot et al., 2006). Scanned immunoblots were quantified using Scion Image software (Scion).

Slice preparation and electrophysiology. Hippocampal slices were prepared from 21- to 35-d-old mice using standard procedures (Vigot et al., 2006). Parasagittal slices (300 μm thick) were cut in ice-cold artificial CSF (ACSF) containing (in mM) 124 NaCl, 2.7 KCl, 1.3 MgCl₂, 2 CaCl₂, 1.24 NaH₂PO₄, 26 NaHCO₃, 18 glucose, 2.25 ascorbate, pH 7.3, equilibrated with 95% O₂/5% CO₂. Slices were kept in oxygenated ACSF at 35°C for at least 45 min before recording. Visualized whole-cell patch-clamp recording was used to investigate presynaptic and postsynaptic GABA_B receptor functions. Holding currents and excitatory synaptic responses were recorded at 30–32°C from the somata of CA3 pyramidal neurons visualized using an infrared-sensitive camera (Till Photonics) and differential interference contrast optics (BX51WI; Olympus). Drugs were applied by superfusion into the recording chamber.

EPSCs were recorded with electrodes (~5 MΩ) filled with a solution containing (in mM): 140 Cs-gluconate, 10 HEPES, 10 phosphocreatine, 5 QX-314, 4 Mg-ATP, 0.3 Na-GTP, at pH 7.25 with CsOH, 285 mOsm. EPSCs were elicited by voltage pulses (100 μs, 2–5 V stimuli) delivered through a bipolar Pt-Ir electrode (25 μm in diameter) placed in the stratum lucidum. MF EPSCs were identified by the presence of a frequency-dependent short-term facilitation. EPSCs were measured at -70 mV in the presence of 100 μM picrotoxin. Presynaptic GABA_B and adenosine receptors were activated by bath application of baclofen (50 μM) and adenosine (100 μM), respectively. GABA_B receptors were inhibited by application of the antagonist CGP54626A (1 μM). For the presynaptic dose-response experiments, baclofen at different concentrations (0.1, 1 and 50 μM) was bath applied for 5 min at 10 min intervals.

To record postsynaptic Kir3-type K⁺ currents, patch pipettes were filled with a solution containing (in mM): 140 K-gluconate, 5 HEPES, 2 MgCl₂, 1.1 EGTA, 2 Na₂-ATP, 5 phosphocreatine, 0.6 Tris-GTP, at pH 7.25 with KOH, 285 mOsm. Kir3-type K⁺ currents induced by baclofen (100 μM) or adenosine (100 μM) were elicited at -50 mV in the presence of tetrodotoxin (TTX, 1 μM). For concentration-response experiments we applied baclofen solutions (0.3–100 μM) for 30 s using the fast gravitation driven application system WAS-02 (Dittert et al., 2006). The inner diameter of the application tube was 300 μm. The distance between the mouth of the tube and the soma of the neuron was ~400 μm. GABA_A- and GABA_B-mediated IPSCs (early and late IPSCs, respectively) were recorded with a solution containing (in mM) 124 K-gluconate, 16 KCl, 5 HEPES, 2 MgCl₂, 1.1 EGTA, 2 MgATP, 3 Na₃GTP, pH 7.25. IPSCs were elicited at -60 mV by 100 μs pulses (3 stimuli at 100 Hz) in the presence of kynurenic acid (2 mM), DNQX (10 μM), naloxone (10 μM) and 8-cyclopentyl-1,3-dipropylxanthine (DPCPX, 1 μM) to block glutamate, opioid and A1 adenosine receptors.

GABA_B-mediated heterosynaptic depression at MF synapses was studied by recording field EPSPs (fEPSPs) in the stratum lucidum (Vogt and Nicoll, 1999; Chandler et al., 2003). The occurrence of heterosynaptic depression is not critically dependent on the temperature, as no significant differences were previously observed between experiments at room temperature and at 34°–36°C (Vogt and Nicoll, 1999). We therefore recorded fEPSPs at room temperature, using low resistance glass pipettes filled with ACSF. Stimulating electrodes filled with ACSF were positioned into the dentate gyrus, and MF responses elicited by 100 μs pulses. MF-evoked fEPSPs were identified through their characteristic short-term plasticity and their sensitivity to the group II mGluR agonist (2S,2'R,3'R)-2-(2',3'-dicarboxycyclopropyl)-glycine (DCG-IV, 2 μM) (Kamiya et al., 1996). Heterosynaptic depression was measured in the presence of naloxone (10 μM) and DPCPX (1 μM) to avoid interference from presynaptic opioid and A1 adenosine receptors, respectively (Weiskopf et al., 1993; Manzoni et al., 1994; Cunha, 2008). Under these con-

ditions heterosynaptic depression was significantly reduced by the GABA_B antagonist CGP54626A (2 μ M). Data were acquired with an Axopatch 200B (Molecular Devices), filtered at 2 kHz and digitized at 10 kHz using a Digidata 1322A Interface (Molecular Devices) driven by pClamp 9.2 software (Molecular Devices). Whole-cell currents and field potentials were analyzed using Clampfit 9.2 software (Molecular Devices). Baclofen and CGP54626A were from Novartis Pharma. Naloxone, DNQX, DPCPX, and DCG-IV were from Tocris Cookson, TTX from Latoxan. All other reagents were from Sigma-Aldrich. Most recordings were made and analyzed in blind. All values are means \pm SEM.

Results

Presynaptic versus postsynaptic distribution of GABA_{B1} isoforms at MF-CA3 pyramidal neuron synapses

Before addressing the contribution of GABA_B receptor subtypes to presynaptic inhibition at MF terminals, we determined the GABA_{B1a} and GABA_{B1b} distribution at presynaptic and postsynaptic sites. We performed pre-embedding immunogold electron microscopy in the hippocampal CA3 stratum lucidum of WT, 1a^{-/-}, and 1b^{-/-} mice, using a pan GABA_{B1} antibody recognizing GABA_{B1a} and GABA_{B1b}. MF-CA3 pyramidal neuron synapses within large MF boutons were identified at the ultrastructural level as asymmetrical synapses at the spines of pyramidal neurons. In WT mice GABA_{B1} protein was present at presynaptic and postsynaptic elements of MF-CA3 pyramidal neuron synapses (Fig. 1A–C). 19.3 \pm 10.7% of all counted immunogold particles were localized at synaptic and extrasynaptic sites of MF boutons, while the remaining 80.7 \pm 10.7% were associated with spines and proximal dendritic shafts of pyramidal neurons (Fig. 1J). A similar distribution was reported for the MF-CA3 pyramidal neuron synapse in rat brain (Kulik et al., 2003). In 1a^{-/-} mice, 92.7 \pm 2.1% of all immunogold particles were observed on spines and dendritic shafts of pyramidal neurons, indicating that GABA_{B1b} protein mainly localizes to postsynaptic elements (Fig. 1D–F, J). In contrast, in 1b^{-/-} mice 55.3 \pm 4.6% of all immunogold particles were associated with the presynaptic membrane of MF boutons, demonstrating that GABA_{B1a} protein is slightly more abundant at presynaptic elements (Fig. 1G–I). Strikingly, the ratios of pre- to postsynaptic immunogold particles in the different genotypes were similar at MF-CA3 pyramidal neuron synapses (ratios for WT: 0.24, 1a^{-/-}: 0.08, 1b^{-/-}: 1.24) and CA3-CA1 synapses (ratios for WT: 0.31, 1a^{-/-}: 0.17, 1b^{-/-}: 1.61; (Vigot et al., 2006)). Quantification from immunoblots indicates an overall GABA_{B1a} to GABA_{B1b} protein ratio of 0.60 \pm 0.04 ($n = 4$ mice, $p < 0.01$, one sample Student's *t* test) in the CA3 region of the hippocampus (data not shown). Considering this ratio and the synaptic distribution of immunogold particles, we approximately estimate that the GABA_{B1a} to GABA_{B1b} protein ratio at presynaptic and postsynaptic sites is 4.5:1 and 1:3.5, respectively. Importantly, we did not observe any MF boutons and associated postsynaptic spines without specific immunogold particle labeling, suggesting that most, if not all, MF synapses express GABA_B receptors.

Subsynaptic distribution of GABA_{B1} isoforms in presynaptic and postsynaptic elements of MF-CA3 pyramidal neuron synapses

We next studied the distribution of GABA_{B1} protein relative to synaptic specializations at MF-CA3 pyramidal neuron synapses. We first determined the percentage of GABA_{B1} immunogold particles in MF boutons that are present at presynaptic membranes opposite to postsynaptic densities (PSDs). In WT and 1b^{-/-} mice 22% of all presynaptic GABA_{B1} immunogold particles were localized opposite to PSDs and 78% at extrasynaptic membranes

(Fig. 2A). In 1a^{-/-} mice 11% of all immunogold particles in MF boutons were found opposite to PSDs, demonstrating that the GABA_{B1b} protein distribution is significantly shifted toward extrasynaptic sites. Considering an overall GABA_{B1a} to GABA_{B1b} protein ratio of 0.60 (see above), we approximately estimate a GABA_{B1a} to GABA_{B1b} protein ratio of 9:1 in the active zones of MF boutons. We additionally analyzed the distribution of GABA_{B1} protein in dendritic spines of CA3 pyramidal neurons. Independent of the genotype we rarely observed immunogold particles in the PSD, likely because the pre-embedding technique limits penetration of immunoreagents into the PSD (Kulik et al., 2002, 2003). However, we did not observe any significant differences between WT, 1a^{-/-}, and 1b^{-/-} mice in the distribution of GABA_{B1} immunoparticles at perisynaptic and extrasynaptic dendritic sites (Fig. 2B). Of note, \sim 20% of all immunoparticles were found within 60 nm from the edge of the PSDs at perisynaptic sites.

GABA_{B(1a,2)} receptors are more efficient than GABA_{B(1b,2)} receptors in inhibiting glutamate release in response to pharmacological activation

We used whole-cell patch-clamp recording in slice preparations from WT, 1a^{-/-}, and 1b^{-/-} mice to examine to what extent GABA_{B(1a,2)} and GABA_{B(1b,2)} receptors can inhibit glutamate release in response to a maximally active concentration of the agonist baclofen. Stimulation of MFs in the stratum lucidum induces EPSCs in CA3 pyramidal neurons that are reduced in amplitude by activation of GABA_B heteroreceptors. A high concentration of baclofen (50 μ M) reduced EPSC amplitudes in all three genotypes (Fig. 3A, B). However, baclofen was significantly less effective in inhibiting release in 1a^{-/-} mice than in WT and 1b^{-/-} mice. As a control, activation of adenosine A1 receptors by adenosine inhibited glutamate release in all three genotypes to a similar extent (Fig. 3A, B). We tested whether lower concentrations of baclofen (0.1, 1 μ M) activate GABA_{B(1a,2)} heteroreceptors without engaging GABA_{B(1b,2)} heteroreceptors (Fig. 3C). This was the case at 0.1 μ M, at which concentration baclofen reduced glutamate release in WT and 1b^{-/-} mice but not in 1a^{-/-} mice (Fig. 3C). Altogether, the electrophysiological data therefore parallel the ultrastructural data described above (Figs. 1, 2). They support that the number of GABA_{B(1a,2)} heteroreceptors in 1b^{-/-} mice is sufficient to produce a maximal level of presynaptic inhibition (similar to WT), while GABA_{B(1b,2)} heteroreceptors in 1a^{-/-} mice are limiting and consequently produce submaximal inhibition. At low concentrations of baclofen, only GABA_{B(1a,2)} heteroreceptors appear to be present in sufficient numbers to inhibit glutamate release.

Recent reports show that certain presynaptic GABA_B receptors can be tonically activated by ambient GABA (Jensen et al., 2003; Lei and McBain, 2003; Liu et al., 2006). Bath application of the GABA_B antagonist CGP54626A had no effect on the amplitudes of evoked EPSCs in WT, 1a^{-/-}, and 1b^{-/-} mice (Fig. 3D, E). This demonstrates that under our experimental conditions ambient GABA does not tonically activate GABA_B heteroreceptors at MF boutons.

GABA_{B(1a,2)} and GABA_{B(1b,2)} receptors activate postsynaptic K⁺ channels to a similar extent in response to pharmacological activation

We next studied the relative contributions of GABA_{B1a} and GABA_{B1b} isoforms to the formation of functional somatodendritic GABA_B receptors on CA3 pyramidal neurons, using somatic whole-cell patch-clamp recordings in slices. Somatoden-

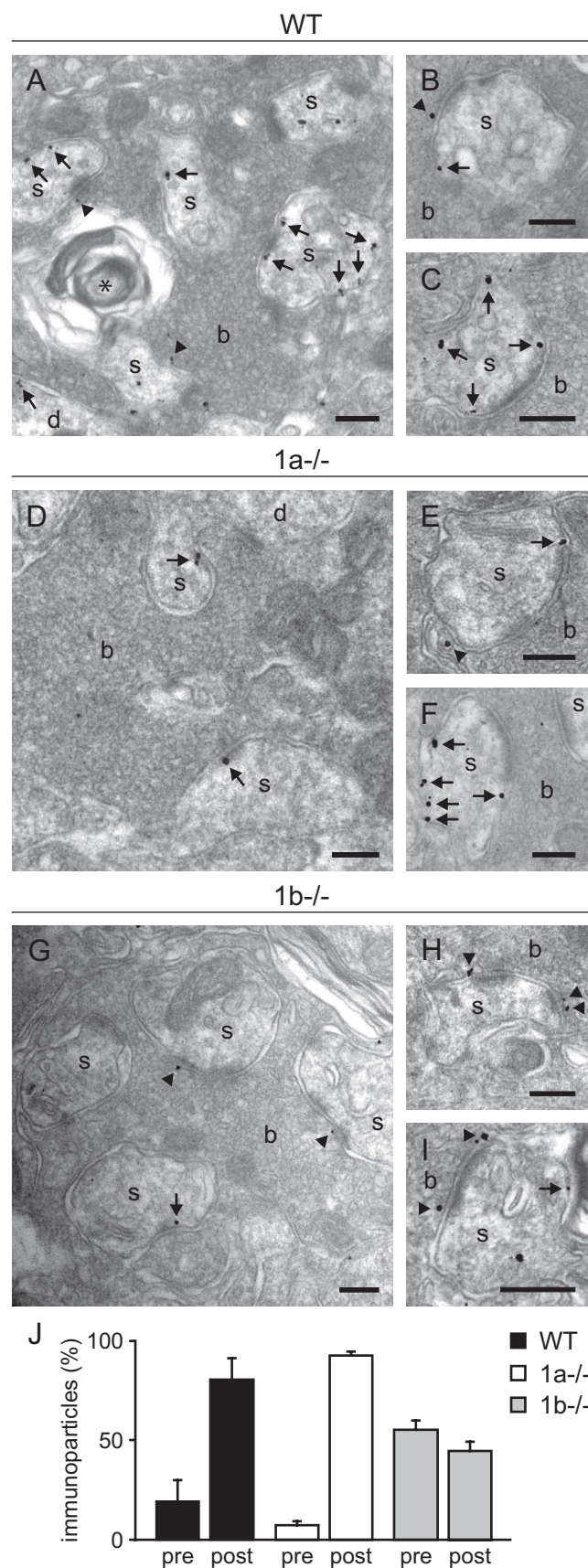


Figure 1. Electron micrographs showing the distribution of GABA_{B1} immunogold particles at MF-CA3 pyramidal neuron synapses in the stratum lucidum. **A–C**, In WT mice, immunogold particles were predominantly detected on dendritic spines and shafts of pyramidal cells (arrows) as well as in MF boutons (arrowheads). Immunogold particles were frequently found at

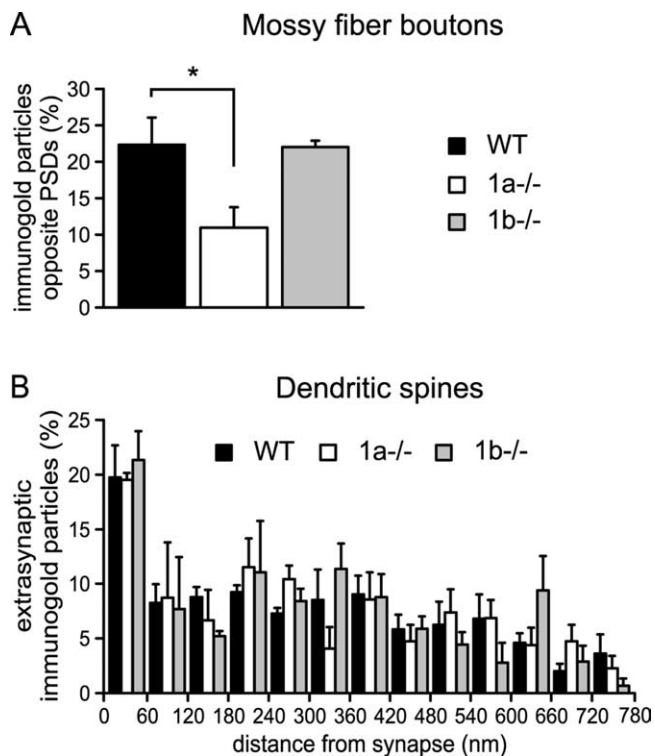


Figure 2. Distribution of GABA_{B1} immunogold particles in presynaptic and postsynaptic elements of MF-CA3 pyramidal neuron synapses. **A**, Percentage of GABA_{B1} immunogold particles at presynaptic membrane specializations of MF boutons opposite to PSDs (WT: 22.5 ± 3.9%; 1a^{-/-}: 11.1 ± 2.8%; 1b^{-/-}: 22.2 ± 0.8%, *n* = 3, **p* < 0.05, ANOVA/Dunnett's multiple comparison *post hoc* test). **B**, Histogram showing the spatial distribution of dendritic GABA_{B1} immunogold particles relative to the postsynaptic density. No significant differences between genotypes were detected. GABA_{B1} immunogold particles were generally enriched in the perisynaptic region within 60 nm from the edge of the PSD. Values are means ± SE.

dritic GABA_B receptors induce a late IPSC by activating Kir3-type K⁺ channels (Lüscher et al., 1997). At a holding potential of -50 mV and at a physiological concentration of extracellular K⁺, pharmacological activation with a maximally active concentration of baclofen (100 μM) elicited smaller outward K⁺ currents in CA3 pyramidal cells of 1a^{-/-} and 1b^{-/-} mice compared with WT mice (Fig. 4A,B). The maximal K⁺ currents induced by baclofen were similar in 1a^{-/-} and 1b^{-/-} mice, thus showing that GABA_{B(1b,2)}} and GABA_{B(1a,2)}} receptors activate K⁺ channels to a similar extent. Pharmacological activation of adenosine A1 receptors, which converge on the same Kir3-type K⁺ channels (Lüscher et al., 1997), induced similar outward currents in all genotypes (Fig. 4A,B). This indicates that the expression levels of

the edge of the presynaptic membrane specialization and at perisynaptic and extrasynaptic sites. **D–F**, In 1a^{-/-} mice, immunogold particles were almost exclusively found in postsynaptic elements, predominantly at perisynaptic and extrasynaptic sites. In rare cases, immunogold particles were also observed in MF boutons (**E**). **G–I**, In 1b^{-/-} mice, immunogold particles were observed in presynaptic and postsynaptic elements. Immunogold particles were frequently found at the presynaptic membrane specialization of MF boutons. **J**, Quantitative analysis of presynaptic versus postsynaptic immunogold particles in WT, 1a^{-/-}, and 1b^{-/-} mice (percentage presynaptic particles: WT, 19.3 ± 10.7%; 1a^{-/-}, 7.3 ± 2.1%; 1b^{-/-}, 55.3 ± 4.6%; *n* = 3 mice per genotype). Immunogold particles were less frequent in 1b^{-/-} compared with 1a^{-/-} and WT mice, which is reflected by the total number of particles that were analyzed (WT: *n* = 1570; 1a^{-/-}: *n* = 1419; 1b^{-/-}: *n* = 1120). b, MF bouton; s, dendritic spine; d, dendritic shaft; asterisk, degenerated unmyelinated axon. Scale bars: 200 nm. Values are means ± SD.

Kir3-type K⁺ channels are not altered as a consequence of the lack of GABA_{B1} isoform proteins. We tested whether lower concentrations of baclofen possibly generate distinct K⁺ outward currents in 1a^{-/-} and 1b^{-/-} mice, which was not the case (Fig. 4C). A reduction of K⁺ current amplitudes in 1a^{-/-} and 1b^{-/-} mice was only observed at high concentrations of baclofen (100 μM), while at lower concentrations (≤ 10 μM) the K⁺ current amplitudes were similar in all genotypes (Fig. 4C). Since at all concentrations of baclofen the GABA_B-induced K⁺ currents in 1a^{-/-} and 1b^{-/-} mice were similar, this suggests that GABA_{B(1b,2)} and GABA_{B(1a,2)} receptors are able to activate K⁺ channels to a similar extent.

GABA_{B(1a,2)} but not GABA_{B(1b,2)} receptors inhibit glutamate release in response to physiological activation

To address to what extent the two GABA_B receptor subtypes contribute to physiological inhibition of glutamate release at MF terminals we examined heterosynaptic depression in WT, 1a^{-/-}, and 1b^{-/-} mice. GABA_B receptor-mediated heterosynaptic depression of MF transmission has been studied using fEPSP recordings and relies on the activation of GABA_B heteroreceptors by GABA released from neighboring interneurons (Vogt and Nicoll, 1999; Chandler et al., 2003). We first verified that the stimulating electrode in the dentate gyrus evokes fEPSPs with properties consistent with MF transmission. MF synaptic responses were identified by the presence of paired-pulse facilitation, frequency-dependent short-term facilitation and sensitivity to the mGluR agonist DCG-IV, which blocks glutamate release from the MF but not from the associational-commissural fibers (Kamiya et al., 1996; Yeckel et al., 1999; Kirschstein et al., 2004; Nicoll and Schmitz, 2005). When fEPSPs were evoked with paired-pulse stimulation (100 ms apart), fEPSPs exhibited a pronounced facilitation of 197.4 ± 14.6% (*n* = 16 slices). In addition, when the stimulation frequency was increased from 0.05 to 1 Hz, fEPSPs exhibited a marked frequency-dependent facilitation of 246.3 ± 26.3% (*n* = 8 slices) (Fig. 5). Finally, as described (Kamiya et al., 1996; Yeckel et al., 1999), bath application of DCG-IV reduced the amplitude of fEPSPs measured at 0.05 Hz to 38.9 ± 5.5% (*n* = 9 slices) (Fig. 5). Bath application of CGP54626A (2 μM) had no significant effect on fEPSP peak amplitudes (control: 100 ± 19.5%, *n* = 7 slices; CGP54626A: 98.9 ± 18.3%, *n* = 7 slices), in keeping with patch-clamp experiments showing that ambient levels of GABA do not tonically activate GABA_B heteroreceptors (Fig. 3D, E).

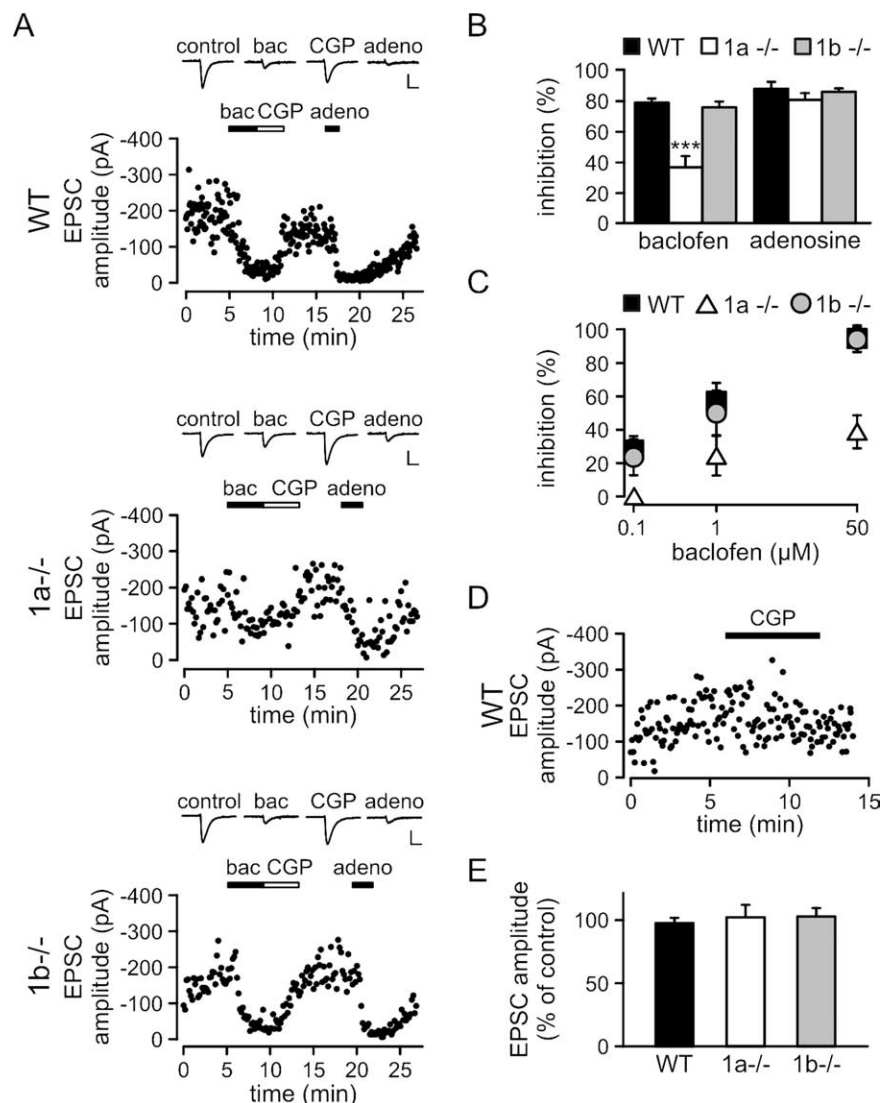


Figure 3. GABA_B heteroreceptor function at MF-CA3 pyramidal neuron synapses. **A, B**, EPSC peak amplitudes plotted versus time, average current traces, and summary histogram of monosynaptic EPSCs inhibition by baclofen (bac) and adenosine (adeno). Baclofen (50 μM) depressed the amplitude of EPSCs to the same extent in WT and 1b^{-/-} mice, but was less effective in 1a^{-/-} mice (WT: 78.6 ± 2.6% inhibition, *n* = 7; 1b^{-/-}: 75.6 ± 3.7% inhibition, *n* = 6; 1a^{-/-}: 36.4 ± 7.3% inhibition, *n* = 10, ****p* < 0.001, 1a^{-/-} compared with WT and 1b^{-/-}, ANOVA/Scheffe *post hoc* test). The inhibitory effect of baclofen was blocked by the GABA_B receptor antagonist CGP54626A (CGP, 1 μM). As a control, adenosine (100 μM) efficiently reduced the peak amplitudes of EPSCs in all genotypes (WT: 87.7 ± 1.6% inhibition, *n* = 6; 1a^{-/-}: 80.4% ± 4.4% inhibition, *n* = 8; 1b^{-/-}: 85.7 ± 2.2% inhibition, *n* = 4). Current traces in **A** show averages of 10 successive EPSCs (calibration: 20 ms/100 pA). **C**, Inhibition of glutamate release by different concentrations of baclofen. In 1a^{-/-} mice, baclofen was ineffective in inhibiting glutamate release at 0.1 μM (*n* = 5). At higher concentrations, baclofen was always less effective in inhibiting glutamate release in 1a^{-/-} mice compared with WT or 1b^{-/-} mice (1 μM, 1a^{-/-}: 24 ± 8.3% inhibition, *n* = 5, **p* < 0.05, 1a^{-/-} compared with WT and 1b^{-/-}; 50 μM, 1a^{-/-}: 38.4 ± 6.6% inhibition, *n* = 5, ****p* < 0.001, 1a^{-/-} compared with WT and 1b^{-/-}, ANOVA/Scheffe *post hoc* test). In WT and 1b^{-/-} mice, baclofen reduced the peak amplitude of EPSCs to the same extent at 0.1 μM (WT: 26.5 ± 3.4% inhibition, *n* = 4; 1b^{-/-}: 23.4 ± 6.1% inhibition, *n* = 4), 1 μM (WT: 57.2 ± 5.6% inhibition, *n* = 4; 1b^{-/-}: 50.1 ± 8.9% inhibition, *n* = 4), and 50 μM (WT: 94.8 ± 2.6% inhibition, *n* = 4; 1b^{-/-}: 94.2 ± 2.2% inhibition, *n* = 4). **D, E**, Lack of evidence for a tonic activity of GABA_B heteroreceptors at MF boutons. **D**, Evoked EPSCs of a WT CA3 pyramidal neuron recorded in the absence and presence of CGP54626A (1 μM). **E**, Summary histogram showing that in all genotypes the peak amplitudes of evoked EPSCs are not significantly altered in the presence of CGP54626A (WT: 98.2 ± 4.5%, *n* = 6; 1a^{-/-}: 100.9 ± 9.0%, *n* = 6; 1b^{-/-}: 102.8 ± 6.1%, *n* = 5). Values are means ± SEM.

To induce heterosynaptic depression at MF synapses we placed a second stimulating electrode into the dentate gyrus. The position of this electrode and the stimulus intensity were adjusted such that two independent MF pathways could be stimulated (Fig. 6A). Pathway one was stimulated at a regular interval of 10 s to evoke MF test fEPSPs (S1). Every tenth stimulus was preceded

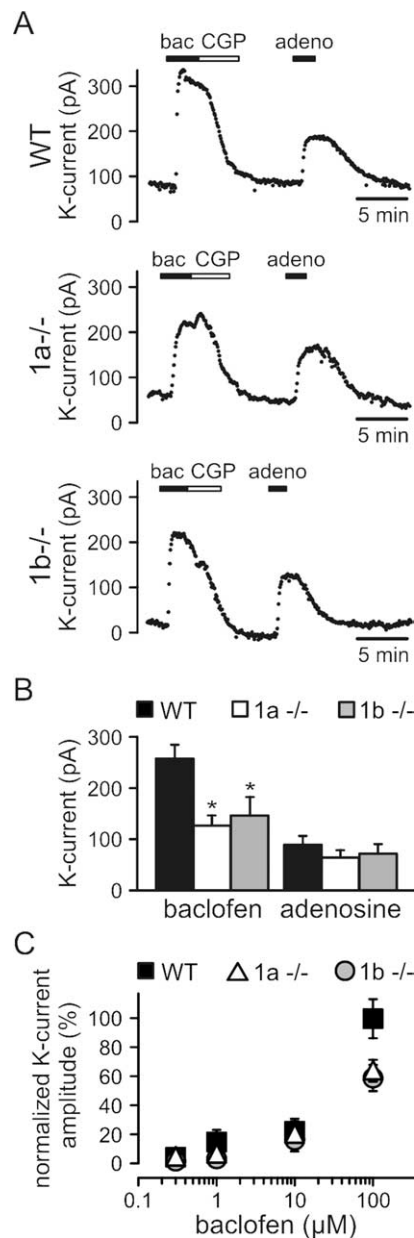


Figure 4. GABA_B-receptor-activated K⁺ currents in CA3 pyramidal neurons. **A, B**, Changes in the holding current of CA3 pyramidal neurons following bath application of baclofen (bac; 100 μM) or adenosine (adeno; 100 μM) and summary histogram of the amplitude of baclofen- and adenosine-induced K⁺ currents. The baclofen-induced outward K⁺ current was blocked by CGP54626A (CGP; 1 μM) and significantly reduced in 1a^{-/-} and 1b^{-/-} mice compared with WT mice (WT: 255.9 ± 23.8 pA, n = 6; 1a^{-/-}: 112.8 ± 17.5 pA, n = 7; 1b^{-/-}: 130.3 ± 31.9 pA, n = 7; *p < 0.05, 1a^{-/-} and 1b^{-/-} compared with WT, ANOVA/Scheffe *post hoc* test). Control adenosine-induced K⁺ currents were similar in all genotypes (WT: 79.4 ± 15.2 pA, n = 6; 1a^{-/-}: 57.1 ± 12.7 pA, n = 7; 1b^{-/-}: 64.0 ± 16.5 pA, n = 7), showing that effector K⁺ channels are not altered in 1a^{-/-} and 1b^{-/-} mice. **C**, Normalized K⁺ current amplitudes in response to increasing concentrations of baclofen. The maximal K⁺ current amplitude for each concentration was normalized to the mean maximal K⁺ current amplitude recorded from WT neurons at a saturating concentration of baclofen (100 μM). In 1a^{-/-} and 1b^{-/-} mice, the amplitude of baclofen-induced K⁺ was significantly reduced compared with WT mice at 100 μM (WT: 100 ± 13.6%, n = 5; 1a^{-/-}: 63.7 ± 7.7%, n = 8; 1b^{-/-}: 58.7 ± 9.1%, n = 5; *p < 0.05, 1a^{-/-} and 1b^{-/-} compared with WT, ANOVA/Scheffe *post hoc* test). Baclofen-induced K⁺ current amplitudes were not statistically different between genotypes at concentrations of 0.3 μM (WT: 3.6 ± 0.9%, n = 5; 1a^{-/-}: 3.6 ± 0.6%, n = 4; 1b^{-/-}: 0.8 ± 0.2%, n = 4), 1 μM (WT: 7.4 ± 2.0%, n = 5; 1a^{-/-}: 5.7 ± 1.1%, n = 5; 1b^{-/-}: 2.4 ± 0.8%, n = 4), and 10 μM (WT: 21.7 ± 3.5%, n = 5; 1a^{-/-}: 19.5 ± 3.4%, n = 6; 1b^{-/-}: 15.5 ± 2.9%, n = 5). Values are means ± SEM.

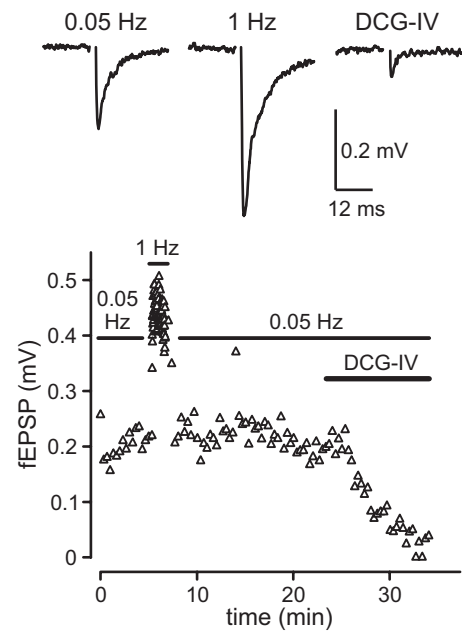


Figure 5. MF fEPSPs exhibit frequency-dependent short-term facilitation and sensitivity to the mGluR agonist DCG-IV. Average traces of fEPSPs recorded in the stratum lucidum at 0.05 Hz and 1 Hz and in the presence of DCG-IV (top) as well as amplitudes of fEPSPs plotted versus time (bottom) are shown. Increasing the stimulus frequency from 0.05 to 1 Hz induced pronounced facilitation. Bath application of DCG-IV (2 μM) strongly inhibited fEPSP amplitudes elicited at 0.05 Hz.

by a conditioning train of 20 stimuli at 100 Hz on pathway two (S2). The two pathways were stimulated 200 ms apart. To prevent interference from presynaptic opioid and A1 adenosine receptors, heterosynaptic depression was measured in the presence of the antagonists naloxone and DPCPX. Under these conditions a marked GABA_B receptor-mediated heterosynaptic depression is observed; only at stronger MF activation levels a direct activation of presynaptic mGluRs through spillover of glutamate will occur (Vogt and Nicoll, 1999). In WT mice, the amplitudes of test fEPSPs evoked after a train on pathway two (conditioned fEPSPs, closed circles) were significantly reduced by 25.7 ± 3.3% (p < 0.01, n = 6 slices) compared with fEPSPs measured in the absence of a conditioning train (unconditioned fEPSPs) (Fig. 6B,E, open circles). CGP54626A largely or totally inhibited the reduction of conditioned fEPSP amplitudes (Fig. 6B,E), confirming that heterosynaptic depression was mainly mediated by GABA_B receptors. No GABA_B-mediated heterosynaptic depression was detectable in 1a^{-/-} mice (conditioned fEPSPs reduced by 2.5 ± 1.4%, p = 0.20, n = 6 slices) and accordingly, CGP54626A had no effect on fEPSPs (Fig. 6C,E). In contrast, we observed a significant heterosynaptic depression in 1b^{-/-} mice (conditioned fEPSP amplitudes reduced by 26.2 ± 2.8%, n = 7 slices; p < 0.001), which was markedly reduced or abolished by CGP54626A (Fig. 6D,E). Confirming that our recordings relate to MF transmission, fEPSPs were always inhibited by application of DCG-IV (Fig. 6B–D). Of note, the amplitudes of unconditioned fEPSPs in WT and 1b^{-/-} mice were increased in the presence of CGP54626A (Fig. 6B,D, open circles), suggesting that the GABA released by the conditioning train lasts long enough to significantly inhibit unconditioned fEPSPs during the 90 s preceding the next conditioning train. In support of this, we found that CGP54626A was without effect on unconditioned fEPSP amplitudes in the absence of the conditioning train (control: 100 ± 18.6%, n = 8 slices; CGP54626A: 100.8 ± 19.1%, n = 8 slices). CGP54626A had no

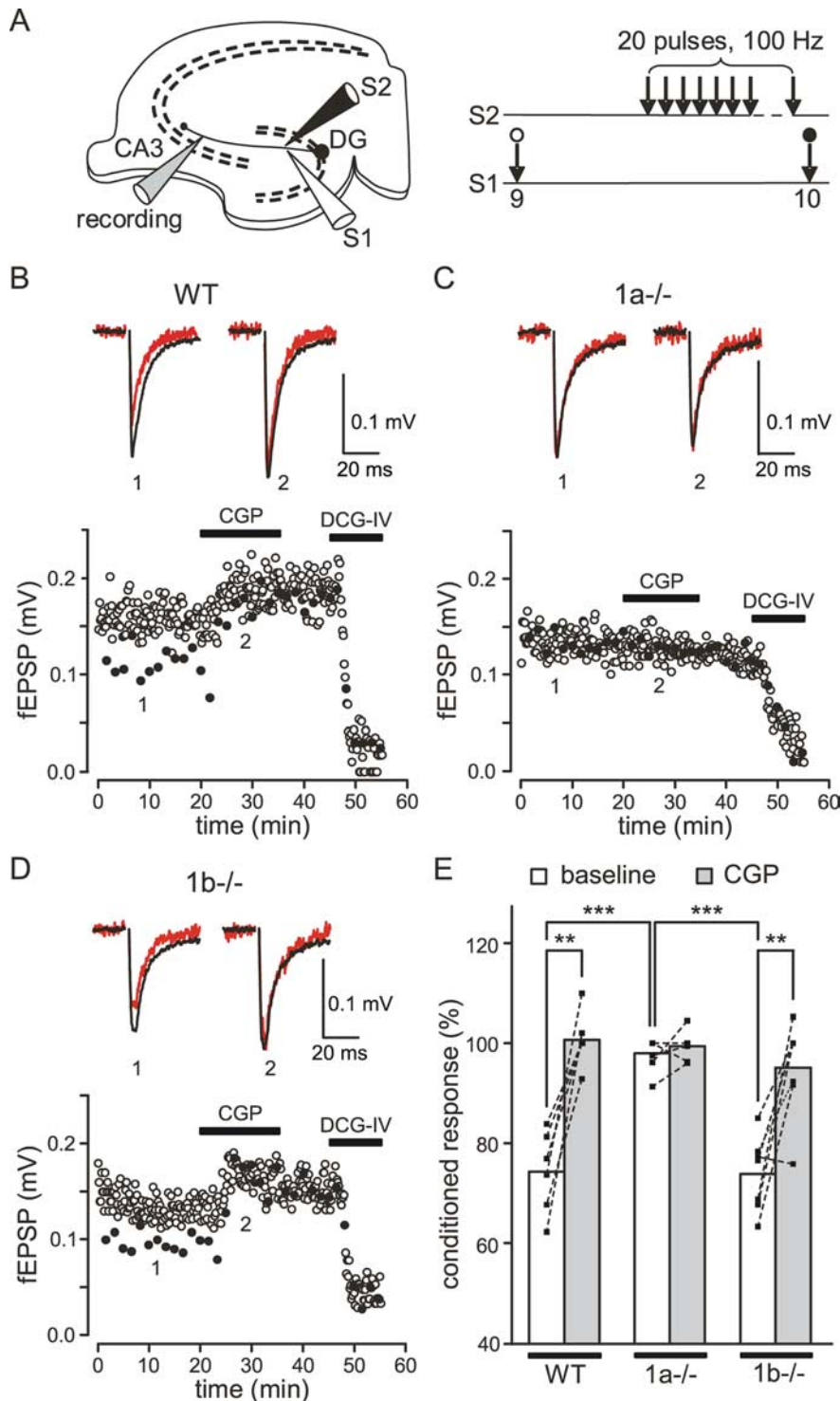


Figure 6. GABA_B-mediated heterosynaptic depression at MF-CA3 pyramidal neuron synapses. **A**, Two electrodes (S1, S2) positioned in the dentate gyrus were used to stimulate two independent pathways. A third electrode in the CA3 stratum lucidum was used to record MF fEPSPs. Pathway 1 was stimulated at a regular interval of 10 s to evoke test fEPSPs (S1, unconditioned response). Pathway 2 was stimulated 200 ms before every tenth test stimulus with a train of 20 stimuli at 100 Hz (S2, conditioned responses). **B**, GABA_B-mediated heterosynaptic depression in slices of WT mice. The amplitudes of fEPSPs plotted over time (bottom) and average traces (top) are shown. The amplitudes of fEPSPs preceded by a train (closed circles, red traces) were reduced compared with those of fEPSPs not preceded by a train (open circles, black traces). Heterosynaptic depression was largely inhibited or lost in the presence of CGP54626A (CGP; 2 μM). Average fEPSP traces are shown in the absence (1) and the presence (2) of CGP54626A (stimulation artifacts were removed). **C**, GABA_B-mediated heterosynaptic depression was absent in slices of 1a^{-/-} mice. The amplitudes of conditioned fEPSPs were similar to those of unconditioned fEPSPs. **D**, GABA_B-mediated heterosynaptic depression in slices of 1b^{-/-} mice was similar to that in WT mice and inhibited by CGP54626A. Note that CGP54626A also increased the amplitude of unconditioned fEPSPs in WT and 1b^{-/-} mice but not in 1a^{-/-} mice (**B–D**). In all genotypes, fEPSPs were inhibited by DCG-IV (2 μM). **E**, Summary histogram of GABA_B-mediated heterosynaptic depression. The amplitudes

of unconditioned fEPSP amplitudes in 1a^{-/-} mice, in agreement with a lack of functional GABA_B heteroreceptors in these mice (Fig. 6C). In summary, our experiments show that exclusively GABA_{B(1a,2)} receptors mediate heterosynaptic depression at MF-CA3 synapses.

Late IPSCs are detectable in WT mice but not in 1a^{-/-} and 1b^{-/-} mice

GABA_{B(1a,2)} and GABA_{B(1b,2)} receptors produce K⁺-currents of similar amplitude in response to pharmacological activation with baclofen (Fig. 4). However, it remains possible that GABA_{B(1a,2)} and GABA_{B(1b,2)} receptors produce distinct postsynaptic responses following physiological activation, due to local differences in their somatodendritic abundance. In the hippocampus, synaptically released GABA induces Cl⁻-dependent early IPSCs and K⁺-dependent late IPSCs that are mediated by GABA_A and GABA_B receptors, respectively (Misgeld et al., 1995; Lüscher et al., 1997). We simultaneously recorded early and late IPSCs in WT, 1a^{-/-}, and 1b^{-/-} mice. The early IPSC allowed us to verify that stimulation of the MF pathway provoked GABA release in all of our recordings. The amplitude of the late IPSC was used to quantify the extent of GABA_B receptor activation in response to synaptically released GABA. Three stimuli at 100 Hz reliably evoked early and late IPSCs in WT mice. The occurrence of late IPSCs was prevented in the presence of CGP54626A, confirming that the late IPSCs are mediated by GABA_B receptors (Fig. 7A,D). No late IPSCs were detectable in 1a^{-/-} and 1b^{-/-} mice, although early IPSCs were always induced (Fig. 7B–D). This suggests that the reduction of functional postsynaptic GABA_B receptors seen in 1a^{-/-} and 1b^{-/-} mice after pharmacological stimulation (Fig. 4) leads to subthreshold late IPSCs under physiological conditions.

←

of conditioned fEPSPs were normalized to amplitudes of unconditioned fEPSPs in the absence (baseline) and presence of CGP54626A. Significant CGP54626A-sensitive heterosynaptic depression was observed in WT mice (baseline: 74.3 ± 4%, n = 6 slices; CGP54626A: 100.8 ± 2.7%, n = 6 slices; **p < 0.01, two-tailed paired Student's *t* test) and 1b^{-/-} mice (baseline: 73.8 ± 2.8%, n = 7 slices; CGP54626A: 95 ± 3.7%, n = 7 slices; **p < 0.01) but not in 1a^{-/-} mice (baseline: 97.5 ± 1.4%, n = 6 slices; CGP54626A: 99.4 ± 1.3%, n = 6 slices; p = 0.32). The ANOVA/Scheffe *post hoc* test was used for the comparison of genotypes (***p < 0.001, normalized conditioned fEPSPs in 1a^{-/-} compared with WT and 1b^{-/-} mice). Values are means ± SEM.

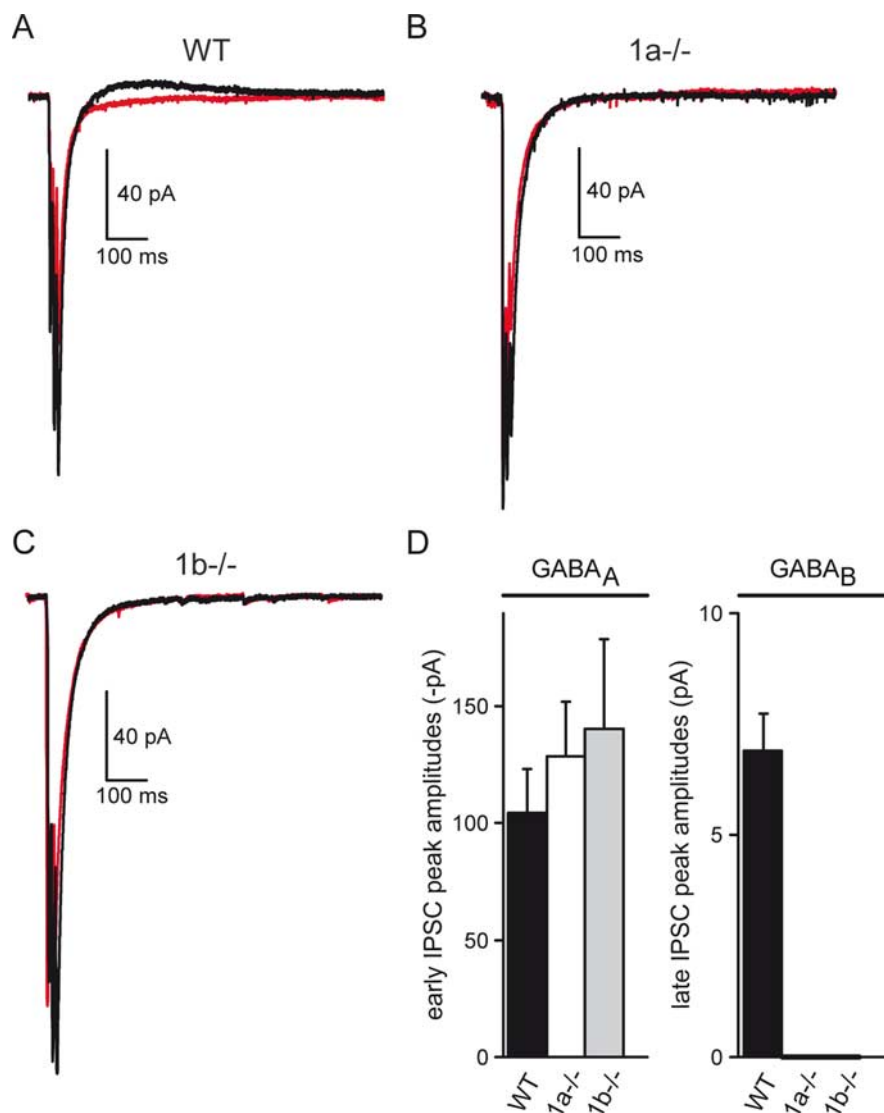


Figure 7. GABA_A-mediated early IPSCs and GABA_B-mediated late IPSCs recorded from CA3 pyramidal neurons in acute hippocampal slices. **A–C**, Average traces of early and late IPSCs recorded from WT, 1a^{-/-}, and 1b^{-/-} brain slices (black traces). IPSCs were recorded at a holding potential of -60 mV and an internal Cl⁻ concentration of 20 mM, which yields inward currents for early IPSCs and outward currents for late IPSCs. Application of CGP54626A (2 μ M) abolished late IPSCs without affecting early IPSCs (red traces). **D**, Mean peak amplitudes of the first early IPSC (GABA_A, left) and the late IPSC (GABA_B, right). Early IPSCs were of similar amplitudes in all three genotypes (WT: 104.5 ± 18.5 pA, $n = 9$; 1a^{-/-}: 128.6 ± 23.4 pA, $n = 9$; 1b^{-/-}: 140.3 ± 38.4 pA, $n = 5$; $p > 0.05$). Late IPSCs were only detectable in WT mice (6.9 ± 0.8 pA, $n = 9$) but not in 1a^{-/-} mice ($n = 9$) or 1b^{-/-} mice ($n = 5$). Currents were recorded in the presence of kynurenic acid (2 mM), DNQX (10 μ M), naloxone (10 μ M), and DPCPX (1 μ M). Values are means \pm SEM.

Discussion

GABA_{B(1a,2)}} and GABA_{B(1b,2)}} receptor subtypes exhibit comparable pharmacological and functional properties when studied in heterologous expression systems (Calver et al., 2002; Bettler et al., 2004; Ulrich and Bettler, 2007). However, the two receptor subtypes produce distinct responses at axonal and dendritic effectors when pharmacologically activated by a saturating concentration of baclofen (Pérez-Garci et al., 2006; Shaban et al., 2006; Vigot et al., 2006; Ulrich and Bettler, 2007; Ulrich et al., 2007). Moreover, the contributions of the two receptor subtypes to axonal or dendritic effector responses can vary in between neuronal populations. Two reasons probably account for neuron-specific differences in the responses of GABA_B receptor subtypes. On the one hand, GABA_{B1a} and GABA_{B1b} subunits are differentially distrib-

uted to axonal and dendritic compartments (Vigot et al., 2006). On the other hand, the expression of GABA_{B1a} and GABA_{B1b} subunits is under separate transcriptional control, which will influence the ratio of receptor subtypes in individual neurons (Steiger et al., 2004). It seems reasonable to propose that separate control of both transcription and distribution of GABA_B receptor subtypes has evolved to provide neurons with a means to independently adjust signaling at select effector systems. To support this concept, it is important to directly demonstrate that endogenously released GABA can differentially activate GABA_B receptor subtypes (Huang, 2006). This is the case for inhibitory synapses at cortical layer 5 pyramidal neurons, where under physiological conditions selectively GABA_{B(1a,2)}} and GABA_{B(1b,2)}} receptors act as autoreceptors and postsynaptic receptors, respectively (Pérez-Garci et al., 2006). Here, we addressed whether this is also the case for GABA_B heteroreceptors at glutamatergic synapses. A physiological phenomenon that is reported to depend on the endogenous activation of GABA_B heteroreceptors is heterosynaptic depression (Isaacson et al., 1993; Vogt and Nicoll, 1999; Chandler et al., 2003). We therefore determined the individual contributions of the two GABA_B receptor subtypes to heterosynaptic depression at MF-CA3 pyramidal neuron synapses, where this phenomenon can be easily studied (Vogt and Nicoll, 1999; Chandler et al., 2003). Our data show that exclusively GABA_{B(1a,2)}} heteroreceptors mediate heterosynaptic depression of MF transmission. Yet the presence of functional GABA_{B(1b,2)}} heteroreceptors at MF boutons can be demonstrated in pharmacological experiments, in which concentrations of baclofen ≥ 1 μ M produce a component of presynaptic inhibition mediated by GABA_{B(1b,2)}} receptors. In pharmacological experiments, a selective presynaptic inhibition via GABA_{B(1a,2)}} heteroreceptors was only observed at a

lower concentration of baclofen (0.1 μ M). The most parsimonious explanation for these data is that the number of GABA_{B(1b,2)}} receptors at presynaptic sites in 1a^{-/-} mice is sufficient to measurably inhibit glutamate release in response to pharmacological activation with moderate to high concentrations of baclofen, but not to inhibit release in response to low concentrations of spillover GABA from neighboring interneurons. This may be accentuated by the fact that presynaptic GABA_B receptors at MF boutons display non-desensitizing properties (Tosetti et al., 2004), which will render sustained pharmacological inhibition particularly effective. Baclofen likely also activates somatic GABA_{B(1b,2)}} receptors in the dentate granule cells. The ensuing hyperpolarizing potentials may passively propagate to the MF boutons and contribute to presynaptic inhibition (Alle and Geiger, 2006). The

exact reason for presynaptic inhibition following pharmacological activation with baclofen is unknown. However, our results support that the spatial segregation of GABA_{B1} isoforms at MF terminals is sufficient to produce a strictly subtype-specific heteroreceptor response under physiological conditions. At other glutamatergic synapses baclofen also produces a significant level of presynaptic inhibition through GABA_{B(1b,2)}} heteroreceptors (Shaban et al., 2006; Vigot et al., 2006; Ulrich et al., 2007). We expect that under physiological conditions exclusively GABA_{B(1a,2)}} receptors mediate heteroreceptor function at those synapses as well.

Heterosynaptic depression at MF-CA3 pyramidal neuron synapses is thought to play an important role in regulating mnemonic processes (Jin and Chavkin, 1999; Vogt and Nicoll, 1999; Vida and Frotscher, 2000; Chandler et al., 2003). Heterosynaptic depression increases the sparseness of input signals to CA3 pyramidal cells, thereby enhancing the storage capacity of the CA3 network. Overt memory deficits in hippocampus-dependent memory tasks in 1a^{-/-} mice (Vigot et al., 2006; Jacobson et al., 2007) may therefore relate, at least in part, to the disinhibition of MF inputs and the ensuing failure to store or recall memory traces. In addition, the control of GABA_{B1a}-mediated inhibition at MF boutons may be important for regulating synaptic plasticity and limbic seizure prevention, since these processes were also shown to be controlled by GABA_B heteroreceptors (Vogt and Nicoll, 1999; Chandler et al., 2003).

We found that baclofen induces similar maximal K⁺ currents in CA3 neurons of 1a^{-/-} and 1b^{-/-} mice. Given the surplus of GABA_{B1b} protein at dendritic sites opposite to MF terminals, it may appear surprising that the maximal K⁺ currents induced by GABA_{B(1b,2)}} receptors are not larger than those induced by GABA_{B(1a,2)}} receptors. However, caution should be exerted when comparing the ultrastructural data with the electrophysiological data. On the one hand, the GABA_B receptors included in the ultrastructural analysis may not necessarily be coupled to K⁺ channels. For example, it is conceivable that a larger fraction of GABA_{B(1a,2)}} receptors is colocalized with Kir3-type K⁺ channels, rendering their coupling to effector channels more efficient (Karschin, 1999). Future studies, for example using high-resolution immunocytochemical techniques (Kulik et al., 2006), will have to address whether GABA_{B1} isoforms exhibit differences in the colocalization with Kir3-type K⁺ channel subunits. On the other hand, baclofen probably mostly activates K⁺ currents via somatodendritic GABA_B receptors remote from MF synapses, and these receptors were excluded from the ultrastructural analysis. It is possible that the relative abundance of GABA_{B(1a,2)}} and GABA_{B(1b,2)}} receptors differs between dendritic spines and shafts, similar as observed in CA1 pyramidal neurons where GABA_{B1a} protein does not efficiently enter the spines (Vigot et al., 2006). It further could be argued that the downregulation of GABA_{B1a} protein levels during early postnatal development (Malitschek et al., 1998; Fritschy et al., 1999) accounts for the difference between the morphological and electrophysiological data. However, ruling out this possibility, all our experiments were performed with mice 3 weeks of age or older, when GABA_{B1a} and GABA_{B1b} protein levels remain stable (Malitschek et al., 1998). While many factors can contribute to the difference between the ultrastructural data of spines and the electrophysiological responses recorded for the soma of CA3 pyramidal neurons, our data further consolidate that the relative contributions of GABA_{B1a} and GABA_{B1b} subunits to the pool of GABA_B receptors coupled to effector K⁺ channels varies in between neurons (Ulrich and Bettler, 2007). Importantly, a physiological activation of somatoden-

dritic GABA_B receptors by synaptically released GABA does not produce a segregation of GABA_{B(1a,2)}} and GABA_{B(1b,2)}} responses in CA3 pyramidal neurons, in contrast to the findings with cortical neurons (Huang, 2006; Pérez-García et al., 2006).

In conclusion, our results are consistent with the proposal that independent regulation of expression and distribution of GABA_B receptor subtypes enables neurons to dynamically adjust GABA_B signaling at axonal and dendritic effectors. The observation that GABA_{B1a} and GABA_{B1b} cannot compensate for each other in response to synaptically released GABA is important from a pharmaceutical perspective. The existence of two functionally distinct GABA_B receptor subtypes enables a more selective interference with the GABA_B receptor system, which may be of therapeutic benefit for the treatment of neurological and psychiatric disorders (Tiao et al., 2008).

References

- Alle H, Geiger JR (2006) Combined analog and action potential coding in hippocampal mossy fibers. *Science* 311:1290–1293.
- Bettler B, Kaupmann K, Mosbacher J, Gassmann M (2004) Molecular structure and physiological functions of GABA_B receptors. *Physiol Rev* 84:835–867.
- Calver AR, Davies CH, Pangalos M (2002) GABA_B receptors: from monogamy to promiscuity. *Neurosignals* 11:299–314.
- Chandler KE, Princiville AP, Fabian-Fine R, Bowery NG, Kullmann DM, Walker MC (2003) Plasticity of GABA_B receptor-mediated heterosynaptic interactions at mossy fibers after status epilepticus. *J Neurosci* 23:11382–11391.
- Cunha RA (2008) Different cellular sources and different roles of adenosine: A1 receptor-mediated inhibition through astrocytic-driven volume transmission and synapse-restricted A2A receptor-mediated facilitation of plasticity. *Neurochem Int* 52:65–72.
- Dittert I, Benedikt J, Vyklický L, Zimmermann K, Reeh PW, Vlachová V (2006) Improved superfusion technique for rapid cooling or heating of cultured cells under patch-clamp conditions. *J Neurosci Methods* 151:178–185.
- Fritschy JM, Meskenaite V, Weinmann O, Honer M, Benke D, Mohler H (1999) GABA_B-receptor splice variants GB1a and GB1b in rat brain: developmental regulation, cellular distribution and extrasynaptic localization. *Eur J Neurosci* 11:761–768.
- Hawrot E, Xiao Y, Shi QL, Norman D, Kirkitadze M, Barlow PN (1998) Demonstration of a tandem pair of complement protein modules in GABA_B receptor 1a. *FEBS Lett* 432:103–108.
- Huang ZJ (2006) GABA_B receptor isoforms caught in action at the scene. *Neuron* 50:521–524.
- Isaacson JS, Solis JM, Nicoll RA (1993) Local and diffuse synaptic actions of GABA in the hippocampus. *Neuron* 10:165–175.
- Jacobson LH, Kelly PH, Bettler B, Kaupmann K, Cryan JF (2007) Specific roles of GABA_{B(1)}} receptor isoforms in cognition. *Behav Brain Res* 181:158–162.
- Jarolimiek W, Misgeld U (1997) GABA_B receptor-mediated inhibition of tetrodotoxin-resistant GABA release in rodent hippocampal CA1 pyramidal cells. *J Neurosci* 17:1025–1032.
- Jensen K, Chiu CS, Sokolova I, Lester HA, Mody I (2003) GABA transporter-1 (GAT1)-deficient mice: differential tonic activation of GABA_A versus GABA_B receptors in the hippocampus. *J Neurophysiol* 90:2690–2701.
- Jin W, Chavkin C (1999) Mu opioids enhance mossy fiber synaptic transmission indirectly by reducing GABA_B receptor activation. *Brain Res* 821:286–293.
- Kamiya H, Shinozaki H, Yamamoto C (1996) Activation of metabotropic glutamate receptor type 2/3 suppresses transmission at rat hippocampal mossy fibre synapses. *J Physiol* 493:447–455.
- Karschin A (1999) G protein regulation of inwardly rectifying K⁺ channels. *News Physiol Sci* 14:215–220.
- Kirschstein T, von der Brélie C, Steinhäuser M, Vinçon A, Beck H, Dietrich D (2004) L-CCG-I activates group III metabotropic glutamate receptors in the hippocampal CA3 region. *Neuropharmacology* 47:157–162.
- Kulik A, Nakadate K, Nyiri G, Notomi T, Malitschek B, Bettler B, Shigemoto R (2002) Distinct localization of GABA_B receptors relative to synaptic

- sites in the rat cerebellum and ventrobasal thalamus. *Eur J Neurosci* 15:291–307.
- Kulik A, Vida I, Luján R, Haas CA, López-Bendito G, Shigemoto R, Frotscher M (2003) Subcellular localization of metabotropic GABA_B receptor subunits GABA_{B(1a/b)} and GABA_{B(2)} in the rat hippocampus. *J Neurosci* 23:11026–11035.
- Kulik A, Vida I, Fukazawa Y, Guetg N, Kasugai Y, Marker CL, Rigato F, Bettler B, Wickman K, Frotscher M, Shigemoto R (2006) Compartment-dependent colocalization of Kir3.2-containing K⁺ channels and GABA_B receptors in hippocampal pyramidal cells. *J Neurosci* 26:4289–4297.
- Lacey CJ, Boyes J, Gerlach O, Chen L, Magill PJ, Bolam JP (2005) GABA_B receptors at glutamatergic synapses in the rat striatum. *Neuroscience* 136:1083–1095.
- Lei S, McBain CJ (2003) GABA_B receptor modulation of excitatory and inhibitory synaptic transmission onto rat CA3 hippocampal interneurons. *J Physiol* 546:439–453.
- Liu X, Tribollet E, Raggenbass M (2006) GABA_B receptor-activation inhibits GABAergic synaptic transmission in parvocellular neurones of rat hypothalamic paraventricular nucleus. *J Neuroendocrinol* 18:177–186.
- López-Bendito G, Shigemoto R, Kulik A, Vida I, Fairén A, Luján R (2004) Distribution of metabotropic GABA receptor subunits GABA_{B1a/b} and GABA_{B2} in the rat hippocampus during prenatal and postnatal development. *Hippocampus* 14:836–848.
- Lüscher C, Jan LY, Stoffel M, Malenka RC, Nicoll RA (1997) G protein-coupled inwardly rectifying K⁺ channels (GIRKs) mediate postsynaptic but not presynaptic transmitter actions in hippocampal neurons. *Neuron* 19:687–695.
- Malitschek B, Rüegg D, Heid J, Kaupmann K, Bittiger H, Fröstl W, Bettler B, Kuhn R (1998) Developmental changes in agonist affinity at GABA_{B(1)} receptor variants in rat brain. *Mol Cell Neurosci* 12:56–64.
- Manzoni OJ, Manabe T, Nicoll RA (1994) Release of adenosine by activation of NMDA receptors in the hippocampus. *Science* 265:2098–2101.
- Misgeld U, Bijak M, Jarolimek W (1995) A physiological role for GABA_B receptors and the effects of baclofen in the mammalian central nervous system. *Prog Neurobiol* 46:423–462.
- Nicoll RA, Schmitz D (2005) Synaptic plasticity at hippocampal mossy fibre synapses. *Nat Rev Neurosci* 6:863–876.
- Pérez-Garci E, Gassmann M, Bettler B, Larkum ME (2006) The GABA_{B1b} isoform mediates long-lasting inhibition of dendritic Ca²⁺ spikes in layer 5 somatosensory pyramidal neurons. *Neuron* 50:603–616.
- Price CJ, Cauli B, Kovacs ER, Kulik A, Lambollez B, Shigemoto R, Capogna M (2005) Neurogliaform neurons form a novel inhibitory network in the hippocampal CA1 area. *J Neurosci* 25:6775–6786.
- Sakaba T, Neher E (2003) Direct modulation of synaptic vesicle priming by GABA_B receptor activation at a glutamatergic synapse. *Nature* 424:775–778.
- Scanziani M (2000) GABA spillover activates postsynaptic GABA_B receptors to control rhythmic hippocampal activity. *Neuron* 25:673–681.
- Scanziani M, Capogna M, Gähwiler BH, Thompson SM (1992) Presynaptic inhibition of miniature excitatory synaptic currents by baclofen and adenosine in the hippocampus. *Neuron* 9:919–927.
- Schuler V, Lüscher C, Blanchet C, Klix N, Sansig G, Klebs K, Schmutz M, Heid J, Gentry C, Urban L, Fox A, Spooren W, Jatton AL, Vigouret J, Pozza M, Kelly PH, Mosbacher J, Froestl W, Käslin E, Korn R, et al. (2001) Epilepsy, hyperalgesia, impaired memory, and loss of pre- and postsynaptic GABA_B responses in mice lacking GABA_{B(1)}. *Neuron* 31:47–58.
- Shaban H, Humeau Y, Herry C, Cassasus G, Shigemoto R, Ciochi S, Barbieri S, van der Putten H, Kaupmann K, Bettler B, Lüthi A (2006) Generalization of amygdala LTP and conditioned fear in the absence of presynaptic inhibition. *Nat Neurosci* 9:1028–1035.
- Steiger JL, Bandyopadhyay S, Farb DH, Russek SJ (2004) cAMP response element-binding protein, activating transcription factor-4, and upstream stimulatory factor differentially control hippocampal GABA_BR1a and GABA_BR1b subunit gene expression through alternative promoters. *J Neurosci* 24:6115–6126.
- Tiao JY, Bradaia A, Biermann B, Kaupmann K, Metz M, Haller C, Rolink AG, Pless E, Barlow PN, Gassmann M, Bettler B (2008) The sushi domains of secreted GABA_{B1} isoforms selectively impair GABA_B heteroreceptor function. *J Biol Chem* 283:31005–31011.
- Tosetti P, Bakels R, Colin-Le Brun I, Ferrand N, Gaiarsa JL, Caillard O (2004) Acute desensitization of presynaptic GABA_B-mediated inhibition and induction of epileptiform discharges in the neonatal rat hippocampus. *Eur J Neurosci* 19:3227–3234.
- Ulrich D, Bettler B (2007) GABA_B receptors: synaptic functions and mechanisms of diversity. *Curr Opin Neurobiol* 17:298–303.
- Ulrich D, Besseyrias V, Bettler B (2007) Functional mapping of GABA_B-receptor subtypes in the thalamus. *J Neurophysiol* 98:3791–3795.
- Vida I, Frotscher M (2000) A hippocampal interneuron associated with the mossy fiber system. *Proc Natl Acad Sci U S A* 97:1275–1280.
- Vigot R, Barbieri S, Bräuner-Osborne H, Turecek R, Shigemoto R, Zhang YP, Luján R, Jacobson LH, Biermann B, Fritschy JM, Vacher CM, Müller M, Sansig G, Guetg N, Cryan JF, Kaupmann K, Gassmann M, Oertner TG, Bettler B (2006) Differential compartmentalization and distinct functions of GABA_B receptor variants. *Neuron* 50:589–601.
- Vogt KE, Nicoll RA (1999) Glutamate and gamma-aminobutyric acid mediate a heterosynaptic depression at mossy fiber synapses in the hippocampus. *Proc Natl Acad Sci U S A* 96:1118–1122.
- Weisskopf MG, Zalutsky RA, Nicoll RA (1993) The opioid peptide dynorphin mediates heterosynaptic depression of hippocampal mossy fibre synapses and modulates long-term potentiation. *Nature* 365:188.
- Yamada J, Saitow F, Satake S, Kiyohara T, Konishi S (1999) GABA_(B) receptor-mediated presynaptic inhibition of glutamatergic and GABAergic transmission in the basolateral amygdala. *Neuropharmacology* 38:1743–1753.
- Yeckel MF, Kapur A, Johnston D (1999) Multiple forms of LTP in hippocampal CA3 neurons use a common postsynaptic mechanism. *Nat Neurosci* 2:625–633.

6.3. A mouse model for visualization of GABA_B receptors

Casanova E*, Guetg N*, Vigot R, Seddik R, Julio-Pieper M, Hyland NP, Cryan JF, Gassmann M, and Bettler B

Genesis (in press)

Genesis 2009; 47:595-602

*Authors contributed equally to this work.

In the following work, a transgenic mouse model for the visualization of GABA_B receptors was generated by using a modified bacterial artificial chromosome (BAC) containing the *GABA_{B1}* gene. The coding sequence for the enhanced green fluorescent protein (eGFP) was inserted into the BAC in frame at the C-terminus of GABA_{B1}. The BAC contained 110 kb of upstream and 50 kb of downstream sequences and was therefore likely to harbor most, if not all, regulatory elements that drive expression of the GABA_{B1a} and GABA_{B1b} subunit isoforms. *GABA_{B1}-eGFP* BAC transgenic mice were backcrossed into the *GABA_{B1}^{-/-}* background in order to assess whether the eGFP-tagged GABA_{B1} subunits were able to form functional receptors.

Expression of eGFP was detected in brains of both young and adult mice. Moreover, immunohistochemistry demonstrated that the GABA_B receptor expression pattern was similar in WT and *GABA_{B1}^{-/-}*, *GABA_{B1}-eGFP BAC^{+/+}* (*GB1^{-/-}*, *BAC^{+/+}*) mice. Immunoblot analysis of *GB1^{-/-}*, *BAC^{+/+}* mice revealed that GABA_{B1a} and GABA_{B1b} are expressed as eGFP-fusion proteins and that protein levels are similar to endogenous GABA_{B1a} and GABA_{B1b} in WT mice. In addition, co-immunoprecipitation demonstrated successful heterodimerization of the *GABA_{B1}-eGFP* fusion proteins with GABA_{B2}. Functional analysis of *GB1^{-/-}*, *BAC^{+/+}* mice revealed complete rescue of GABA_B functions, indicating that *GABA_{B1}-eGFP* fusion proteins are forming functional pre- and postsynaptic receptors with GABA_{B2}. Next the temporal expression of *GABA_{B1}-eGFP* fusion proteins was assessed in cultured hippocampal neurons of *GB1^{-/-}*, *BAC^{+/+}* mice. *GABA_{B1}-eGFP* expression was observed as early as day *in vitro* (DIV) 2, predominantly in the soma and the axon. From DIV4, *GABA_{B1}-eGFP* expression was observed in the soma, dendrites and axon.

Furthermore, we demonstrated by examining the ileum and colon that this mouse model can be used as a new tool to localize GABA_B receptor expressing cells in peripheral tissues. In conclusion, the mouse model presented in the following publication provides a validated tool for direct visualization of endogenous GABA_B receptors and therefore allows the study of receptor dynamics under physiological and experimental conditions.

Statement of personal contribution:

- Characterization of the GB1^{-/-}, BAC^{+/+} mouse model including western blot and immunohistochemical analysis of the brain
- Experiments with primary hippocampal neuronal cultures
- Breeding and genotyping of the mice
- Contribution to the preparation of the manuscript
- Design of all figures

TECHNOLOGY REPORT

A Mouse Model for Visualization of GABA_B Receptors

Emilio Casanova,¹ Nicole Guetg,¹ Réjan Vigot,¹ Riad Seddik,¹ Marcela Julio-Pieper,² Niall P. Hyland,^{2,3} John F. Cryan,^{2,3} Martin Gassmann,¹ and Bernhard Bettler^{1*}

¹Department of Biomedicine, Institute of Physiology, University of Basel, Basel, Switzerland

²Alimentary Pharmabiotic Centre, University College Cork, Cork, Ireland

³Department of Pharmacology and Therapeutics, University College Cork, Cork, Ireland

Received 17 December 2008; Revised 22 April 2009; Accepted 26 April 2009

Summary: GABA_B receptors are the G-protein-coupled receptors for the neurotransmitter γ -aminobutyric acid (GABA). Receptor subtypes are based on the subunit isoforms GABA_{B1a} and GABA_{B1b}, which combine with GABA_{B2} subunits to form heteromeric receptors. Here, we used a modified bacterial artificial chromosome (BAC) containing the GABA_{B1} gene to generate transgenic mice expressing GABA_{B1a} and GABA_{B1b} subunits fused to the enhanced green fluorescence protein (eGFP). We demonstrate that the GABA_{B1}-eGFP fusion proteins reproduce the cellular expression patterns of endogenous GABA_{B1} proteins in the brain and in peripheral tissue. Crossing the GABA_{B1}-eGFP BAC transgene into the GABA_{B1}^{-/-} background restores pre and postsynaptic GABA_B functions, showing that the GABA_{B1}-eGFP fusion proteins substitute for the lack of endogenous GABA_{B1} proteins. Finally, we demonstrate that the GABA_{B1}-eGFP fusion proteins replicate the temporal expression patterns of native GABA_B receptors in cultured neurons. These transgenic mice therefore provide a validated tool for direct visualization of native GABA_B receptors. *genesis* 47:595–602, 2009. © 2009 Wiley-Liss, Inc.

Key words: enhanced GFP; enteric; GABA-B; GABA(B); GABA_{B1}; GPCR; transgenic

GABA_B receptors are the G-protein-coupled receptors (GPCRs) for γ -aminobutyric acid (GABA), the main inhibitory neurotransmitter in the brain. They are considered as promising drug targets for the treatment of neurological and psychiatric disorders (Bettler *et al.*, 2004; Bowery *et al.*, 2002). Depending on their subcellular localization, GABA_B receptors exert distinct regulatory effects on synaptic transmission (Couve *et al.*, 2000; Ulrich and Bettler, 2007). Presynaptic GABA_B receptors inhibit the release of GABA (autoreceptors) and other neurotransmitters (heteroreceptors). Postsynaptic GABA_B receptors inhibit neuronal excitability by activating K⁺ channels that shunt excitatory currents and induce membrane hyperpolarization. Functional GABA_B receptors are obligate heteromers composed of GABA_{B1} and

GABA_{B2} subunits (Gassmann *et al.*, 2004; Marshall *et al.*, 1999; Prosser *et al.*, 2001; Schuler *et al.*, 2001). Molecular diversity in the GABA_B system is based on the subunit isoforms GABA_{B1a} and GABA_{B1b}, which are encoded by the same gene but independently regulated at the transcriptional level (Steiger *et al.*, 2004). GABA_{B1a} and GABA_{B1b} constitute two distinct receptor subtypes, GABA_{B(1a,2)}} and GABA_{B(1b,2)}}, which contribute differentially to synaptic and nonsynaptic functions (Ulrich and Bettler, 2007). At hippocampal mossy fiber-to-CA3 and CA3-to-CA1 synapses, mainly GABA_{B1a} assembles heteroreceptors inhibiting glutamate release, while GABA_{B1b} is more abundant at postsynaptic sites (Guetg *et al.*, 2009; Vigot *et al.*, 2006). A large body of work has addressed the regulation of GABA_B receptor assembly and surface trafficking (Bettler and Tiao, 2006). However, the mechanisms regulating the distribution of GABA_B receptors to axons and dendrites are less well understood. Likewise, it remains unclear whether GABA_B receptor localization and surface expression is altered in disease and in response to pharmacological treatment. Mice that allow direct visualization of endogenous GABA_B receptors would therefore be useful to study receptor dynamics under physiological and experimental conditions (Scherrer *et al.*, 2006).

Tagging proteins with GFP from the jellyfish *Aequorea victoria* has been widely used to study the spatial and

Current address for Emilio Casanova: Ludwig Boltzmann Institute for Cancer Research (LBI-CR), Vienna, Austria.

Emilio Casanova and Nicole Guetg contributed equally to this work.

*Correspondence to: Bernhard Bettler, Pharmazentrum, Klingelbergstrasse 50-70, Basel CH-4056, Switzerland.

E-mail: bernhard.bettler@unibas.ch

Contract grant sponsor: Swiss Science Foundation, Contract grant number: 3100A0-117816; Contract grant sponsor: European Community's Seventh Framework Programme (FP7/2007-2013), Contract grant number: Grant Agreement 201714

Published online 14 July 2009 in

Wiley InterScience (www.interscience.wiley.com).

DOI: 10.1002/dvg.20535

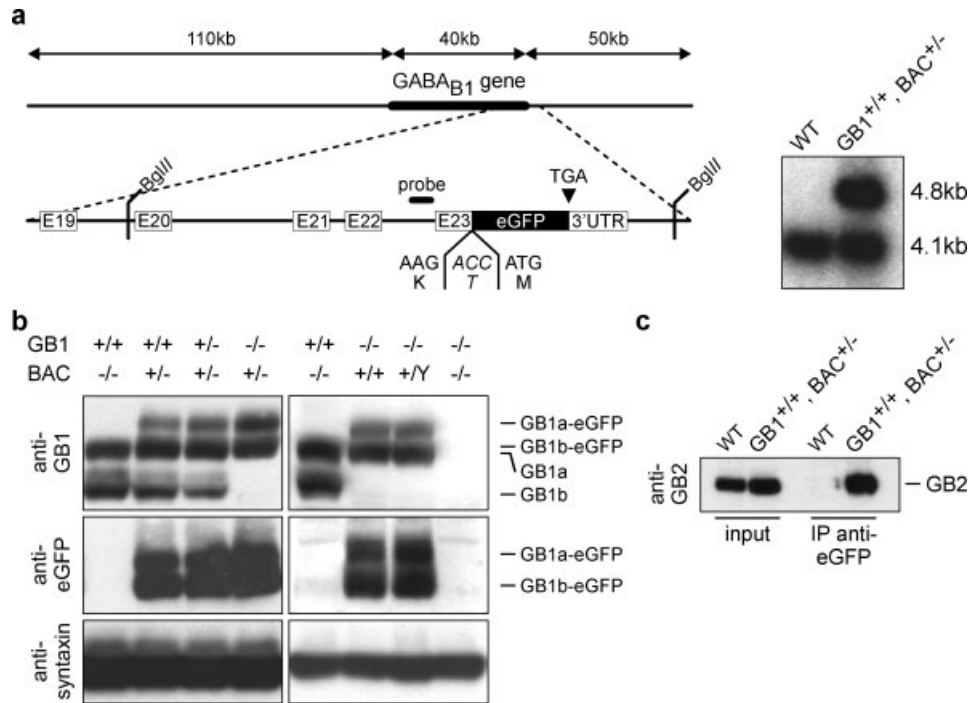


FIG. 1. Generation of a *GABA_{B1}-eGFP* BAC transgenic mouse line. **(a)** Schematic representation of the modified BAC containing the *GABA_{B1}* gene. The eGFP cDNA was inserted in frame 5' of the stop codon (TGA) of exon 23 (E23) in the *GABA_{B1}* gene. The junction sequence between the *GABA_{B1}* C-terminus and the eGFP coding region contains an ACC insertion encoding a threonine (T). The 3' untranslated region (3' UTR) is indicated. Southern blot analysis with the indicated probe detects *Bgl*II restriction fragments of 4.1 and 4.8 kb for the endogenous *GABA_{B1}* gene and the BAC transgene, respectively. **(b)** Immunoblot analysis of total brain lysates prepared from adult mice of different genotypes. In *GB1^{+/+}, BAC^{+/-}* mice, an antibody recognizing the common C-terminus of *GABA_{B1}* (anti-GB1) detects the endogenous *GABA_{B1}* subunit isoforms GB1a and GB1b as well as the C-terminal eGFP fusion proteins GB1a-eGFP and GB1b-eGFP. Of note, GB1b-eGFP and GB1a migrate at a similar molecular weight and are not resolved on the blot. Immunoblot analysis with an anti-eGFP antibody confirms that both GB1a and GB1b are expressed as eGFP fusion proteins from the modified BAC. Anti-syntaxin antibodies control for sample loading. **(c)** Anti-eGFP antibodies co-immunoprecipitate endogenous *GABA_{B2}* protein from total brain lysates of *GB1^{+/+}, BAC^{+/-}* but not of WT control mice. This demonstrates that the *GABA_{B1}-eGFP* fusion proteins associate with *GABA_{B2}* protein in vivo.

temporal expression patterns of proteins in various model organisms. To faithfully recapitulate the endogenous expression patterns, the tagged proteins are ideally expressed under control of promoter elements of their own gene. However, using traditional transgenic approaches that usually rely on promoter elements in the vicinity of the transcriptional start site, the tagged proteins often failed to reproduce the endogenous expression patterns. In particular, this has been a problem when expressing proteins in the mammalian central nervous system (Heintz, 2001). The use of bacterial artificial chromosomes (BACs) for transgenic expression potentially circumvents this problem as BACs are more likely to contain all the cis regulatory elements that are required for accurate expression of the transgene (Yang *et al.*, 1997; Zhang *et al.*, 1998). However, because of the random integration of the BAC into the genome, the expression of the transgene may still be influenced by sequences at the integration site. Moreover, overexpression of genes contained in the BAC in addition to the gene of interest may produce unwanted effects. With these potential drawbacks in mind, BAC transgenic mice have been a very useful tool for analyzing protein distri-

bution and function in the brain. To generate transgenic mice expressing eGFP-tagged *GABA_{B1}* subunits under control of *GABA_{B1}* promoter elements, we therefore resorted to BAC technology.

Specifically, we used homologous recombination in *Escherichia coli* (ET-recombination) to modify a 200 kb BAC encompassing the *GABA_{B1}* gene. The BAC contained 110 kb of upstream and 50 kb of downstream sequences and was therefore likely to harbor most, if not all, regulatory elements that drive expression of the *GABA_{B1a}* and *GABA_{B1b}* subunit isoforms. An eGFP cDNA was inserted in frame at the C-terminus of the *GABA_{B1}* coding sequence (Fig. 1a). Transgenic mice were generated by pronuclear injection of the modified BAC. One founder mouse was identified by Southern blot analysis of genomic tail DNA (Fig. 1a). Breeding of the founder mouse revealed that the BAC transgene was integrated in the X chromosome. BAC transgenic mice were viable and did not express any overt phenotypes. We next analyzed BAC transgenic mice for expression of *GABA_{B1}-eGFP* fusion proteins. Immunoblot analysis of brain membranes showed that, as expected, the subunit isoforms *GABA_{B1a}* and *GABA_{B1b}* are both expressed as

eGFP fusion proteins (Fig 1b). Crossing of the *GABA_{B1}-eGFP* BAC into the *GABA_{B1}^{-/-}* (from here on referred to as *GBI^{-/-}*) background (Schuler *et al.*, 2001) showed a progressive increment in the levels of expression of the GABA_{B1}-eGFP fusion proteins, reaching a maximum when endogenous GABA_{B1} proteins are completely lacking (Fig. 1b, left panels). Because the BAC integrated in the X chromosome, we also compared the expression levels of the GABA_{B1}-eGFP fusion proteins in *GBI^{-/-}, BAC^{+/+}* females and *GBI^{-/-}, BAC^{+/+}* males. The expression levels of the GABA_{B1}-eGFP fusion proteins were similar in both sexes and comparable to the expression level of endogenous GABA_{B1} protein in wild-type (WT; *GBI^{+/+}, BAC^{-/-}*) mice (Fig. 1b, right panels). It is known that GABA_{B2} protein stabilizes the GABA_{B1} proteins (Gassmann *et al.*, 2004). It is therefore likely that the maximal expression levels of the transgenic GABA_{B1}-eGFP fusion proteins cannot exceed the levels of the endogenous GABA_{B1} proteins because of the limited availability of GABA_{B2} protein. Co-immunoprecipitation experiments with anti-eGFP antibodies confirmed that the GABA_{B1}-eGFP fusion proteins heteromerize with endogenous GABA_{B2} protein (Fig. 1c). Immunoblot analysis using antibodies against the common C-terminus of GABA_{B1a} and GABA_{B1b} or against eGFP did not reveal any detectable protein degradation of the fusion proteins (Fig. 1b).

We next examined expression of the GABA_{B1}-eGFP fusion proteins in *GBI^{-/-}, BAC^{+/+}* mice by fluorescence imaging and immunohistochemistry (see Fig. 2). Strong eGFP fluorescence was observed in whole brain as well as in brain sections (Fig. 2a). Immunohistochemistry using anti-GABA_{B1} and anti-eGFP antibodies confirmed that the GABA_{B1}-eGFP fusion proteins are expressed across the entire brain (Fig. 2b), consistent with the known expression pattern of the endogenous GABA_{B1} proteins in WT mice (Fritschy *et al.*, 2004). We also assessed whether the *GBI^{-/-}, BAC^{+/+}* mice can be used to identify cell types expressing GABA_B receptors in peripheral tissues. Given the extensive distribution of GABA_B receptors previously reported in rat intestine (Nakajima *et al.*, 1996), we examined GABA_{B1}-eGFP expression in the mouse ileum and colon (see Fig. 3). GABA_{B1}-eGFP immunoreactivity was observed in both the myenteric and submucosal plexus of longitudinal sections of ileum (Fig. 3a) and colon (Fig. 3b), consistent with the immunostaining for the endogenous GABA_{B1} proteins in WT mice (Fig. 3i,j). Predominantly cytoplasmic GABA_{B1}-eGFP immunoreactivity was detected in whole mount preparations of both the ileum and colon (Fig. 3c,d; submucosal plexus). As a control, no eGFP immunoreactivity was detectable in WT tissues (Fig. 3e-h). No epithelial GABA_{B1}-eGFP was detected in either colonic or ileal preparations, nor did we observe any enteroendocrine-like GABA_{B1}-eGFP, suggesting that GABA_B receptor localization in mouse ileum and colon is almost exclusively neuronal in nature. This is consistent with a prejunctional inhibitory role for GABA_B receptors in modulating ileal contraction, via actions within the

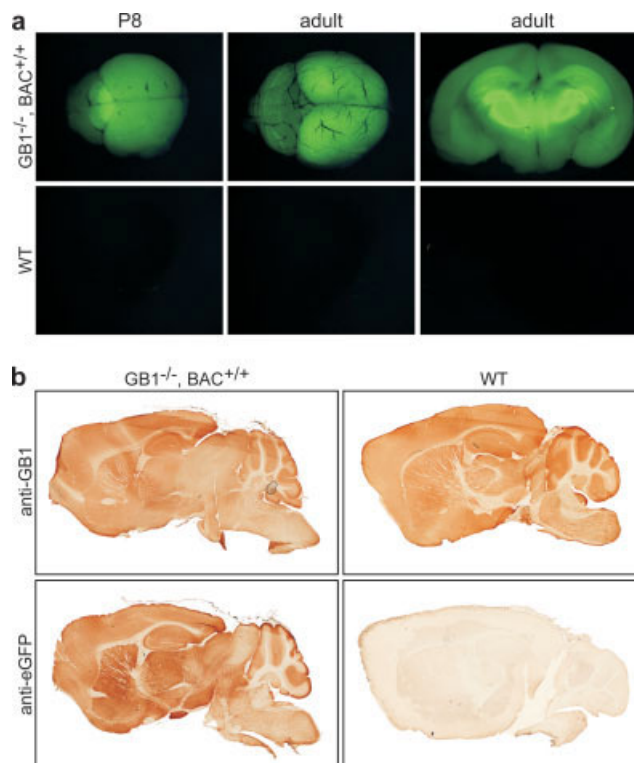


FIG. 2. GABA_{B1}-eGFP fusion proteins reproduce the expression pattern of endogenous GABA_{B1} proteins in the brain. (a) GABA_{B1}-eGFP fluorescence in whole brain of P8 and adult *GBI^{-/-}, BAC^{+/+}* mice. In coronal sections of adult *GBI^{-/-}, BAC^{+/+}* mice strong fluorescence was detected in the hippocampus and the striatum. (b) Immunohistochemistry using anti-GB1 and anti-eGFP antibodies revealed that the GABA_{B1}-eGFP fusion proteins are expressed in the entire brain of adult *GBI^{-/-}, BAC^{+/+}* mice, similar to the expression pattern of endogenous GABA_{B1} proteins in WT mice (top). No specific eGFP-immunoreactivity was detected in WT mice (bottom).

enteric nervous system (Sanger *et al.*, 2002). The *GBI^{-/-}, BAC^{+/+}* mice recently also allowed us to localize GABA_B receptors in cochlear neurons (Maison *et al.*, 2009). This shows that these mice represent a useful tool to identify GABA_B receptors in cells that are not yet linked to GABA_B receptor physiology. Importantly, the eGFP fluorescence allows studying the roles of GABA_B receptors in identified cells, using for example electrophysiological techniques.

GBI^{-/-} mice heterozygous or homozygous for the *GABA_{B1}-eGFP* BAC were fertile and did not show any of the overt behavioral abnormalities described for *GBI^{-/-}* mice, such as sporadic episodes of intensive running and epileptiform activity (Schuler *et al.*, 2001). We next investigated whether the *GABA_{B1}-eGFP* BAC rescues pre and postsynaptic GABA_B receptor functions, which are completely absent in *GBI^{-/-}* mice (Schuler *et al.*, 2001). Using whole-cell patch-clamp recordings in acute hippocampal slices, we first checked for the presence of GABA_B heteroreceptors on excitatory terminals. Stimulation of the Schaffer collateral-commissural fibers induces

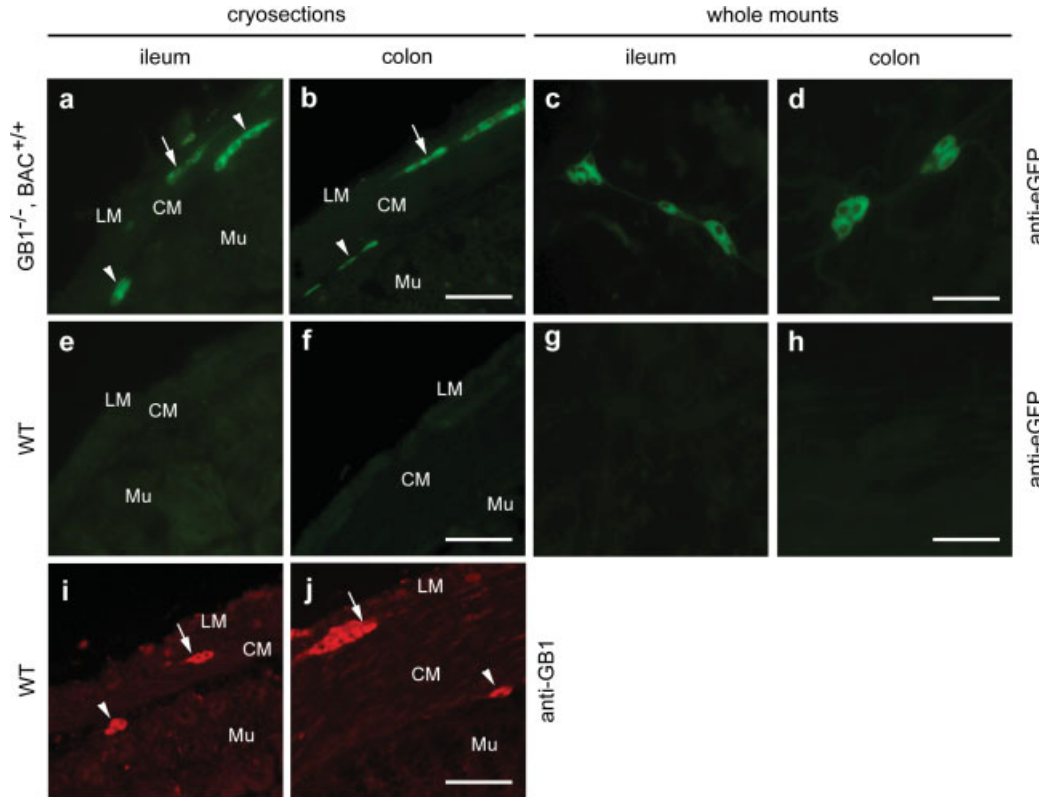


FIG. 3. GABA_{B1}-eGFP expression in the ileum and colon of *GB1*^{-/-}, *BAC*^{+/+} mice. Fluorescence immunohistochemistry using anti-eGFP antibodies revealed GABA_{B1}-eGFP localization in the submucosal (arrowheads) and myenteric plexus (arrows) of *GB1*^{-/-}, *BAC*^{+/+} ileum (a) and colon (b), comparable to the localization of endogenous GABA_{B1} protein in WT sections, as detected with anti-GB1 antibodies (i,j). GABA_{B1}-eGFP was not detected in either the epithelial layer or enteroendocrine cells of *GB1*^{-/-}, *BAC*^{+/+} ileum and colon (a,b). Whole mount preparations of ileum (c) and colon (d) revealed a cytoplasmic, nonnuclear, distribution of GABA_{B1}-eGFP in enteric neurons of *GB1*^{-/-}, *BAC*^{+/+} mice. No GABA_{B1}-eGFP activity was detected in WT tissues (e-h). Scale bars = 100 μm. LM, longitudinal muscle; CM, circular muscle; Mu, mucosa.

excitatory postsynaptic currents (EPSCs) in CA1 pyramidal neurons, which are reduced by blocking the release of glutamate through activation of GABA_B heteroreceptors. Baclofen (50 μM), a GABA_B agonist, was similarly effective in reducing the EPSC amplitude in WT and *GB1*^{-/-}, *BAC*^{+/+} mice (Fig. 4a). Next, we examined autoreceptor-mediated responses to baclofen on GABAergic terminals. We recorded inhibitory postsynaptic currents (IPSCs) in CA1 pyramidal neurons in the presence of the ionotropic glutamate receptor antagonist kynurenatate (2 mM). Baclofen reduced the amplitude of IPSCs in both genotypes (Fig. 4b). Finally, we assessed postsynaptic GABA_B receptors, which induce a late IPSC by activating Kir3-type K⁺ channels (Luscher *et al.*, 1997). At a holding potential of -50 mV and in physiological extracellular K⁺ concentration, baclofen at 1, 10, or 100 μM elicited similar outward currents in CA1 pyramidal neurons in WT and *GB1*^{-/-}, *BAC*^{+/+} mice (Fig. 4c,d). Normalization of the current amplitudes to cell capacitance showed that there were no significant differences in the baclofen-induced current densities between WT and *GB1*^{-/-}, *BAC*^{+/+} mice (WT: 2.2 ± 0.3 pA/pF, *n* = 10; *GB1*^{-/-}, *BAC*^{+/+}: 2.3 ± 0.2 pA/pF, *n* = 22; *P* = 0.78). In conclusion, the *GABA_{B1}-eGFP* BAC restores

normal GABA_B functions in mice lacking endogenous GABA_{B1} subunits, thus demonstrating that the GABA_{B1}-eGFP fusion proteins fully substitute for the lack of endogenous GABA_{B1a} and GABA_{B1b} proteins.

We finally assessed expression of the GABA_{B1}-eGFP fusion proteins in cultured primary hippocampal neurons, which are widely used to study the dynamics of receptor trafficking. The subcellular distribution of GABA_{B1}-eGFP protein was studied by fluorescence imaging of neurons established from embryos obtained from *GB1*^{-/-}, *BAC*^{+/+} females mated with *GB1*^{-/-}, *BAC*^{+/+} males (Fig. 5a). GABA_{B1}-eGFP fluorescence was detected as early as 2 days in vitro (DIV). At this stage, the GABA_{B1}-eGFP fusion proteins were mainly present in the soma as well as in axon-like processes expressing the marker protein Tau1 (Kosik and Finch, 1987). From DIV4 on, the GABA_{B1}-eGFP fusion proteins were also observed in dendritic processes expressing the marker protein microtubule-associated protein 2 (MAP2) (Caceres *et al.*, 1986). Interestingly, a strong green fluorescence signal was often observed in the distensions at the termini of growing axons, most likely representing axonal growth cones. At DIV14, the GABA_{B1}-eGFP fusion proteins displayed a punctuate distribution in the

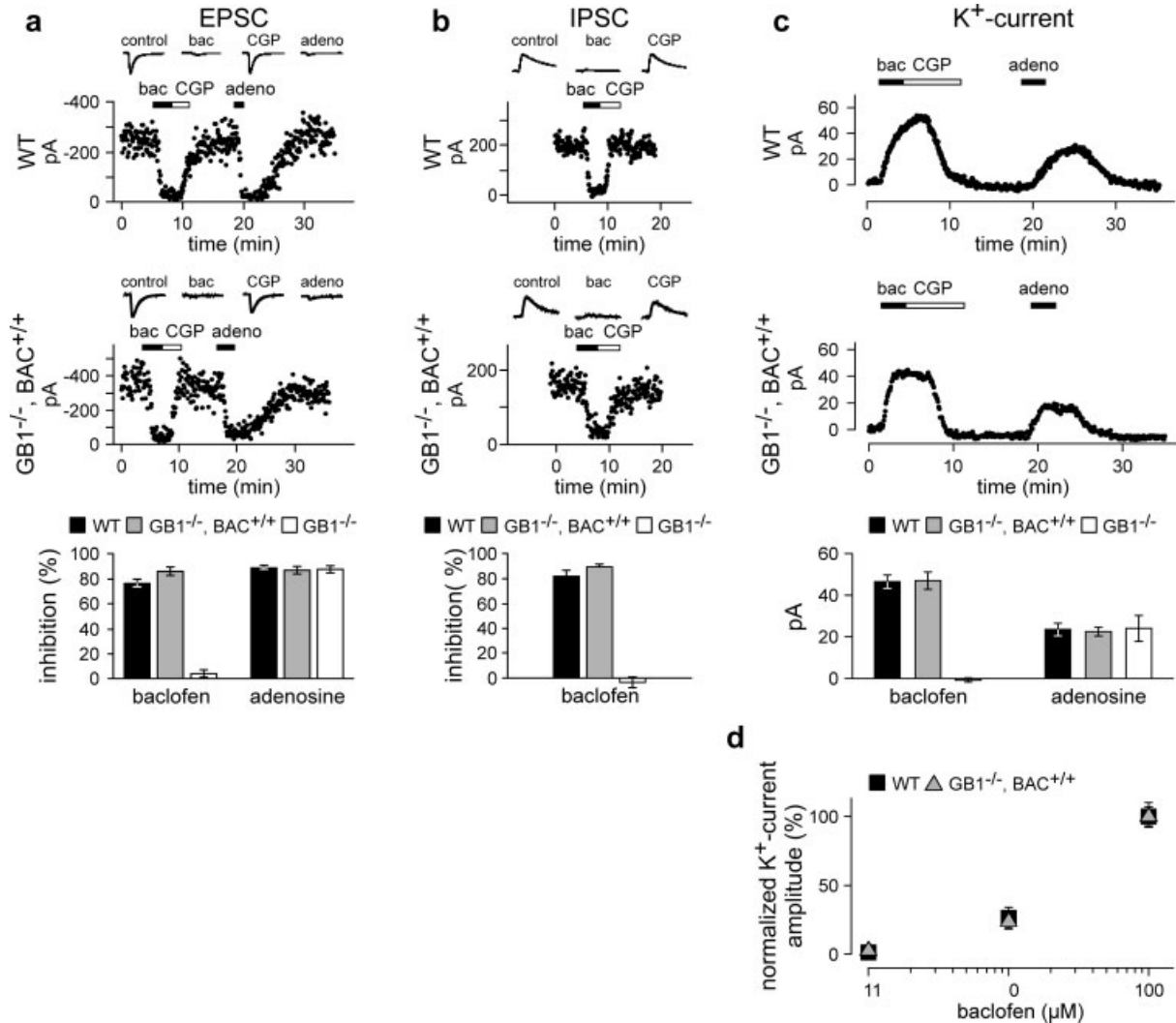


FIG. 4. GABA_{B1}-eGFP fusion proteins assemble with endogenous GABA_{B2} protein into functional pre and postsynaptic GABA_B receptors. (a) Rescue of GABA_B heteroreceptor function in CA1 pyramidal neurons of *GB1^{-/-}, BAC^{+/+}* mice. Peak amplitudes and representative traces plotted over time and summary bar graph of monosynaptic EPSC inhibition by baclofen (bac, 50 μM) and adenosine (adeno, 100 μM). Baclofen similarly depressed the amplitude of EPSCs in WT (76.5% ± 3.1% inhibition, *n* = 6) and *GB1^{-/-}, BAC^{+/+}* (86.3% ± 3.2% inhibition, *n* = 3), but not in *GB1^{-/-}* (4.0% ± 3.0% inhibition, *n* = 5) mice. As a control, adenosine-induced depression of EPSC amplitudes did not differ between genotypes (WT: 89.1% ± 1.6% inhibition, *n* = 6; *GB1^{-/-}, BAC^{+/+}*: 87.2% ± 3.1% inhibition, *n* = 3; *GB1^{-/-}*: 89.5% ± 2.8% inhibition, *n* = 5). (b) Rescue of GABA_B autoreceptor function in *GB1^{-/-}, BAC^{+/+}* mice. Peak amplitudes and representative traces plotted versus time and summary bar graph of IPSC inhibition by baclofen (50 μM). Baclofen depressed the amplitude of IPSCs to the same extent in WT (82.7% ± 4.8% inhibition, *n* = 6) and *GB1^{-/-}, BAC^{+/+}* (90.1% ± 2.3% inhibition, *n* = 4) but not in *GB1^{-/-}* (-3.4% ± 4.2% inhibition, *n* = 5) mice. (c) Rescue of postsynaptic GABA_B receptor function in *GB1^{-/-}, BAC^{+/+}* mice. Changes in the holding currents of CA1 pyramidal neurons and summary bar graph of the amplitudes of baclofen- and adenosine-induced K⁺ currents. The baclofen-induced K⁺ outward current is similar in WT (46.5 ± 3.2 pA, *n* = 10) and *GB1^{-/-}, BAC^{+/+}* (46.9 ± 4.1 pA, *n* = 22) and absent in *GB1^{-/-}* (-0.8 ± 0.7 pA, *n* = 5) mice. Control adenosine-induced currents did not differ between genotypes (WT: 23.5 ± 3.1 pA, *n* = 9; *GB1^{-/-}, BAC^{+/+}*: 22.5 ± 2.1 pA, *n* = 19; *GB1^{-/-}*: 25.3 ± 5.0 pA, *n* = 5). (d) Normalized K⁺ current amplitudes in response to increasing concentrations of baclofen. No significant differences were observed between WT and *GB1^{-/-}, BAC^{+/+}* neurons at 1, 10, and 100 μM. All baclofen-induced responses were fully blocked by the GABA_B antagonist CGP54626A (CGP, 1 μM). Values are represented as means ± SEM.

somatodendritic compartment, as previously described for the endogenous GABA_{B1} proteins (Correa *et al.*, 2004). In addition, the dense plexus of fine-caliber axonal processes extending throughout the cultures also expressed GABA_{B1}-eGFP fusion proteins. At all developmental stages, the GABA_{B1}-eGFP fusion proteins dis-

played a subcellular distribution similar to that of the endogenous GABA_{B1} proteins (Fig. 5b).

In conclusion, we have generated a BAC transgenic mouse line that faithfully expresses GABA_{B1a}-eGFP and GABA_{B1b}-eGFP fusion proteins under control of transgenic *GABA_{B1}* promoter elements. We show that the

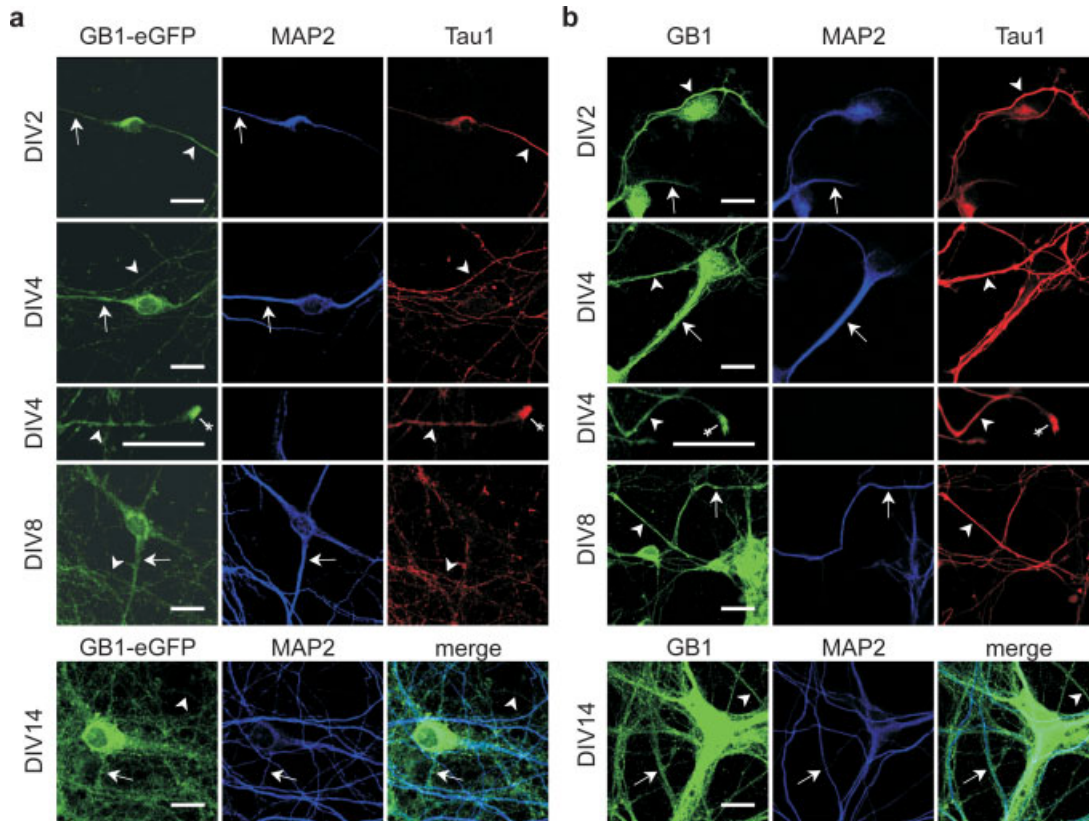


FIG. 5. GABA_{B1}-eGFP fusion proteins replicate the temporal expression pattern of endogenous GABA_{B1} subunits in cultured hippocampal neurons. Fluorescence detection of GABA_{B1}-eGFP expression in cultured primary hippocampal neurons derived from *GB1*^{-/-}, *BAC*^{+/+} or *GB1*^{-/-}, *BAC*^{+/-} embryos (a) compared to endogenous GABA_{B1} immunostaining in WT neurons (b). Somatodendritic and axonal compartments were identified using antibodies directed against MAP2 (blue) and Tau1 (red), respectively. (a) At DIV2, GABA_{B1}-eGFP is predominantly observed in the soma and in the axon (arrowhead) but not in dendrites (arrow). From day DIV4, eGFP fluorescence is evident throughout the soma, axon, and dendrites. Strong eGFP fluorescence was observed in the distensions at the termini of growing axons, indicated by an asterisk (DIV4, lower panels). At DIV14, eGFP fluorescence displayed a punctuate distribution in the somatodendritic compartment (MAP2-positive) as well as in axonal processes extending throughout the cultures (MAP2-negative). The merged image of the green and blue channel is shown on the right. At all developmental stages the distribution of GABA_{B1}-eGFP fluorescence was similar to the distribution of the endogenous GABA_{B1} proteins in WT neurons (b). Scale bars = 10 μm.

eGFP-tagged GABA_{B1} subunits combine with endogenous GABA_{B2} subunits to form fully functional pre and postsynaptic GABA_B receptors. These mice therefore provide a useful tool to visualize the spatio-temporal distribution of GABA_B receptors in vivo and in vitro.

METHODS

Generation of *GABA_{B1}-eGFP BAC* Transgenic Mice

The BAC clone RP23-98F21 (Children Hospital Oakland Research Institute, CA) containing the *GABA_{B1}* gene was modified by homologous recombination in *E. coli* (ET-recombination) using standard techniques (Casanova *et al.*, 2001; Zhang *et al.*, 1998). In the targeting construct the eGFP cDNA was inserted in front of the stop codon of the *GABA_{B1}* gene generating a C-terminal fusion protein. The 200 bp 5' homology arm upstream of the stop codon was amplified from the *GABA_{B1}* BAC using primers P1 (5'-CCCACACTCCCAATTGTGTTT-3')

and P2 (5'-CCATGGTCTTGTAAGCAAATGTACTCG-3'). The 200 bp 3' homology arm within the 3' untranslated region was amplified with primers P3 (5'-TTAATTAATTCGAGAAGGATGAGGCCAGC-3') and P4 (5'-GCTAGCGAATAGCTCCAAGCAGGGTTC-3'). Downstream of the eGFP the targeting construct contained an ampicillin cassette flanked by two FRT sites. Correct homologous recombination of the targeting construct with the *GABA_{B1}* BAC was confirmed by Southern blot analysis and direct sequencing of the recombined BAC. The ampicillin cassette was removed from the modified BAC by expressing the FLP recombinase in BAC-containing bacteria (Buchholz *et al.*, 1996). The isolated BAC DNA was linearized with the homing endonuclease PI-*SceI* (New England Biolabs), purified by pulse-field electrophoresis and injected into the pronucleus of B6D2/F1 oocytes at 1 ng/μl. *GABA_{B1}-eGFP* BAC transgenic mice were backcrossed three times to BALB/c mice and genotyped by PCR using primers P6 (5'-CACATGGTCCTGCTGGAGTTCGTG-3') and P7 (5'-CAAACGAGATGCCCC

TCTGGAGTC-3') yielding a band of 390 bp for the BAC transgene.

Whole Brain eGFP Imaging and Immunohistochemistry

For eGFP imaging, brains were removed and washed in phosphate buffered saline (PBS; pH 7.4) at 4°C. Whole brains and 1 mm coronal sections were imaged with a Zeiss Axiovert 25 binocular equipped for GFP detection. For immunohistochemistry, adult mice were perfused with 4% paraformaldehyde (PFA; Sigma-Aldrich) in PBS; pH 7.4. Brains were removed and postfixed overnight in 4% PFA at 4°C. Fifty micrometer parasagittal vibratome sections were blocked in PBS with 0.3% Triton X-100 (Sigma-Aldrich) and 10% normal goat serum (NGS) and probed with rabbit polyclonal anti-eGFP antibody (1:200; Molecular Probes, Invitrogen) or anti-GABA_{B1} antibody Ab174.1 (1:200) (Malitschek *et al.*, 1998). Immunostaining was visualized with an ABC kit (Vector Labs). For immunohistochemistry of the enteric nervous system, animals were killed by cervical dislocation, and ileum and colon removed. Submucosal plexus preparations were prepared as described (Nasser *et al.*, 2006). For longitudinal sections, segments of colon and ileum were flushed with PBS, fixed overnight at 4°C in 4% PFA, transferred to 30% sucrose, and cryosectioned at 10 µm. Tissues were permeabilized in PBS, 0.1% Triton X-100, blocked in 5% donkey serum, and probed with rabbit polyclonal anti-eGFP antibody (1:500) or anti-GABA_{B1} antibody Ab25 (1:1,000) (Engle *et al.*, 2006). Immunostaining was visualized using FITC-conjugated secondary antibody (1:400; Jackson ImmunoResearch).

Immunoblot and Immunoprecipitation

Mouse brain membranes were prepared as described (Gassmann *et al.*, 2004). For Western blot analysis 50 µg protein were separated by 8% SDS-PAGE, blotted and probed with rabbit polyclonal anti-GABA_{B1} antibody Ab174.1 (1:3,000) recognizing the common C-terminus of GABA_{B1a} and GABA_{B1b}, rabbit polyclonal anti-eGFP antibody (1:2,000; Molecular Probes), or mouse monoclonal anti-syntaxin antibody (1:10,000; Sigma-Aldrich) and peroxidase-conjugated secondary antibodies (1:3,000; Amersham Biosciences). For immunoprecipitation, brain membranes were resuspended in RIPA buffer without SDS (50 mM Tris-HCl pH 7.4, 150 mM NaCl, 1% NP-40, 0.5% DOC) and centrifuged at 10,000g for 30 min to remove insoluble material. Supernatants (1 mg protein) were precleared for 3 h with 50 µl of Protein G-agarose beads (Roche), incubated with 2.5 µg mouse monoclonal anti-eGFP antibody (Molecular probes) for 1 h followed by an overnight incubation with 50 µl protein G-agarose beads. Immunoprecipitated complexes were washed three times with RIPA buffer, separated by 8% SDS-PAGE, blotted and probed with polyclonal guinea pig anti-GABA_{B2} antibody (1:5000; Chemicon).

Electrophysiology

Standard procedures were used to prepare 300 µm thick parasagittal hippocampal slices from P18 to P28 mice. Pre and postsynaptic GABA_B responses were assessed by visualized whole-cell patch-clamp recording techniques from CA1 pyramidal neurons as described previously (Vigot *et al.*, 2006). For dose-response experiments, baclofen at different concentrations was bath applied at 10 min intervals. Recordings were amplified with an Axopatch 200B (Axon Instruments), filtered at 2 kHz, digitized at 10 kHz and analyzed with pClamp9 (Axon Instruments). Data are expressed as means ± SEM.

Neuronal Cultures and Immunocytochemistry

Hippocampal neurons were prepared from 16.5-day mouse embryos and cultured at a density of ~ 750 cells/mm² on poly-L-lysine coated glass cover slips (Brewer, 1993; Goslin *et al.*, 1998). Neurons were fixed with 4% PFA in PBS containing 120 mM sucrose for 20 min at room temperature (RT), permeabilized with 0.25% Triton-X-100 in PBS for 10 min, and blocked for 2 h in 10% NGS. Antibodies were diluted in 10% NGS and incubated at RT for 2 h. Primary antibodies: rabbit anti-GABA_{B1} Ab174.1 (1:500), chicken anti-MAP2 (1:100; Abcam), and mouse anti-Tau1 (1:700; Chemicon). Secondary antibodies: Alexa goat anti-chicken 647 and goat anti-mouse 568 (1:500; Molecular Probes). Images were acquired on a Leica TCS SPE confocal microscope and identically processed with ImageJ software (NIH).

ACKNOWLEDGMENT

We thank Thorsten Fritzius for helpful comments on the manuscript.

LITERATURE CITED

- Bettler B, Kaupmann K, Mosbacher J, Gassmann M. 2004. Molecular structure and physiological functions of GABA_B receptors. *Physiol Rev* 84:835-867.
- Bettler B, Tiao JY. 2006. Molecular diversity, trafficking and subcellular localization of GABA_B receptors. *Pharmacol Ther* 110:533-543.
- Bowery NG, Bettler B, Froestl W, Gallagher JP, Marshall F, Raiteri M, Bonner TI, Enna SJ. 2002. International Union of Pharmacology. XXXIII. Mammalian γ -aminobutyric acid_B receptors: Structure and function. *Pharmacol Rev* 54:247-264.
- Brewer GJ. 1993. Optimized survival of hippocampal neurons in B-27 supplemented Neurobasal, a new serum-free medium combination. *J Neurosci Res* 35:567-576.
- Buchholz F, Angrand PO, Stewart AF. 1996. A simple assay to determine the functionality of Cre or FLP recombination targets in genomic manipulation constructs. *Nucleic Acids Res* 24:3118-3119.
- Caceres A, Banker GA, Binder L. 1986. Immunocytochemical localization of tubulin and microtubule-associated protein 2 during the development of hippocampal neurons in culture. *J Neurosci* 6: 714-722.
- Casanova E, Fehsenfeld S, Mantamadiotis T, Lemberger T, Greiner E, Stewart AF, Schutz G. 2001. A CamKII α iCre BAC allows brain-specific gene inactivation. *Genesis* 31:37-42.
- Correa SA, Munton R, Nishimune A, Fitzjohn S, Henley JM. 2004. Development of GABA_B subunits and functional GABA_B receptors in rat cultured hippocampal neurons. *Neuropharmacology* 47:475-484.

- Couve A, Moss SJ, Pangalos MN. 2000. GABA_B receptors: A new paradigm in G protein signaling. *Mol Cell Neurosci* 16:296-312.
- Engle MP, Gassman M, Sykes KT, Bettler B, Hammond DL. 2006. Spinal nerve ligation does not alter the expression or function of GABA_B receptors in spinal cord and dorsal root ganglia of the rat. *Neuroscience* 138:1277-1287.
- Fritschy JM, Sidler C, Parpan F, Gassmann M, Kaupmann K, Bettler B, Benke D. 2004. Independent maturation of the GABA_B receptor subunits GABA_{B1} and GABA_{B2} during postnatal development in rodent brain. *J Comp Neurol* 477:235-252.
- Gassmann M, Shaban H, Vigot R, Sansig G, Haller C, Barbieri S, Humeau Y, Schuler V, Muller M, Kinzel B, Klebs K, Schmutz M, Froestl W, Heid J, Kelly PH, Gentry C, Jatón AL, Van der Putten H, Mombereau C, Lecourtier L, Mosbacher J, Cryan JF, Fritschy JM, Luthi A, Kaupmann K, Bettler B. 2004. Redistribution of GABA_{B(1)} protein and atypical GABA_B responses in GABA_{B(2)}-deficient mice. *J Neurosci* 24:6086-6097.
- Goslin K, Asmussen H, Banker G. 1998. Rat hippocampal neurons in low-density culture. In: Banker G, Goslin K, editors. *Culturing nerve cells*, 2nd ed. Cambridge, MA: MIT Press. pp 339-370.
- Guéteg N, Seddik R, Vigot R, Turecek R, Gassmann M, Vogt KE, Brauner-Osborne H, Shigemoto R, Kretz O, Frotscher M, Kulik A, Bettler B. 2009. The GABA_{B1a} isoform mediates heterosynaptic depression at hippocampal mossy fiber synapses. *J Neurosci* 29:1414-1423.
- Heintz N. 2001. BAC to the future: The use of bac transgenic mice for neuroscience research. *Nat Rev Neurosci* 2:861-870.
- Kosik KS, Finch EA. 1987. MAP2 and tau segregate into dendritic and axonal domains after the elaboration of morphologically distinct neurites: An immunocytochemical study of cultured rat cerebrum. *J Neurosci* 7:3142-3153.
- Lüscher C, Jan LY, Stoffel M, Malenka RC, Nicoll RA. 1997. G protein-coupled inwardly rectifying K⁺ channels (GIRKs) mediate postsynaptic but not presynaptic transmitter actions in hippocampal neurons. *Neuron* 19:687-695.
- Maison SF, Casanova E, Holstein GR, Bettler B, Liberman MC. 2009. Loss of GABA_B receptors in cochlear neurons: Threshold elevation suggests modulation of outer hair cell function by type II afferent fibers. *J Assoc Res Otolaryngol* 10:50-63.
- Malitschek B, Rüegg D, Heid J, Kaupmann K, Bittiger H, Fröstl W, Bettler B, Kuhn R. 1998. Developmental changes in agonist affinity at GABA_{B(1)} receptor variants in rat brain. *Mol Cell Neurosci* 12:56-64.
- Marshall FH, Jones KA, Kaupmann K, Bettler B. 1999. GABA_B receptors—The first 7TM heterodimers. *Trends Pharmacol Sci* 20:396-399.
- Nakajima K, Tooyama I, Kuriyama K, Kimura H. 1996. Immunohistochemical demonstration of GABA_B receptors in the rat gastrointestinal tract. *Neurochem Res* 21:211-215.
- Nasser Y, Ho W, Sharkey KA. 2006. Distribution of adrenergic receptors in the enteric nervous system of the guinea pig, mouse, and rat. *J Comp Neurol* 495:529-553.
- Prosser HM, Gill CH, Hirst WD, Grau E, Robbins M, Calver A, Soffin EM, Farmer CE, Lanneau C, Gray J, Schenck E, Warmerdam BS, Clapham C, Reavill C, Rogers DC, Stean T, Upton N, Humphreys K, Randall A, Geppert M, Davies CH, Pangalos MN. 2001. Epileptogenesis and enhanced prepulse inhibition in GABA_{B(1)}-deficient mice. *Mol Cell Neurosci* 17:1059-1070.
- Sanger GJ, Munonyara ML, Dass N, Prosser H, Pangalos MN, Parsons ME. 2002. GABA_B receptor function in the ileum and urinary bladder of wildtype and GABA_{B(1)} subunit null mice. *Auton Autacoid Pharmacol* 22:147-154.
- Scherrer G, Tryoen-Toth P, Filliol D, Matifas A, Laustriat D, Cao YQ, Basbaum AI, Dierich A, Vonesh JL, Gaveriaux-Ruff C, Kieffer BL. 2006. Knockin mice expressing fluorescent delta-opioid receptors uncover G protein-coupled receptor dynamics in vivo. *Proc Natl Acad Sci USA* 103:9691-9696.
- Schuler V, Lüscher C, Blanchet C, Klux N, Sansig G, Klebs K, Schmutz M, Heid J, Gentry C, Urban L, Fox A, Spooren W, Jatón AL, Vigouret JM, Pozza M, Kelly PH, Mosbacher J, Froestl W, Käslin E, Korn R, Bischoff S, Kaupmann K, van der Putten H, Bettler B. 2001. Epilepsy, hyperalgesia, impaired memory, and loss of pre- and postsynaptic GABA_B responses in mice lacking GABA_{B(1)}. *Neuron* 31:47-58.
- Steiger JL, Bandyopadhyay S, Farb DH, Russek SJ. 2004. cAMP response element-binding protein, activating transcription factor-4, and upstream stimulatory factor differentially control hippocampal GABA_BR1a and GABA_BR1b subunit gene expression through alternative promoters. *J Neurosci* 24:6115-6126.
- Ulrich D, Bettler B. 2007. GABA_B receptors: Synaptic functions and mechanisms of diversity. *Curr Opin Neurobiol* 17:298-303.
- Vigot R, Barbieri S, Brauner-Osborne H, Turecek R, Shigemoto R, Zhang YP, Lujan R, Jacobson LH, Biermann B, Fritschy JM, Vacher CM, Muller M, Sansig G, Guéteg N, Cryan JF, Kaupmann K, Gassmann M, Oertner TG, Bettler B. 2006. Differential compartmentalization and distinct functions of GABA_B receptor variants. *Neuron* 50:589-601.
- Yang XW, Model P, Heintz N. 1997. Homologous recombination based modification in *Escherichia coli* and germline transmission in transgenic mice of a bacterial artificial chromosome. *Nat Biotechnol* 15:859-865.
- Zhang Y, Buchholz F, Muirers JP, Stewart AF. 1998. A new logic for DNA engineering using recombination in *Escherichia coli*. *Nat Genet* 20:123-128.

**6.4. NMDA Receptor-Dependent GABA_B Receptor Internalization via CaMKII
Phosphorylation of Serine 867 in GABA_{B1}**

Guetg N*, Abdel Aziz S*, Holbro N, Turecek R, Rose T, Seddik R, Gassmann M, Moes S, Jenoe P, Oertner TG, Casanova E and Bettler B

Submitted (PNAS)

*Authors contributed equally to this work.

Statement of personal contribution:

- Design and realization of all functional experiments in primary hippocampal neuronal cultures
- Quantitative analysis of GABA_B surface levels
- Design and realization biochemical experiments
- Preparation of the entire manuscript
- Design of all figures

NMDA Receptor-Dependent GABA_B Receptor Internalization via CaMKII Phosphorylation of Serine 867 in GABA_{B1}

Nicole Guetg^{a,1}, Said Abdel Aziz^{a,1}, Niklaus Holbro^b, Rostislav Turecek^{a,c}, Tobias Rose^b, Riad Seddik^a, Martin Gassmann^a, Suzette Moes^d, Paul Jenoe^d, Thomas G. Oertner^b, Emilio Casanova^{a,2} and Bernhard Bettler^{a,3}

^aDepartment of Biomedicine, Institute of Physiology, Pharmazentrum, University of Basel, 4056 Basel, Switzerland; ^bFriedrich Miescher Institute for Biomedical Research, 4058 Basel, Switzerland; ^cInstitute of Experimental Medicine ASCR, 14220 Prague, Czech Republic; ^dBiozentrum, University of Basel, 4056 Basel, Switzerland.

¹N.G. and S.A.A. contributed equally to this work.

²Present address: Ludwig Boltzmann Institute for Cancer Research, Vienna, Austria

³To whom correspondence should be addressed: Bernhard Bettler, Pharmazentrum, Klingelbergstrasse 50-70, CH-4056 Basel, Switzerland. Phone: ++41 61 267 1632. Fax: ++41 61 267 1628. E-mail: bernhard.bettler@unibas.ch.

The authors declare no conflict of interest.

Key words: γ -aminobutyric acid, GABA(B), GABA-B, spines, endocytosis

Abstract

GABA_B receptors are the G-protein coupled receptors for γ -aminobutyric acid (GABA), the main inhibitory neurotransmitter in the brain. GABA_B receptors are abundant on dendritic spines, where they dampen postsynaptic excitability and inhibit Ca²⁺ influx through N-methyl-D-aspartic acid (NMDA) receptors when activated by spillover of GABA from neighboring GABAergic terminals. Here, we show that an excitatory signaling cascade enables spines to counteract this GABA_B-mediated inhibition. We found that NMDA application to cultured hippocampal neurons promotes dynamin-dependent endocytosis of GABA_B receptors. NMDA-dependent internalization of GABA_B receptors requires activation of Ca²⁺/Calmodulin-dependent protein kinase II (CaMKII), which associates with GABA_B receptors *in vivo* and phosphorylates serine 867 (S867) in the intracellular C-terminus of the GABA_{B1} subunit. Blockade of either CaMKII or phosphorylation of S867 renders GABA_B receptors refractory to NMDA-mediated internalization. Time-lapse two-photon imaging of organotypic hippocampal slices reveals that activation of NMDA receptors removes GABA_B receptors within minutes from the surface of dendritic spines and shafts. NMDA-dependent phosphorylation of S867 is detectable at the GABA_{B1b} subunit isoform, which is the isoform that clusters with inhibitory effector K⁺ channels in the spines. Consistent with this, NMDA receptor activation in neurons impairs the ability of GABA_B receptors to activate K⁺ channels. Thus, our data support that NMDA receptor activity endocytoses postsynaptic GABA_B receptors through CaMKII-mediated phosphorylation of S867. This provides a means to spare NMDA receptors at individual glutamatergic synapses from reciprocal inhibition through GABA_B receptors.

Introduction

GABA_B receptors modulate the excitability of neurons throughout the brain. They are therapeutic targets for a variety of disorders, including cognitive impairments, addiction, anxiety, depression and epilepsy (1). Depending on their subcellular localization GABA_B receptors exert distinct regulatory effects on synaptic transmission (2-4). Presynaptic GABA_B receptors inhibit neurotransmitter release (5,6). Postsynaptic GABA_B receptors dampen neuronal excitability by gating Kir3-type K⁺ channels, which generates slow inhibitory postsynaptic potentials (IPSPs) and local shunting (7). Molecular diversity in the GABA_B system arises from the GABA_{B1a} and GABA_{B1b} subunit isoforms, both of which combine with GABA_{B2} subunits to form the heteromeric receptor subtypes GABA_{B(1a,2)}} and GABA_{B(1b,2)}} (8). Genetically modified mice revealed that the two receptor subtypes convey non-redundant synaptic functions at glutamatergic synapses, owing to their differing distribution to axonal and dendritic compartments (3,9). Selectively GABA_{B(1a,2)}} receptors control the release of glutamate while predominantly GABA_{B(1b,2)}} receptors activate postsynaptic Kir3 channels in dendritic spines (10-12). Activation of GABA_B receptors on spines inhibits NMDA receptors through hyperpolarization and the PKA pathway, which enhances Mg²⁺ block (13,14) and reduces Ca²⁺ permeability (15) of NMDA receptors. Reciprocally, there is evidence that glutamate receptors decrease surface expression of GABA_B receptors (16-18). This supports that glutamate receptors and GABA_B receptors crosstalk with each other in dendrites and spines.

Neither the glutamate receptors nor the signaling pathways controlling surface availability of GABA_B receptors have been identified yet. Here we show that NMDA receptor-dependent phosphorylation via CaMKII targets GABA_B receptors for internalization. This postsynaptic regulation of GABA_B receptors has implications for the control of local excitability and Ca²⁺-dependent neuronal functions.

Results

NMDA receptors mediate GABA_B receptor internalization. We used transfected cultured hippocampal neurons to identify the glutamate receptors regulating cell surface expression of GABA_B receptors. Robust cell surface expression of tagged GABA_{B1b} subunits (HA-GB1b-eGFP) was observed upon co-transfection with GABA_{B2} subunits (Fig. 1A), which are mandatory for GABA_{B1} surface expression (8,19,20). GABA_{B1b} surface expression was monitored by immunolabeling of the extracellular HA-tag prior to permeabilization of cells (red fluorescence). Total GABA_{B1b} expression was monitored by immunolabeling of the intracellular eGFP-tag after permeabilization of cells (green fluorescence). To quantify the level of surface GABA_{B1b} protein, we calculated the ratio of red to green fluorescence intensity (Fig. 1B and C). Upon glutamate treatment (50 μM glutamate/5 μM glycine for 30 min), surface GABA_{B1b} protein was significantly reduced ($41.4 \pm 5.3\%$ of control, $n = 10$, $P < 0.001$), consistent with published data (18). The NMDA receptor antagonist APV (100 μM for 2 h) prevented the glutamate-induced decrease in surface GABA_{B1b} protein ($98.4 \pm 12.6\%$ of control, $n = 9$, $P > 0.05$). We tested whether a selective activation of NMDA receptors is sufficient to decrease surface GABA_{B1b} protein. Following NMDA treatment (75 μM NMDA/5 μM glycine for 3 min) and recovery in conditioned medium for 27 min, surface GABA_{B1b} protein was significantly reduced ($54.8 \pm 3.2\%$ of control, $n = 10$, $P < 0.01$). Heteromerization with GABA_{B2} is mandatory for exit of GABA_{B1} from the endoplasmic reticulum and for receptor function (19,20). As expected from the assembly with GABA_{B1}, surface GABA_{B2} protein was also significantly decreased following glutamate or NMDA application and this decrease was prevented by APV (Fig. S1A). We also observed a trend towards decreased surface GABA_{B1a} protein in response to glutamate or NMDA but this did not reach statistical significance (Fig. S1B). Likewise, surface biotinylation of the endogenous GABA_B subunits in NMDA-treated cultured cortical neurons showed that GABA_{B1b} was more efficiently removed from the cell surface than GABA_{B1a} (Fig. 2B). Endogenous surface GABA_{B2} protein was also significantly down-regulated following NMDA treatment (Fig. 2B). This supports that preferentially the GABA_{B(1b,2)}} receptor subtype is removed from the cell surface in response to NMDA application, possibly as a consequence of its selective localization in the somatodendritic compartment (10).

We examined whether the decrease in surface GABA_{B1b} protein following glutamate or NMDA treatment is due to endocytosis. We observed basal endocytosis of surface GABA_{B1b} protein under control conditions (Fig. S2A), as reported (21). Glutamate or NMDA treatment visibly increased endocytosis of GABA_{B1b} protein, which was inhibited in the presence of APV (Fig. S2A).

Constitutively internalized GABA_{B1b} protein co-localized with Rab11-eGFP (22,23), a marker for recycling endosomes (Fig. S2B). Following glutamate or NMDA treatment a fraction of internalized GABA_{B1b} protein segregated into structures devoid of Rab11-eGFP, possibly indicating GABA_{B1b} protein targeted for degradation (24,25). Preincubation of neurons with dynasore (80 μM for 15 min), a cell-permeable inhibitor of dynamin-dependent endocytosis (26), interfered with the NMDA-mediated removal of surface GABA_{B1b} protein (NMDA: 58.8 ± 5.4% of control, *n* = 8, *P* < 0.05; NMDA + dynasore: 105 ± 10% of control, *n* = 10, *P* > 0.05; dynasore: 98.4 ± 9.0% of control, *n* = 9, *P* > 0.05; Fig. 1C). Agonists accelerate basal endocytosis of GABA_B receptors (25). Antagonizing GABA_B receptor activity with CGP54626A (2 μM for 10 min) did not attenuate NMDA-mediated removal of surface GABA_{B1b} protein (NMDA + CGP54626A: 60.2 ± 9.6% of control, *n* = 10, *P* < 0.05; Fig. 1C). Thus NMDA receptor activation triggers dynamin-dependent endocytosis of GABA_B receptors, irrespective of whether GABA_B receptors are active or not.

Removal of surface GABA_B receptors requires CaMKII activity. NMDA failed to reduce surface GABA_{B1b} protein in transfected hippocampal neurons in the presence of the membrane-permeable Ca²⁺-chelator EGTA-AM (100 μM for 10 min; NMDA: 51.7 ± 6.7% of control, *n* = 10, *P* < 0.01; NMDA + EGTA-AM: 83.4 ± 9.0% of control, *n* = 9, *P* > 0.05; Fig. 2A). NMDA also failed to reduce surface GABA_{B1b} protein in the presence of the CaMKII inhibitor KN-93 (10 μM for 10 min; NMDA + KN-93: 85.6 ± 11.1% of control, *n* = 10, *P* > 0.05), implicating activation of CaMKII by NMDA receptors (27) in the removal of surface GABA_{B1b}. Likewise, KN-93 also prevented the NMDA-induced decrease of exogenous (Fig. S1A) and endogenous surface GABA_{B2} protein (Fig. 2B). In contrast, the NMDA-mediated decrease in surface GABA_{B1b} protein was not inhibited in the presence of KN-92 (28), an inactive structural analogue of KN-93 (10 μM for 10 min; NMDA + KN-92: 48.9 ± 7.9% of control, *n* = 9, *P* < 0.01; Fig. 2A).

S867 in GABA_{B1} is phosphorylated by CaMKII. Both anti-GABA_{B1} and anti-GABA_{B2} antibodies efficiently co-immunoprecipitated CaMKII from purified mouse brain membranes while control sera did not (Fig. 2C). This indicates that CaMKII associates with the GABA_{B1} and/or GABA_{B2} subunits of heteromeric GABA_B receptors (29). We corroborated this finding by performing pull-down assays with GST fusion proteins encoding the GABA_{B1} and GABA_{B2} C-termini (GST-GB1, GST-GB2). CaMKII in whole-brain lysate associated to a larger extent with GST-GB1 than with GST-GB2, supporting that CaMKII preferentially associates with GABA_{B1} (Fig. 2D). For *in vitro* phosphorylation, the GST-fusion

proteins were incubated for 30 min at 30°C with [γ - 32 P]-ATP and recombinant CaMKII. CaMKII-dependent phosphorylation was detectable on GST-GB1 but not on GST-GB2 or GST alone (Fig. 2E). Thus CaMKII associates with native GABA_B receptors and phosphorylates site(s) in the C-terminus of GABA_{B1}.

To identify the CaMKII phosphorylation site(s) in GABA_{B1}, we digested phosphorylated GST-GB1 protein with LysC and trypsin, separated the resulting peptides by reverse-phase high-performance liquid chromatography (RP-HPLC) and collected fractions at 1 min intervals (Fig. 3A). The majority of radiolabel eluted in a single peak in fraction 54, which we further analyzed using mass spectrometry (ESI-MS/MS). Database searches of the ESI-MS/MS scans revealed the presence of the phosphopeptide GEWQSETQDTMK (whose methionine was oxidized). The fragmentation spectrum indicated phosphorylation of the serine residue corresponding to S867 in the full-length GABA_{B1a} protein (Fig. 3B). S867 is localized in the juxtamembrane domain, a regulatory region for many transmembrane proteins, including G-protein coupled receptors (30). S867 does not conform to the consensus sequence for phosphorylation by CaMKII (31) or other kinases (Table S1). Nonetheless, alanine substitution of putative phosphorylation sites within the GEWQSETQDTMK motif (GST-GB1S867A, GST-GB1T869A, GST-GB1T872A, GST-GB1T869A/T872A) confirmed that recombinant CaMKII only phosphorylates S867 in this sequence (Fig. 3C). In addition, we found that CaMKII in brain extracts also specifically phosphorylates S867 in GST-GB1 (Fig. S3).

NMDA increases phosphorylation at S867 in native GABA_B receptors. To analyze S867 phosphorylation in native tissue we generated a S867 phosphorylation-state specific antibody, anti-GB1pS867. After phosphorylation of GST fusion proteins with recombinant CaMKII this antibody labeled GST-GB1 but not GST-GB1S867A (Fig. S4A). No S867 phosphorylation was seen when using recombinant PKC instead of CaMKII for phosphorylation (Fig. S4B). Importantly, the anti-GB1pS867 antibody revealed weak basal S867 phosphorylation (i) in mouse brain membranes after enrichment of GABA_B receptors by immunoprecipitation and (ii) in synaptic plasma membranes after subcellular fractionation (Fig. 4A and B). Application of NMDA to cultured cortical neurons significantly increased phosphorylation of S867 (Fig. 4C). Phosphorylation of S867 in brain membranes or cortical neurons was only detectable in the GABA_{B1b} subunit isoform. However, we cannot exclude that NMDA treatment also weakly phosphorylates the GABA_{B1a} subunit and that this phosphorylation is below our detection limit. Of note, GABA_{B(1b,2)}} but not GABA_{B(1a,2)}} receptors reside

in spines (10) where NMDA and GABA_B receptors are particularly abundant (15). This may explain why NMDA receptor activation preferentially targets GABA_{B1b} for phosphorylation.

Removal of surface GABA_B receptors requires S867 phosphorylation. Cultured hippocampal neurons expressing HA-GB1b-eGFP or HA-GB1bS867A-eGFP in combination with exogenous GABA_{B2} were analyzed for surface expression of transfected GABA_{B1b} protein (Fig. 4D and S5). HA-GB1bS867A-eGFP exhibited a similar surface expression level as HA-GB1b-eGFP, showing that lack of S867 phosphorylation does not prevent surface expression. However, HA-GB1bS867A-eGFP was refractory to removal from the surface upon NMDA treatment, as determined by the ratio of surface to total fluorescence intensity (GB1b NMDA: $52.6 \pm 4.8\%$, $n = 10$, $P < 0.01$; GB1bS867A control: $82.4 \pm 6.3\%$, $n = 9$, $P > 0.05$; GB1bS867A NMDA: 98.1 ± 16.0 , $n = 8$, $P > 0.05$; data normalized to GB1b control; Fig. 4D). This implicates S867 phosphorylation in GABA_B receptor removal from the cell surface.

NMDA-mediated CaMKII activation reduces GABA_B-induced K⁺ currents. Well-known effectors of dendritic GABA_B receptors are the Kir3-type K⁺ channels, which cluster with GABA_B receptors in spines (12). We used whole-cell patch-clamp recording to address whether NMDA-treatment reduces baclofen-induced K⁺ currents due to GABA_B receptor internalization. Baclofen-evoked K⁺ currents were recorded from cultured hippocampal neurons clamped at -50 mV after pharmacological blockade of Na⁺ channels, GABA_A, glycine, AMPA and kainate receptors (Fig. 5A). Baclofen-induced K⁺ currents were recorded before and 30 min after NMDA treatment (30 μM NMDA/5 μM glycine in Mg²⁺-free solution for 1 min). During NMDA applications neurons were held at -70 mV to minimize Ca²⁺ entry through voltage-gated Ca²⁺ channels. Following NMDA treatment the maximal amplitudes of the baclofen-induced K⁺ currents were reduced ($19.1 \pm 6.5\%$, $n = 5$; Fig. 5C). Likewise, baclofen-induced K⁺ currents was decreased following glutamate treatment (5 μM glutamate/5 μM glycine in Mg²⁺-free solution for 1 min; $35.2 \pm 5.1\%$, $n = 3$) and this decrease was prevented by the NMDA-receptor antagonist dCPP (20 μM; $93.5 \pm 0.5\%$, $n = 3$, $P < 0.001$ compared to NMDA alone; Fig. 5A and C). Intracellular dialysis with the CaMKII inhibitor KN-93 (5 μM) significantly attenuated the NMDA-mediated reduction of K⁺ currents ($65.5 \pm 9.0\%$, $n = 5$, $P < 0.001$ compared to NMDA alone). Ca²⁺/calmodulin-dependent protein kinase kinase β (CaMKKβ) promotes phosphorylation of the GABA_{B2} subunit by 5'AMP-dependent protein kinase (32). Intracellular dialysis with the CaMKK inhibitor STO-609 (5 μM) resulted in a modest attenuation of

NMDA-mediated reduction of K⁺-currents that, however, did not reach significance ($41.3 \pm 2.9\%$, $n = 5$, $P > 0.05$ compared to NMDA alone; Fig. 5A and C). We next addressed whether phosphorylation at S867 is critical for the NMDA-mediated decrease in K⁺-current amplitude. We transfected cultured hippocampal neurons from GABA_{B1}^{-/-} (GB1^{-/-}) mice (33) with expression constructs for GABA_{B1b} (GB1b), GABA_{B1a} (GB1a) or GB1bS867A. All exogenous GABA_{B1} subunits, including GB1bS867A, fully rescued GABA_B receptor function, demonstrating that they heteromerize with endogenous GABA_{B2} subunits (Fig. 5B and D). In GB1^{-/-} neurons reconstituted with GB1b, NMDA application decreased the baclofen-induced K⁺ currents to a similar extent as in wild-type neurons. In contrast, in GB1^{-/-} neurons reconstituted with GB1a or GB1bS867A NMDA application decreased the K⁺ currents significantly less (GB1b: $28.3 \pm 3.0\%$, $n = 5$; GB1a: $54.2 \pm 7.2\%$, $n = 6$, $P < 0.05$; GB1bS867A: $64.1 \pm 7.0\%$, $n = 5$, $P < 0.01$). Thus predominantly phosphorylation of GABA_{B1b} at S867 is implicated in the NMDA-mediated decrease of the K⁺-current amplitude.

NMDA-mediated endocytosis of GABA_B receptors in dendritic shafts and spines. The GABA_{B(1b,2)} receptor subtype, which appears to be the main substrate for S867 phosphorylation, resides in dendritic spines and shafts (10). We therefore addressed whether GABA_B receptors at these locations internalize in response to NMDA. We transfected GABA_{B1b} fused to a pH-sensitive eGFP (Super Ecliptic pHluorin, SEP-GB1b) together with GABA_{B2} into organotypic hippocampal slice cultures. SEP-GB1b selectively visualizes GABA_{B1b} protein at the cell surface (34). In addition, we expressed the freely diffusible red fluorescent protein (RFP) t-dimer2 to visualize the morphology of transfected cells (10). Time-lapse two-photon images of transfected CA1 pyramidal cells were collected at days-in-vitro (DIV) 14-21 (Fig. 6A). Dendrites were imaged at 5 min intervals before and after bath-application of NMDA (30 μM for 1 min). NMDA application resulted in a long-lasting decrease in green fluorescence in dendritic spines and shafts, indicating GABA_B receptor internalization (Fig. 6B and C, green traces; SEP-GB1b fluorescence ratio after/before NMDA: spine, 0.82 ± 0.05 , $n = 22$, $P < 0.001$; shaft, 0.73 ± 0.04 , $n = 8$, $P < 0.001$; 5 cells analyzed). NMDA application did not significantly affect RFP fluorescence in dendritic spines and shafts (Fig. 6B and C, red traces; RFP fluorescence ratio after/before NMDA: spine, 1.04 ± 0.05 , $n = 22$, $P > 0.05$; shaft, 0.88 ± 0.03 , $n = 8$, $P > 0.05$). The decrease in green fluorescence was inhibited in the presence of the NMDA receptor antagonist dCPP (20 μM; Fig. 6B and C, green traces; SEP-GB1b fluorescence ratio after/before NMDA: spine, 1.00 ± 0.05 , $n = 15$, $P > 0.05$; shaft, 0.99 ± 0.04 , $n = 3$, $P > 0.05$; 2 cells analyzed). No significant change in the red fluorescence under NMDA receptor blockade was

observed (Fig. 6B and C, red traces; RFP fluorescence ratio after/before NMDA: spine, 1.06 ± 0.07 , $n = 15$, $P > 0.05$; shaft, 1.02 ± 0.03 , $n = 3$, $P > 0.05$). Thus NMDA receptor stimulation leads to GABA_B receptor internalization in dendritic spines and shafts. In agreement with experiments described above (Figs. 4D, 5 D and S5B) the SEP-GB1bS867A protein is refractory to NMDA-induced internalization in dendritic spines and shafts (Fig. S6).

Discussion

Activity-dependent phosphorylation and internalization of dendritic GABA_B receptors. A previous report showed that glutamate application to cortical neurons decreases the number of GABA_B receptors at the cell surface (18). Another report showed that glutamate application increases the steady-state level of GABA_B receptor endocytosis while at the same time reducing the rate of endocytosis (35). Here, we show that glutamate acts via NMDA receptors to activate CaMKII (36), which directly phosphorylates S867 in the C-terminus of GABA_{B1} to trigger endocytosis. Intriguingly, NMDA-dependent phosphorylation of S867 is only detectable in the GABA_{B1b} subunit, which mostly resides in the dendrites and, in contrast to the GABA_{B1a} subunit, efficiently penetrates spines (10). Consistent with this we found that GABA_B receptors undergo endocytosis in dendritic spines and shafts within minutes of NMDA receptor activation. Notably, endocytosis of GABA_B receptors prevents them from activating effector K⁺ channels that cluster with GABA_B receptors in spines (12).

Physiological implications. GABA from interneurons firing in synchrony can spill over to pre- and postsynaptic GABA_B receptors on excitatory synapses (11,37). This will reduce glutamate release and produce hyperpolarizing inhibitory postsynaptic potentials (IPSP) that enhance Mg²⁺ block of NMDA receptors and thus reduce their Ca²⁺ signals (13,14). In addition to modulating the electrical properties of neurons, GABA_B receptors can also reduce the Ca²⁺ permeability of NMDA receptors in dendritic spines via activation of the PKA signaling pathway (15). Here, we demonstrate that NMDA receptors can counter this suppression of Ca²⁺ signals and rapidly endocytose GABA_B receptors from the surface of dendritic shafts and spines. Hence, there appears to be a reciprocal regulation where both NMDA and GABA_B receptors can cancel each other out. The temporal interplay of NMDA and GABA_B receptors may be particularly relevant to phenomena controlling synaptic strength, where NMDA receptor activity is of importance. Of note, the same NMDA receptor/CaMKII signaling cascade regulating synaptic strength also internalizes GABA_B receptors. This provides a means to keep individual glutamatergic synapses modifiable (38,39) and to spare them from volume inhibition through spillover of GABA. A previous study reported that NMDA receptor activation promotes surface expression of Kir3 channels in hippocampal neurons (40), which was paralleled with an increase in basal Kir3 currents and adenosine A₁-mediated Kir3 currents (41). However, GABA_B mediated Kir3 currents were not altered, in apparent conflict with an earlier report (42) and our own findings. The reasons for these discrepancies are unclear but may relate to differences in the signaling pathways activated under the different experimental conditions used. Reciprocal

regulation of NMDA and GABA_B receptors is reminiscent of the recently reported interplay of NMDA and muscarinic receptors (43). In this crosstalk, NMDA receptors phosphorylate and inactivate muscarinic receptors in a CaMKII-dependent manner, much in the same way as now observed with GABA_B receptors.

Materials and Methods

Neuronal cultures. Dissociated hippocampal and cortical neurons were prepared from embryonic day 18.5 Wistar rats or from embryonic day 16.5 wild-type and GABA_{B1}^{-/-} mice (33,44) and cultured in Neurobasal medium (GIBCO) supplemented with B27 (GIBCO). Neurons were transfected at DIV7 using Lipofectamin 2000 (Invitrogen). Pharmacological treatments were performed in conditioned medium at 37°C/5% CO₂.

Biochemistry. Surface biotinylation, immunoprecipitation, *in vitro* phosphorylation, HPLC analysis and mass spectrometry were essentially performed as described (24,45,46). To generate GST-GB1 and GST-GB2, the full-length C-termini of GABA_{B1} (amino acids 857–960) and GABA_{B2} (amino acid 745–940) were amplified by PCR from the rat cDNAs and inserted in-frame into the pGEX-4T-1 fusion vector (GE Healthcare). GST-fusion proteins were expressed in *E. coli* BL21(DE3).

Electrophysiology. Recordings in cultured hippocampal neurons were performed with an Axopatch 200B patch-clamp amplifier. GABA_B responses were evoked by fast application of 100 μM baclofen (47). Normalized K⁺ current amplitudes were calculated as the maximal baclofen-induced K⁺ current amplitudes recorded 30 min after pharmacological treatment relative to the maximal baclofen-induced K⁺ current amplitudes recorded before pharmacological treatment of the same neuron.

Two-photon imaging. Organotypic hippocampal slice cultures for two-photon time-lapse imaging (48) were prepared from Wistar rats at postnatal day 5 (49). For time-lapse imaging, we used a custom-built two-photon laser scanning microscope based on a BX51WI microscope (Olympus) and a pulsed Ti:Sapphire laser (Chameleon XR, Coherent) tuned to λ = 930 nm, controlled by the open source software ScanImage. Fluorescence was detected in epi- and transfluorescence mode using four photomultiplier tubes (R2896, Hamamatsu). The slice was placed into a perfusion chamber and superfused with ACSF containing (in mM): 127 NaCl, 25 NaHCO₃, 25 D-glucose, 2.5 KCl, 4 CaCl₂, 1.25 NaH₂PO₄, 0.03 serine and 0.001 TTX (320 mosm, pH 7.4). In a subset of experiments 0.02 mM dCPP was added to the ACSF. Experiments were performed at 28°C. Stacks of images (256 × 256 pixels) from secondary dendritic branches were obtained from transfected CA1 pyramidal neurons (Z step: 0.5 μm). Green fluorescence (SEP-GB1b or SEP-GB1bS867A) and red fluorescence (RFP) was imaged

at 5 min intervals before and after bath-application of NMDA and quantified in regions of interest (ROIs) containing either a dendritic shaft or spines. Control ROIs in the image background were always included and did not show changes in fluorescence during the course of the experiment. To quantify NMDA-mediated changes the green and red fluorescence intensities after NMDA application (7 values) were normalized to the intensities before NMDA application (2 values). For the ratio images, we used a hue/saturation/brightness model, where hue was determined by the G/R ratio (using a rainbow color table), and the intensity in the red channel was used to set the brightness.

Data analysis. Data are given as mean \pm SEM and statistical significance was assessed using ANOVA with the Dunnett's multiple comparison test or non-parametric Mann-Whitney test using GraphPad Prism 5.0.

Additional experimental procedures are described in *SI Materials and Methods* published on the PNAS Web site.

Acknowledgments

B.B. was supported by the Swiss Science Foundation (3100A0-117816) and the European Community's Seventh Framework Programme FP7/2007-2013 under Grant Agreement 201714. R.T. was supported by the Wellcome Trust International Senior Research Fellowship and EU Synapse grant (LSHM-CT-2005-019055). We thank N. Hardel for the Rab11-eGFP plasmid, K. Ivankova and A. Cremonesi for technical help and F. Schatzmann for comments on the manuscript.

References

1. Bettler B, Kaupmann K, Mosbacher J, Gassmann M (2004) Molecular structure and physiological functions of GABA_B receptors. *Physiol Rev* 84:835-867.
2. Couve A, Moss SJ, Pangalos MN (2000) GABA_B receptors: a new paradigm in G-protein signaling. *Mol Cell Neurosci* 16:296-312.
3. Ulrich D, Bettler B (2007) GABA_B receptors: synaptic functions and mechanisms of diversity. *Curr Opin Neurobiol* 17:298-303.
4. Kornau HC (2006) GABA_B receptors and synaptic modulation. *Cell Tissue Res* 326:517-533.
5. Jarolimek W, Misgeld U (1997) GABA_B receptor-mediated inhibition of tetrodotoxin-resistant GABA release in rodent hippocampal CA1 pyramidal cells. *J Neurosci* 17:1025-1032.
6. Scanziani M, Capogna M, Gähwiler BH, Thompson SM (1992) Presynaptic inhibition of miniature excitatory synaptic currents by baclofen and adenosine in the hippocampus. *Neuron* 9:919-927.
7. Luscher C, Jan LY, Stoffel M, Malenka RC, Nicoll RA (1997) G protein-coupled inwardly rectifying K⁺ channels (GIRKs) mediate postsynaptic but not presynaptic transmitter actions in hippocampal neurons. *Neuron* 19:687-695.
8. Marshall FH, Jones KA, Kaupmann K, Bettler B (1999) GABA_B receptors - the first 7TM heterodimers. *Trends Pharmacol Sci* 20:396-399.
9. Biermann B, et al. (2010) The Sushi domains of GABA_B receptors function as axonal targeting signals. *J Neurosci* 30:1385-1394.
10. Vigot R, et al. (2006) Differential Compartmentalization and Distinct Functions of GABA_B Receptor Variants. *Neuron* 50:589-601.
11. Guetg N, et al. (2009) The GABA_{B1a} isoform mediates heterosynaptic depression at hippocampal mossy fiber synapses. *J Neurosci* 29:1414-1423.
12. Kulik A, et al. (2006) Compartment-dependent colocalization of Kir3.2-containing K⁺ channels and GABA_B receptors in hippocampal pyramidal cells. *J Neurosci* 26:4289-4297.
13. Morrisett RA, Mott DD, Lewis DV, Swartzwelder HS, Wilson WA (1991) GABA_B-receptor-mediated inhibition of the N-methyl-D-aspartate component of synaptic transmission in the rat hippocampus. *J Neurosci* 11:203-209.
14. Otmakhova NA, Lisman JE (2004) Contribution of I_h and GABA_B to synaptically induced afterhyperpolarizations in CA1: a brake on the NMDA response. *J Neurophys* 92:2027-2039.

15. Chalifoux JR, Carter AG (2010) GABA_B Receptors Modulate NMDA Receptor Calcium Signals in Dendritic Spines. *Neuron* 66:101-113.
16. Cimarosti H, Kantamneni S, Henley JM (2009) Ischaemia differentially regulates GABA_B receptor subunits in organotypic hippocampal slice cultures. *Neuropharmacol* 56:1088-1096.
17. Straessle A, Loup F, Arabadzisz D, Ohning GV, Fritschy JM (2003) Rapid and long-term alterations of hippocampal GABA_B receptors in a mouse model of temporal lobe epilepsy. *Eur J Neurosci* 18:2213-2226.
18. Vargas KJ, *et al.* (2008) The availability of surface GABA_B receptors is independent of γ -aminobutyric acid but controlled by glutamate in central neurons. *J Biol Chem* 283:24641-24648.
19. Pagano A, *et al.* (2001) C-terminal interaction is essential for surface trafficking but not for heteromeric assembly of GABA_B receptors. *J Neurosci* 21:1189-1202.
20. Margeta-Mitrovic M, Jan YN, Jan LY (2000) A trafficking checkpoint controls GABA_B receptor heterodimerization. *Neuron* 27:97-106.
21. Grampp T, Sauter K, Markovic B, Benke D (2007) γ -aminobutyric acid type B receptors are constitutively internalized via the clathrin-dependent pathway and targeted to lysosomes for degradation. *J Biol Chem* 282:24157-24165.
22. Hardel N, Harmel N, Zolles G, Fakler B, Klocker N (2008) Recycling endosomes supply cardiac pacemaker channels for regulated surface expression. *Cardiovasc Res* 79:52-60.
23. Maxfield FR, McGraw TE (2004) Endocytic recycling. *Nat Rev Mol Cell Biol* 5:121-132.
24. Fairfax BP, *et al.* (2004) Phosphorylation and Chronic Agonist Treatment Atypically Modulate GABA_B Receptor Cell Surface Stability. *J Biol Chem* 279:12565-12573.
25. Grampp T, Notz V, Broll I, Fischer N, Benke D (2008) Constitutive, agonist-accelerated, recycling and lysosomal degradation of GABA_B receptors in cortical neurons. *Mol Cell Neurosci* 39:628-637.
26. Macia E, *et al.* (2006) Dynasore, a cell-permeable inhibitor of dynamin. *Dev Cell* 10:839-850.
27. Lisman J, Schulman H, Cline H (2002) The molecular basis of CaMKII function in synaptic and behavioural memory. *Nat Rev Neurosci* 3:175-190.
28. Tombes RM, Grant S, Westin EH, Krystal G (1995) G₁ cell cycle arrest and apoptosis are induced in NIH 3T3 cells by KN-93, an inhibitor of CaMK-II (the multifunctional Ca²⁺/CaM kinase). *Cell Growth Differ* 6:1063-1070.

29. Kaupmann K, *et al.* (1998) GABA_B-receptor subtypes assemble into functional heteromeric complexes. *Nature* 396:683-687.
30. Kim CH, Lee J, Lee JY, Roche KW (2008) Metabotropic glutamate receptors: phosphorylation and receptor signaling. *J Neurosci Res* 86:1-10.
31. Pearson RB, Woodgett JR, Cohen P, Kemp BE (1985) Substrate specificity of a multifunctional calmodulin-dependent protein kinase. *J Biol Chem* 260:14471-14476.
32. Kuramoto N, *et al.* (2007) Phospho-Dependent Functional Modulation of GABA_B Receptors by the Metabolic Sensor AMP-Dependent Protein Kinase. *Neuron* 53:233-247.
33. Schuler V, *et al.* (2001) Epilepsy, hyperalgesia, impaired memory, and loss of pre- and postsynaptic GABA_B responses in mice lacking GABA_{B(1)}. *Neuron* 31:47-58.
34. Kopec CD, Li B, Wei W, Boehm J, Malinow R (2006) Glutamate receptor exocytosis and spine enlargement during chemically induced long-term potentiation. *J Neurosci* 26:2000-2009.
35. Wilkins ME, Li X, Smart TG (2008) Tracking cell surface GABA_B receptors using an alpha-bungarotoxin tag. *J Biol Chem* 283:34745-34752.
36. Nicoll RA, Malenka RC (1999) Expression mechanisms underlying NMDA receptor-dependent long-term potentiation. *Ann N Y Acad Sci* 868:515-525.
37. Scanziani M (2000) GABA spillover activates postsynaptic GABA_B receptors to control rhythmic hippocampal activity. *Neuron* 25:673-681.
38. Lee SJ, Escobedo-Lozoya Y, Szatmari EM, Yasuda R (2009) Activation of CaMKII in single dendritic spines during long-term potentiation. *Nature* 458:299-304.
39. Zhang YP, Holbro N, Oertner TG (2008) Optical induction of plasticity at single synapses reveals input-specific accumulation of α CaMKII. *Proc Natl Acad Sci U S A* 105:12039-12044.
40. Chung HJ, Qian X, Ehlers M, Jan YN, Jan LY (2009) Neuronal activity regulates phosphorylation-dependent surface delivery of G protein-activated inwardly rectifying potassium channels. *Proc Natl Acad Sci U S A* 106:629-634.
41. Chung HJ, *et al.* (2009) G protein-activated inwardly rectifying potassium channels mediate depotentiation of long-term potentiation. *Proc Natl Acad Sci U S A* 106:635-640.
42. Huang CS, *et al.* (2005) Common molecular pathways mediate long-term potentiation of synaptic excitation and slow synaptic inhibition. *Cell* 123:105-118.
43. Butcher AJ, *et al.* (2009) N-methyl-D-aspartate receptors mediate the phosphorylation and desensitization of muscarinic receptors in cerebellar granule neurons. *J Biol Chem* 284:17147-17156.

44. Brewer GJ (1993) Optimized survival of hippocampal neurons in B-27 supplemented Neurobasal, a new serum-free medium combination. *J Neurosci Res* 35:567-576.
45. Gassmann M, *et al.* (2004) Redistribution of GABA_{B(1)} protein and atypical GABA_B responses in GABA_{B(2)}-deficient mice. *J Neurosci* 24:6086-6097.
46. Gander S, *et al.* (2008) Identification of the rapamycin-sensitive phosphorylation sites within the Ser/Thr-rich domain of the yeast Npr1 protein kinase. *Rapid Commun Mass Spectrom* 22:3743-3753.
47. Schwenk J, *et al.* (2010) Native GABA_B receptors are heteromultimers with a family of auxiliary subunits. *Nature* in press.
48. Holbro N, Grunditz A, Oertner TG (2009) Differential distribution of endoplasmic reticulum controls metabotropic signaling and plasticity at hippocampal synapses. *Proc Natl Acad Sci U S A* 106:15055-15060.
49. Stoppini L, Buchs PA, Muller D (1991) A simple method for organotypic cultures of nervous tissue. *J Neurosci Methods* 37:173-182.
50. Couve A, *et al.* (2002) Cyclic AMP-dependent protein kinase phosphorylation facilitates GABA_B receptor-effector coupling. *Nat Neurosci* 5:415-424.

Figure Legends

Fig. 1. NMDA-dependent removal of surface GABA_B receptors. (A) Rat hippocampal neurons coexpressing exogenous HA-GB1b-eGFP and GABA_{B2} were treated at DIV14 as indicated. Surface GABA_{B1b} (GB1b) protein was fluorescence-labeled with anti-HA antibodies prior to permeabilization. Total GB1b protein was fluorescence-labeled with anti-eGFP antibodies after permeabilization. Single optical planes captured with a confocal microscope are shown. Scale bar = 15 μm. Insets show representative spines at higher magnification. (B) Surface GABA_{B1b} protein was quantified by the ratio of surface to total fluorescence intensity. Values were normalized to control values in the absence of any pharmacological treatment. Surface GABA_{B1b} protein was significantly decreased following glutamate or NMDA treatment. No significant reduction was observed with glutamate treatment after preincubation with APV. $n = 9-10$, $**P < 0.01$, $***P < 0.001$. (C) Dynasore but not CGP54626A prevented the NMDA-induced reduction of surface GABA_{B1b} protein. $n = 8-10$, $*P < 0.05$. Quantification was from non-saturated images, data are presented as mean ± SEM.

Fig. 2. NMDA-induced removal of surface GABA_B receptors requires CaMKII. (A) Rat hippocampal neurons coexpressing exogenous HA-GB1b-eGFP and GABA_{B2} were analyzed at DIV14. Surface GABA_{B1b} protein was quantified by the ratio of surface to total fluorescence intensity. Preincubation of neurons with the Ca²⁺-chelator EGTA-AM or the CaMKII inhibitor KN-93 prevented the NMDA-induced reduction in surface GABA_{B1b} protein. KN-92 was ineffective. Data are means ± SEM, $n = 9-10$, $**P < 0.01$. (B) NMDA-mediated removal of endogenous surface GABA_B receptors. Live cortical neurons were treated at DIV14 as indicated and then biotinylated. Cell homogenates (total) and avidin-purified cell surface proteins (surf) were probed on Western blots with anti-GABA_{B1} (anti-GB1) and anti-GABA_{B2} (anti-GB2) antibodies. While all GABA_B subunits were removed from the cell surface in response to NMDA, GABA_{B1b} was more efficiently removed than GABA_{B1a}. NMDA-mediated removal of surface protein was inhibited by KN-93. Anti-tubulin antibodies were used as a control. (C) CaMKII interacts with GABA_B receptors in the brain. Anti-GB1 and anti-GB2 antibodies co-immunoprecipitated CaMKII from purified mouse brain membranes, while control rabbit (serum rb) or guinea-pig serum (serum gp) did not. (D) Pull-down assays with GST-fusion proteins containing the entire C-terminal domain of GABA_{B1} (GST-GB1) or GABA_{B2} (GST-GB2) and whole brain lysates. CaMKII bound to a larger extent to GST-GB1 than to GST-GB2. Control assays were with glutathione beads alone or with beads together with GST protein. (E) *In vitro* phosphorylation of GST-fusion proteins with [γ -³²P]-ATP in the presence or absence of recombinant CaMKII.

Phosphorylated proteins were separated by SDS-PAGE and exposed to autoradiography. CaMKII specifically phosphorylated GST-GB1 but not GST-GB2 or GST alone. Coomassie blue staining controlled for loading. The GST-GB2 fusion protein tended to degrade (50).

Fig. 3. CaMKII phosphorylates S867 in the GABA_{B1} subunit. (A) RP-HPLC analysis of proteolytically digested GST-GB1 after phosphorylation with recombinant CaMKII and [γ -³²P]-ATP. Peptide elution was monitored at 214 nm and radioactivity (red) determined by liquid scintillation counting. The asterisk marks elution of the ³²P-labeled peptide in fraction 54. (B) Fragmentation spectrum of the doubly charged 768.29 Da precursor from the phosphorylated peptide of fraction 54. The fragmentation pattern agrees with the predicted ESI-MS/MS spectrum for the phosphopeptide GEWQpS⁸⁶⁷ETQDTMK. The γ - and b-ions matching the GEWQpS⁸⁶⁷ETQDTMK sequence are labeled. Phosphorylated ions are marked by asterisks. (C) *In vitro* phosphorylation of GST fusion proteins with recombinant CaMKII and [γ -³²P]-ATP. Phosphorylated proteins were separated by SDS-PAGE and exposed to autoradiography. Substitution of S867 with alanine in GST-GB1S867A prevented phosphorylation by CaMKII, while alanine substitutions of other putative phosphorylation sites in proximity of S867 (GST-GB1T869A, GST-GB1T872A and GST-GB1T869A/T872A) did not. Coomassie blue staining controlled for loading.

Fig. 4. S867 phosphorylation in brain tissue and cultured neurons. (A) S867 phosphorylation was detectable after immunoprecipitation of GABA_B receptors with anti-GABA_{B1} antibodies (IP:GB1) from WT but not GB1^{-/-} brain membranes. S867 phosphorylation was detected on Western blots with a phosphorylation-state specific antibody (anti-GB1pS867). The same blot was reprobbed with anti-GB1 antibodies. Immunoprecipitation with rabbit IgG (IP:IgG) was used as a control. Note the specific phosphorylation of the GABA_{B1b} subunit. (B) S867 phosphorylation of GABA_{B1b} was clearly detectable in synaptic plasma membranes (SPM) and barely detectable in the P2 membrane fraction purified from total mouse brain homogenates. (C) NMDA application to cultured cortical neurons increased S867 phosphorylation in the GABA_{B1b} subunit. Neurons were treated with NMDA for 3 min and harvested at the times indicated. Whole cell lysates (input) were subjected to immunoprecipitation with anti-GB1 antibodies (IP:GB1). S867 phosphorylation was detected on Western blot with anti-GB1pS867; anti-tubulin antibodies were used as control. (D) Alanine mutation of S867 in GABA_{B1b} prevents NMDA-induced internalization. Cultured hippocampal neurons expressing exogenous HA-GB1b-eGFP (GB1b) or HA-GB1bS867A-eGFP (GB1bS867A)

together with GABA_{B2} were analyzed at DIV14. Surface GABA_{B1b} protein was quantified by the ratio of surface to total fluorescence intensity. Values were normalized to GB1b control in the absence of NMDA. Data are means ± SEM, $n = 8-10$, $**P < 0.01$.

Fig. 5. CaMKII reduces GABA_B-mediated K⁺ currents in cultured hippocampal neurons. (A) Representative baclofen-induced K⁺ currents recorded at -50 mV before and after application of NMDA or glutamate. Baclofen-induced K⁺ currents were strongly reduced 30 min after NMDA or glutamate application. KN-93 and dCPP but not STO-609 attenuated the NMDA-mediated K⁺ current reduction. (B) Representative baclofen-induced K⁺ currents recorded from neurons of GABA_{B1}^{-/-} (GB1^{-/-}) mice transfected with GABA_{B1a} (GB1a) GABA_{B1b} (GB1b) or GB1bS867A expression vectors. NMDA was less effective in decreasing the K⁺ current in neurons transfected with GB1bS867A or GABA_{B1a}. (C) Bar graph illustrating that dCPP and KN-93 attenuated the NMDA-mediated reduction of baclofen-induced K⁺ currents. (D) NMDA was significantly less effective in decreasing the K⁺ current in GB1^{-/-} neurons transfected with GB1a or GB1bS867A than with GB1b. Maximal K⁺-current amplitudes after NMDA application were normalized to the maximal K⁺-current amplitudes before NMDA application. Data are means ± SEM, $n = 3-6$, $*P < 0.05$, $**P < 0.01$, $***P < 0.001$.

Fig. 6. NMDA-mediated endocytosis of GABA_B receptors in dendritic spines and shafts. (A) Red fluorescence (R), green fluorescence (G) and G/R ratio images of dendrites expressing freely diffusible RFP and SEP-GB1b before and after NMDA application. NMDA application leads to a decrease in green fluorescence in dendritic spines and shafts. The G/R ratio is coded in rainbow colors and is scaled to encompass 2 standard deviations (2σ) of the average dendritic ratio before NMDA application. Scale bar = 5 μm. (B and C) Time course of red and green fluorescence in dendritic spines (B) and shafts (C) before and after NMDA application. NMDA leads to a long-lasting decrease in SEP-fluorescence within minutes, which is prevented by prior application of dCPP. Data are means ± SEM.

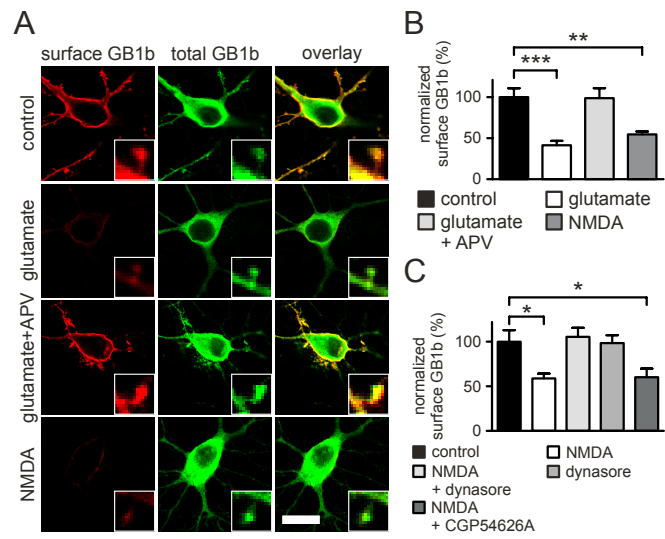


Figure 1
Guetg et al.

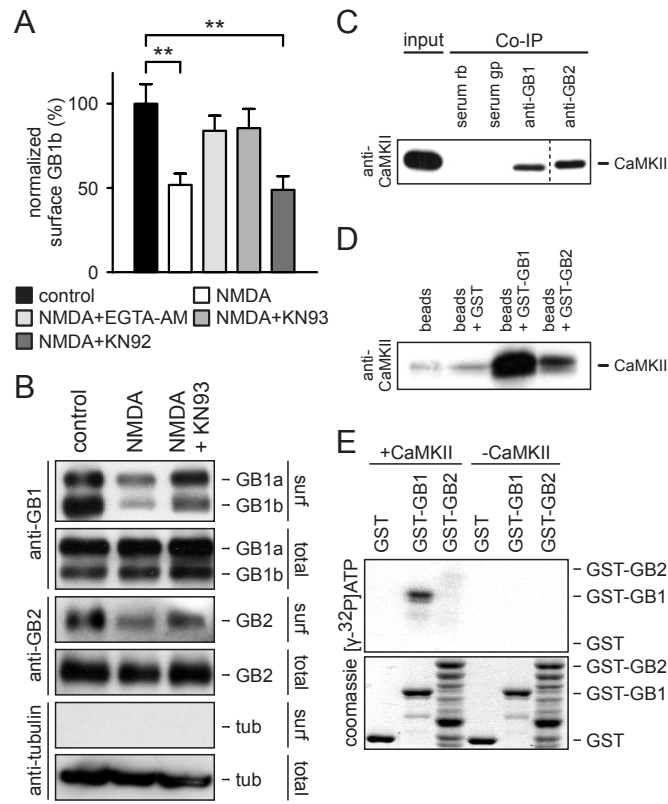


Figure 2
Guetg et al.

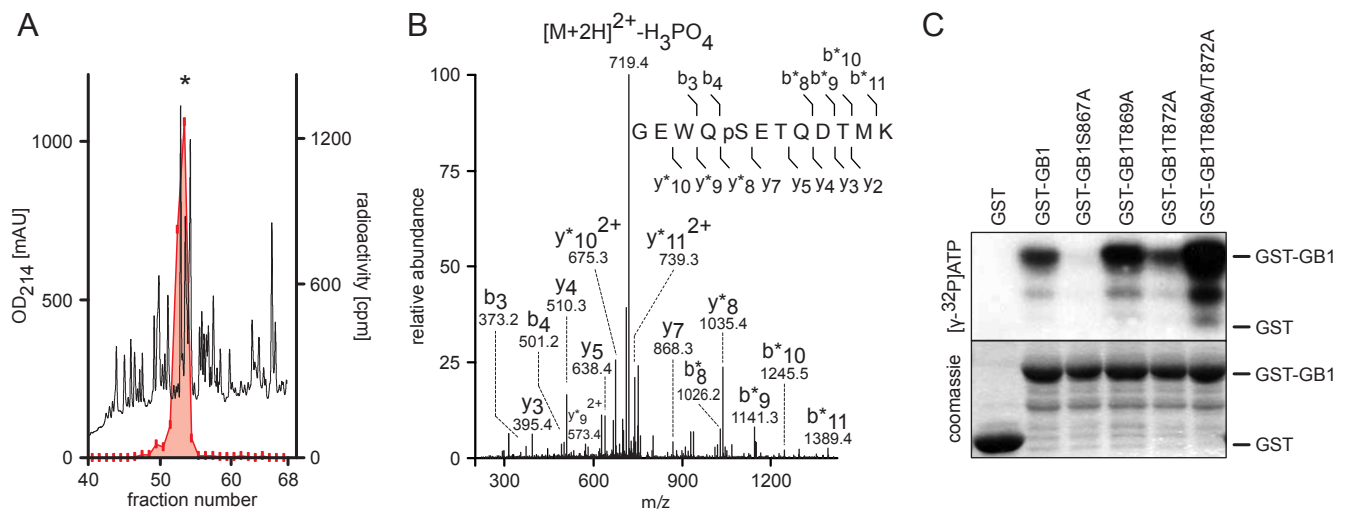


Figure 3
Guetg et al.

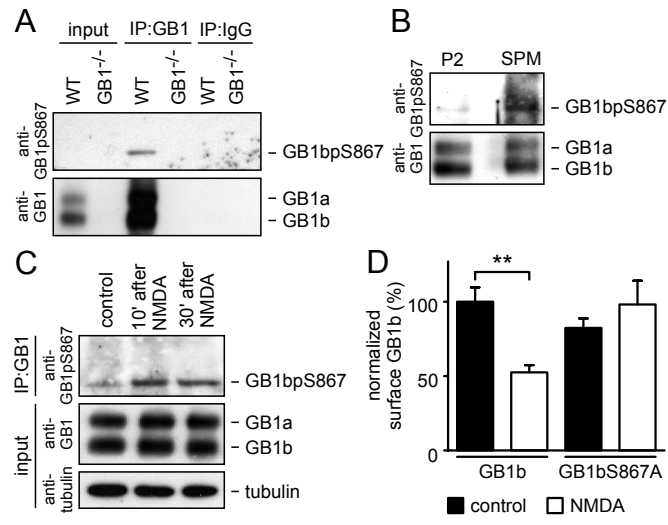


Figure 4
Guetg et al.

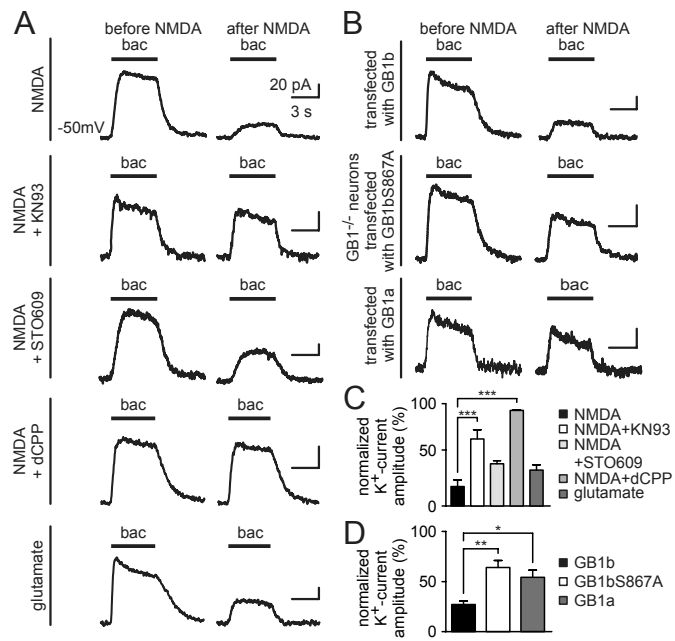


Figure 5
Guetg et al.

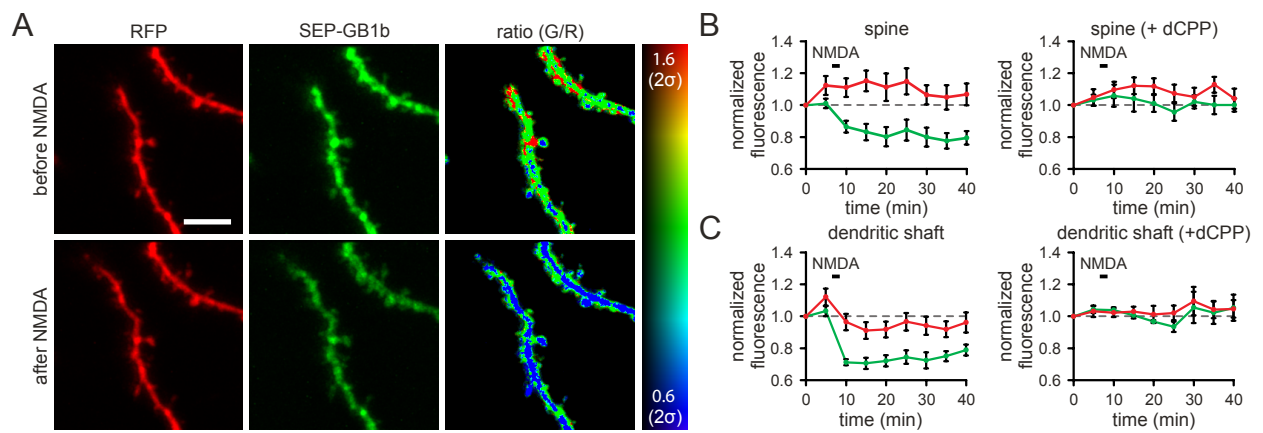


Figure 6
Guetg et al.

Supporting Information

SI Materials and Methods

Transfection of neuronal cultures. High-density primary hippocampal neuronal cultures were prepared from 18.5-day embryonic rats or 16.5-day embryonic mice and cultured in Neurobasal medium (GIBCO) supplemented with B27 (GIBCO) at a density of ~ 750 cells/mm² on poly-L-lysine coated coverslips as described previously (1). At day-in-vitro (DIV) 7, neurons were co-transfected with (i) GABA_{B1b} (HA-GB1b-eGFP or HA-GB1bS867A-eGFP) and GABA_{B2} (GB2) expression vectors, (ii) GABA_{B1b} (Myc-GB1b) and GABA_{B2} (HA-GB2), (iii) GABA_{B1a} (HA-GB1a-eGFP) and GB2 or (iv) Myc-GB1b, GB2 and Rab11-eGFP using Lipofectamin 2000 (Invitrogen) according to the manufacturer's instruction. The HA- and Myc-tags are located at the extracellular N-terminus and the eGFP-tag at the intracellular C-terminus. Gene expression was under control of the neuron specific *synapsin-1* promoter (gift from K. Svoboda).

Treatment protocols for neuronal cultures. All treatments were performed in conditioned medium at 37°C / 5% CO₂. Control neurons were incubated for 30 min with 5 μ M glycine. Glutamate-treated neurons were incubated for 30 min with 50 μ M glutamate and 5 μ M glycine. NMDA-treated neurons were incubated for 3 min with 75 μ M NMDA (Tocris) / 5 μ M glycine (adapted from (2)). The following inhibitors were dissolved in DMSO and applied to the cultures prior to glutamate or NMDA treatment: D-(-)-2-Amino-5-phosphonopentanoic acid (APV, 100 μ M for 2 h, Tocris), dynasore (80 μ M for 15 min, Sigma), ethylene glycol-bis-(2-aminoethyl)-N,N,N',N'-tetraacetic acid (EGTA-AM, 100 μ M for 10 min (adapted from (3)), Molecular Probes), KN-93 (10 μ M for 10 min, Tocris) and KN-92 (10 μ M for 10 min, Calbiochem). Inhibitors were kept in the medium during the glutamate or NMDA treatment. After glutamate or NMDA treatment neurons were returned to conditioned medium for 27 min before analysis. The final DMSO concentration never exceeded 1% (v/v). Preincubation of neurons with DMSO 1% (v/v) for 2 h did not significantly affect the NMDA-mediated reduction in surface GABA_{B1b} levels (control: 100% \pm 13%; NMDA: 49.7 \pm 7.4%, $P < 0.001$ compared to control; NMDA + DMSO: 58.6 \pm 3.7%, $P < 0.01$ compared to control; mean \pm SEM, $n = 10$. No significant difference was observed between NMDA and NMDA + DMSO treatment.)

Immunocytochemistry and quantification of surface receptors. Neurons were fixed after treatment with 4% paraformaldehyde (PFA) in phosphate-buffered saline (PBS) containing 120 mM sucrose for

20 min and blocked for 2 h in 10% normal goat serum (GIBCO) in PBS (NGS/PBS). Neurons were incubated with primary mouse anti-HA antibodies (1:500 in 10% NGS/PBS; Covance) for 2 h to visualize surface GABA_{B1b} receptors. Subsequently neurons were permeabilized with 0.25% Triton-X-100 in PBS for 10 min. The total amount of GABA_{B1b} receptors was detected by staining with rabbit anti-GFP antibodies (1:500 in 10% NGS/PBS; Molecular Probes). Secondary antibodies Alexa Fluor 568 goat anti-mouse and Alexa Fluor 488 goat anti-rabbit (1:500; Molecular Probes) were incubated for 1 h in 10% NGS/PBS. Stained neuronal cultures were mounted in FluorSave Reagent (Calbiochem) and viewed on a Leica TCS SPE confocal microscope. Digital pictures were captured with Leica Software (LAS AF) and identically processed with ImageJ software (4). The fluorescence intensity of labeled surface HA-GB1b-eGFP proteins was measured on the soma of transfected neurons and visualized in single optical planes using ImageJ software. For quantification of surface HA-GB1b-eGFP protein levels, the fluorescence intensity of surface HA-GB1b-eGFP (red) was normalized to the total HA-GB1b-eGFP (green) fluorescence intensity. Statistical analysis was performed with GraphPad Prism 5.0. For each statistical analysis independent sample groups were analyzed. All steps were performed at room temperature. For visualization of surface Myc-GB1a-eGFP and HA-GB2 proteins mouse anti-Myc (1:500, Roche) and mouse anti-HA antibodies were used. Total protein levels were determined by using rabbit anti-GFP and rabbit anti-GB2 (1:500, Abcam) antibodies.

Immunocytochemistry of internalized receptors. Anti-HA antibodies (1:50, Immunology Consultants Laboratory) were used to label the N-terminal HA-tag of GABA_{B1b} protein at the cell surface. Live neurons were then incubated at 37°C/5% CO₂ for 30 min to allow internalization in the presence or absence of glutamatergic agonists and antagonists. After removal of residual anti-HA antibodies from the cell surface by acid wash (2 min wash in Neurobasal medium pH 2.0 on ice, followed by intensive washing with Neurobasal medium pH 7.4 on ice), internalized anti-HA antibodies were visualized with fluorescence-labeled secondary antibodies. Following fixation and permeabilization of neurons, the total amount of HA-GB1b-eGFP protein was determined by staining with mouse anti-GFP antibodies (1:500 in 10% NGS/PBS, Molecular Probes). Secondary antibodies (Alexa Fluor 568 goat anti-rabbit and Alexa Fluor 488 goat anti-mouse, 1:500, Molecular Probes) were incubated for 1 h in 10% NGS/PBS. To control for complete removal of anti-HA antibodies from the cell surface upon acid wash, some non-permeabilization cultures were stained with Alexa Fluor 568 goat anti-rabbit antibodies. For colocalization experiments, neurons were co-transfected with Myc-GABA_{B1b}, GABA_{B2}

and Rab11-eGFP (5). Internalization experiments were performed as described above by surface labeling of live neurons with mouse anti-Myc antibodies (1:50, Roche).

Surface biotinylation of neuronal cultures. After treatment with pharmacological agents, rat cortical neurons were rinsed twice with PBS on ice. Neurons were then incubated with 1 mg/ml EZ-Link Sulfo-NHS-SS-Biotin (Pierce Chemicals) in PBS for 30 min. The biotinylation solution was removed by washing with PBS followed by 5 min quenching with 50 mM glycine in PBS. Neurons were rinsed with Tris-buffered saline (TBS) and PBS, collected in 2 ml PBS and transferred into tubes. Neurons were washed twice by resuspension in PBS followed by centrifugation at 2000 x g. Finally, neurons were lysed in RIPA buffer and incubated for 30 min on a rotor wheel. Lysates were cleared by centrifugation for 20 min at 16000 x g and incubated with immobilized NeutrAvidin gel (Pierce Chemicals) overnight on a rotor wheel. Beads were washed five times with RIPA buffer and the adsorbed proteins eluted with SDS sample buffer for 60 min at room temperature. All steps were performed on ice or at 4°C unless indicated differently.

Whole-brain lysate and brain membrane preparation. Whole brains from BALB/c mice were polytron-homogenized in HEPES buffer (4 mM HEPES pH 7.4, 320 mM sucrose, 1 mM EDTA, 1 mM EGTA) containing Complete Protease Inhibitor Cocktail (Roche) and centrifuged for 10 min at 1000 x g to remove debris and the crude nuclear fraction. Samples were kept at 4°C throughout the procedure. The supernatant (S2) containing the cytosolic fraction of whole brain lysates was removed and stored at -80°C until used for *in vitro* phosphorylation assays. The remaining pellets (P2) containing the membrane fraction were solubilized in RIPA buffer (50 mM Tris-HCl pH 7.4, 150 mM NaCl, 1% NP-40, 0.5% deoxycholate) and were centrifuged for 30 min at 10000 x g to remove insoluble material. Solubilized brain membranes were stored at -80°C until used for immunoprecipitation and/or Western blot analysis. Synaptic plasma membranes were purified from total mouse brain by combined flotation-sedimentation density gradient centrifugation as described previously (6).

Co-immunoprecipitation. Solubilized brain membranes were precleared for 3 h by incubation with protein G-agarose beads (Roche). Rabbit anti-GABA_{B1} antibody 174.1 (7) or guinea pig anti-GABA_{B2} antibody (Chemicon) were added to the precleared lysates and incubated for 1 h followed by overnight incubation with protein G-agarose beads. Rabbit and guinea preimmune pig serum were

used as a control. Immunoprecipitated complexes were repeatedly washed with RIPA buffer, separated by SDS-PAGE and probed with an anti-CaMKII α antibody (1:1000, Santa Cruz).

GST-fusion proteins. To generate GST-GB1, the full-length C-terminus of GABA_{B1} (amino acids 857–960) was amplified by PCR from rat GABA_{B1} cDNA (8), digested with *Bam*HI and *Xho*I, and subcloned in-frame into pGEX-4T-1 fusion vector (GE Healthcare). GST-fusion protein expression vectors containing alanine substitutions of serine or threonine residues in the GABA_{B1} C-terminus (GST-GB1S867A, GST-GB1T869A, GST-GB1T872A and GST-GB1T869A/T872A) were generated by overlapping PCR from GST-GB1. To generate GST-GB2, the full-length C-terminus of GABA_{B2} (amino acid 745-940) was amplified by PCR from rat GABA_{B2} cDNA (9), digested with *Bam*HI and *Eco*RI and subcloned in-frame into pGEX-4T-1. GST-fusion proteins were expressed in *E. coli* BL21(DE3). Expression of the fusion-proteins was induced by 1 mM isopropyl 1-thio- β -D-galactopyranoside (IPTG) for 4 h. Cells were lysed by sonication and GST-fusion proteins were purified by incubation with Glutathione Sepharose 4B (Amersham Biosciences) overnight at 4°C and washed with PBS.

Pull-down assay. Whole-brain lysates from BALB/c mice were prepared by polytron-homogenization in modified RIPA buffer (50 mM Tris-HCl pH 7.4, 150 mM NaCl, 1 mM EDTA, 1% NP-40, 0.5% Triton X-100) containing Complete Protease Inhibitor Cocktail. Lysates were cleared by centrifugation at 15700 x g for 30 min at 4°C and incubated for 4 h with GST-fusion proteins immobilized on sepharose beads. Following extensive washing in RIPA buffer, isolated proteins were eluted by boiling in Laemmli buffer, separated by SDS-PAGE and probed with anti-CaMKII antibody (1:5000, BD Biosciences).

In vitro phosphorylation assay. GST-fusion proteins immobilized on sepharose beads were phosphorylated with recombinant CaMKII (New England Biolabs) or the cytosolic P2 fraction of whole-brain lysates prepared from BALB/c mice by polytron-homogenization in HEPES buffer. Recombinant CaMKII was activated in phosphorylation buffer for 10 min at 30°C, according to the manufacturer's instructions. For whole-brain lysates the following phosphorylation buffer was used (in mM): 20 HEPES pH7.4, 1.7 CaCl₂, 100 dithiothreitol, 10 MgCl₂, 1.6 unlabeled ATP. For each phosphorylation reaction, 20 μ g GST fusion-protein was incubated with recombinant CaMKII (500 units) or whole-brain lysates (50 μ g) in the appropriate phosphorylation buffer in the presence of 1 μ l [γ -³²P]-ATP (3000 Ci/mmol) for 30 min at 30°C. Free [γ -³²P]-ATP was removed by extensive washing

with ice-cold phosphorylation buffer. To inhibit CaMKII activity, whole-brain extracts were preincubated with 10 μ M KN-93 for 20 min at 4°C. Phosphorylated GST-fusion proteins were either separated by SDS-PAGE and subjected to autoradiography or subsequently used for RP-HPLC and ESI-MS/MS analysis.

Reverse-phase high-pressure liquid chromatography (RP-HPLC). For HPLC analysis, 20 μ g of phosphorylated GST-fusion protein was digested with the endoproteinase Lys C (Wako Chemicals) followed by a second digestion with trypsin (Promega). Digestion was stopped by adding TFA (Applied Biosystems) to a final concentration of 0.1% (v/v). Insoluble material was removed by centrifugation (12000 rpm, 5 min) and the supernatant was subjected to RP-HPLC on Vydac C18 reverse-phase columns (218TP52, 2.1 x 250 mm; Grace Vydac) connected to a Hewlett Packard 1090 HPLC system. Bound peptides were eluted during 60 min at 150 μ l/min with a linear gradient of 0.1% TFA/2% acetonitrile to 0.09% TFA/75% acetonitrile. The effluent was monitored at 214 nm. Fractions were collected at 1 min intervals. Phosphopeptides in the fractions were located by liquid scintillation counting.

Electrospray ionization mass spectrometry (ESI-MS/MS). The radioactively labeled peptides were analyzed by capillary liquid chromatography tandem MS (LC/MS/MS) using a set up of a trapping 300SB C-18 column (0.3x50 mm) (Agilent Technologies) and a separating column (0.1x100 mm) packed with Magic 300 Å C18 reverse-phase material (5 μ m particle size, Michrom Bioresources Inc.). The columns were connected on line to an Orbitrap FT hybrid instrument (Thermo Finnigan). A linear gradient from 2 to 80% solvent B (0.1% acetic acid and 80% acetonitrile in water) in solvent A (0.1% acetic acid and 2% acetonitrile in water) in 85 min was delivered with a Rheos 2200 pump (Flux Instruments) at a flow rate of 100 μ l/min. A pre-column split was used to reduce the flow to 100 μ l/min. The eluting peptides were ionized at 1.7 kV. The mass spectrometer was operated in a data-dependent fashion. The precursor scan was done in the Orbitrap set to 60000 resolution, while the fragment ions were mass analyzed in the LTQ instrument. The five most intense precursors were selected for fragmentation. The MS/MS spectra were searched against the NCBI non-redundant database using TurboSequest or Mascot software (10, 11).

Electrophysiology in cultured hippocampal neurons. Recordings were performed 1-2 weeks after transfection at DIV14-21 at room temperature (23-24°C). Neurons were continuously superfused

with an extracellular solution (ECS) composed of (in mM): 145 NaCl, 2.5 KCl, 1 MgCl₂, 2 CaCl₂, 10 HEPES, 25 Glucose; pH 7.3, 323 mosm supplemented with 5 μM DNQX, 0.5 μM TTX, 0.3 μM strychnine, 100 μM picrotoxin. Patch pipettes had resistances between 3-4 MΩ when filled with intracellular solution composed of (in mM): 107.5 potassium gluconate, 32.5 KCl, 10 HEPES, 0.1 EGTA, 4 MgATP, 0.6 NaGTP, 10 Tris phosphocreatine; pH 7.2, 297 mosm. Series resistance (< 5 MΩ) was compensated by 80%. GABA_B responses were evoked by fast application of baclofen and recorded with an Axopatch 200B patch-clamp amplifier; filtering and sampling frequencies were set to 1 kHz and 5 kHz, respectively. Normalized K⁺ current amplitudes were calculated as the maximal baclofen-induced K⁺ current amplitudes recorded 30 min after pharmacological treatment relative to the maximal baclofen-induced K⁺ current amplitudes recorded before pharmacological treatment of the same neuron.

Transfection of organotypic slice cultures and two-photon time-lapse imaging. Organotypic hippocampal slices were prepared from Wistar rats at postnatal day 5 as described (12). After 3 days in vitro, cultures were biolistically co-transfected with a Helios Gene Gun (Bio-Rad) with the following plasmids: GABA_{B1b} or GABA_{B1b}S867A N-terminally tagged with a pH-sensitive eGFP (Super Ecliptic pHluorin, SEP-GB1b or SEP-GB1bS867A, 2.2 μg DNA per mg gold), GABA_{B2} (2 μg/mg) and a freely diffusible red fluorescent protein (RFP) tdimer2 (1 μg/mg). Gene expression was under control of the neuron specific *synapsin-1* promoter. For time-lapse imaging, we used a custom-built two-photon laser scanning microscope based on a BX51WI microscope (Olympus) and a pulsed Ti:Sapphire laser (Chameleon XR, Coherent) tuned to λ = 930 nm, controlled by the open source software ScanImage written in Matlab (13). Fluorescence was detected in epi- and transfluorescence mode using four photomultiplier tubes (R2896, Hamamatsu). The slice was placed into a perfusion chamber and superfused with ACSF containing (in mM): 127 NaCl, 25 NaHCO₃, 25 D-glucose, 2.5 KCl, 4 CaCl₂, 1.25 NaH₂PO₄, 0.03 serine and 0.001 TTX (320 mosm, pH 7.4). In a subset of experiments 0.02 mM dCPP was added to the ACSF. Experiments were performed at 28°C. Stacks of images (256 × 256 pixels) from secondary dendritic branches were obtained from transfected CA1 pyramidal neurons (Z step: 0.5 μm) Green fluorescence (SEP-GB1b or SEP-GB1bS867A) and red fluorescence (RFP) was imaged at 5 min intervals before and after bath-application of NMDA and quantified in regions of interest (ROIs) containing either a dendritic shaft or spines. Control ROIs in the image background were always included and did not show changes in fluorescence during the course of the experiment. To quantify NMDA-mediated changes the green and red fluorescence intensities after NMDA application

(7 values) were normalized to the intensities before NMDA application (2 values). For the ratio images, we used a hue/saturation/brightness model, where hue was determined by the G/R ratio (using a rainbow color table), and the intensity in the red channel was used to set the brightness. To allow the comparison of ratio images the rainbow color table is scaled to encompass 2 standard deviations (2σ) of the average dendritic G/R pixel ratios before NMDA application.

References

1. Brewer GJ (1993) Optimized survival of hippocampal neurons in B-27 supplemented Neurobasal, a new serum-free medium combination. *J Neurosci Res* 35:567-576.
2. Kim MJ, *et al.* (2007) Synaptic accumulation of PSD-95 and synaptic function regulated by phosphorylation of serine-295 of PSD-95. *Neuron* 56:488-502.
3. Faure C, *et al.* (2007) Calcineurin is essential for depolarization-induced nuclear translocation and tyrosine phosphorylation of PYK2 in neurons. *J Cell Sci* 120:3034-3044.
4. Abramoff MD, Magelhaes PJ, Ram SJ (2004) Image Processing with ImageJ. *Biophot Int* 11:36-42.
5. Hardel N, Harmel N, Zolles G, Fakler B, Klocker N (2008) Recycling endosomes supply cardiac pacemaker channels for regulated surface expression. *Cardiovasc Res* 79:52-60.
6. Jones DH, Matus AI (1974) Isolation of synaptic plasma membrane from brain by combined flotation-sedimentation density gradient centrifugation. *Biochim Biophys Acta* 356:276-287.
7. Malitschek B, *et al.* (1998) Developmental changes in agonist affinity at GABA_{B(1)} receptor variants in rat brain. *Mol Cell Neurosci* 12:56-64.
8. Kaupmann K, *et al.* (1997) Expression cloning of GABA_B receptors uncovers similarity to metabotropic glutamate receptors. *Nature* 386:239-246.
9. Kaupmann K, *et al.* (1998) GABA_B-receptor subtypes assemble into functional heteromeric complexes. *Nature* 396:683-687.
10. Gatlin CL, Eng JK, Cross ST, Detter JC, Yates JR, 3rd (2000) Automated identification of amino acid sequence variations in proteins by HPLC/microspray tandem mass spectrometry. *Anal Chem* 72:757-763.
11. Perkins DN, Pappin DJ, Creasy DM, Cottrell JS (1999) Probability-based protein identification by searching sequence databases using mass spectrometry data. *Electrophoresis* 20:3551-3567.
12. Stoppini L, Buchs PA, Muller D (1991) A simple method for organotypic cultures of nervous tissue. *J Neurosci Methods* 37:173-182.

13. Pologruto TA, Sabatini BL, Svoboda K (2003) ScanImage: flexible software for operating laser scanning microscopes. *Biomed Eng Online* 2:13.
14. Vigot R, *et al.* (2006) Differential Compartmentalization and Distinct Functions of GABA_B Receptor Variants. *Neuron* 50:589-601.

Figure Legends

Fig. S1. NMDA-dependent internalization of GABA_B receptors. (A) Rat hippocampal neurons coexpressing exogenous HA-GB2 and GABA_{B1b} were treated at DIV14 as indicated. Surface GABA_{B2} (GB2) protein was fluorescence-labeled with anti-HA antibodies prior to permeabilization. Total GB2 protein was fluorescence-labeled with anti-GB2 antibodies after permeabilization. Single optical planes captured with a confocal microscope are shown (scale bar = 15 μm). Insets show representative spines at higher magnification. Surface GB2 protein was quantified by the ratio of surface to total fluorescence intensity. Values were normalized to control values in the absence of any pharmacological treatment. Surface GB2 protein was significantly decreased following glutamate or NMDA treatment. No significant reduction was observed with glutamate treatment after preincubation with APV and with NMDA treatment after preincubation with KN-93 (glutamate: 54.4 ± 13.2% of control, *n* = 10, ***P* < 0.01; glutamate + APV: 111 ± 8.7%, *n* = 8; NMDA: 55.9 ± 6.2%, *n* = 10, ***P* < 0.01; NMDA + KN-93: 105 ± 13.2, *n* = 10). (B) Rat hippocampal neurons coexpressing exogenous Myc-GB1a-eGFP and GABA_{B2} were treated at DIV14 as indicated. Surface GABA_{B1a} (GB1a) protein was fluorescence-labelled with anti-Myc antibodies prior to permeabilization. Total GB1a protein was fluorescence-labeled with anti-eGFP antibodies after permeabilization. Single optical planes captured with a confocal microscope are shown (scale bar = 15 μm). Insets show representative spines at higher magnification. Note that GB1a does not efficiently penetrate the spines. Surface GB1a protein was quantified by the ratio of surface to total fluorescence intensity. Values were normalized to control values in the absence of any pharmacological treatment. Surface GB1a protein was decreased following glutamate or NMDA treatment, but this decrease did not reach statistical significance. No reduction in surface GB1a protein was observed with glutamate treatment after preincubation with APV and with NMDA treatment after preincubation with KN-93 (glutamate: 62.5 ± 7.5% of control, *n* = 10; glutamate + APV: 108 ± 10.7%, *n* = 9; NMDA: 67.4 ± 9.6%, *n* = 8; NMDA + KN-93: 108 ± 15.5, *n* = 9). Quantification was from non-saturated images, data are presented as mean ± SEM; ns, not significant.

Fig. S2. NMDA receptor-dependent internalization of GABA_B receptors in neurons. (A) Rat hippocampal neuronal cultures were co-transfected with HA-GB1b-eGFP and GABA_{B2} expression vectors and analyzed at DIV14. Constitutive internalization was observed under control conditions. After glutamate treatment the rate of HA-GB1b-eGFP internalization was visibly increased. Preincubation with APV prevented glutamate-induced internalization of HA-GB1b-eGFP above

constitutive levels. NMDA treatment was sufficient to increase internalization of HA-GB1b-eGFP. Maximum projections of representative neurons visualized by confocal microscopy are shown. Scale bar = 15 μ m. (B) Rat hippocampal neurons were co-transfected with Myc-GB1b, GABA_{B2} and Rab11-eGFP, which labels recycling endosomes. Under control conditions constitutively internalized GB1b appears to mostly co-localize with Rab11-eGFP. Following glutamate or NMDA treatment a fraction of internalized Myc-GB1b is observed in structures that are not labelled by Rab11-eGFP (arrowheads). Single optical planes of representative neurons visualized with confocal microscopy are shown. Scale bar = 15 μ m.

Fig. S3. Endogenous CaMKII phosphorylates S867 in GABA_{B1}. (A-C) GST-fusion proteins were incubated with the cytosolic fraction of whole mouse brain extracts in the presence of [γ -³²P]-ATP. Proteolytic peptides were separated by RP-HPLC (top panels) and the radioactivity in the eluted fractions determined (lower panels). (A) The C-terminal GABA_{B1} peptide GEWQSETQDTMK was identified by ESI-MS/MS as a major constituent of a highly radiolabeled fraction (asterisk) of the GST-GB1 effluent. Because the phosphorylation stoichiometry with brain extracts was low, a direct demonstration of phosphorylation at S867 was impossible. (B) Following phosphorylation of GST-GB1S867A with brain extracts no radiolabel was detected in the RP-HPLC fraction containing the peptide GEWQA⁸⁶⁷ETQDTMK (arrow head), supporting that brain extracts normally phosphorylate S867. (C) No radiolabel was detected in the fraction containing GEWQSETQDTMK (arrow head) after phosphorylation of GST-GB1 in the presence of KN-93, implicating native CaMKII in phosphorylation of S867.

Fig. S4. Validation of the phosphorylation-state specific anti-GB1pS867 antibody. (A) The anti-GB1pS867 antibody was generated against the phosphorylated peptide ITRGEWQpS867EAQDT and recognized GST-GB1 but not GST-GB1S867A after phosphorylation with recombinant CaMKII. Moreover, unphosphorylated GST-GB1 was not recognized by the anti-GB1p867 antibody demonstrating its specificity for phosphorylated S867 (top panel). The same blot was probed with an anti-GABA_{B1} antibody (anti-GB1) to demonstrate expression of the GST-fusion proteins (bottom panel). (B) *In vitro* phosphorylation of GST-GB1 with recombinant CaMKII and PKC in the presence of [γ -³²P]-ATP. Phosphorylated proteins were separated by SDS-PAGE and exposed to autoradiography (top panel) or probed with anti-GB1pS867 (middle panel) or anti-GB1 (bottom panel). Anti-GB1pS867 recognized GST-GB1 phosphorylated by CaMKII but not by PKC.

Fig. S5. Surface localization of transfected GABA_{B1b} protein. Cultured hippocampal neurons expressing exogenous (A) HA-GB1b-eGFP (GB1b) or (B) HA-GB1bS867A-eGFP (GB1bS867A) together with GABA_{B2} were treated at DIV14 as indicated. Surface GB1b or GB1bS867A protein was fluorescence-labeled with anti-HA antibodies prior to permeabilization. Total GB1b or GB1bS867A protein was fluorescence-labeled with anti-eGFP antibodies after permeabilization. Alanine mutation of S867 prevented the NMDA-induced reduction of surface GB1b protein (quantification of data presented in Fig. 4D). Single optical planes captured with a confocal microscope are shown. Scale bar = 15 μm . Insets show representative spines at higher magnification.

Fig. S6. Reduced NMDA-mediated internalization of SEP-GB1bS867A protein in dendritic spines and shafts. (A) Red fluorescence (R), green fluorescence (G) and G/R ratio images of dendrites expressing freely diffusible RFP and SEP-GB1bS867A before and after NMDA application. NMDA application does not lead to a decrease in green fluorescence in spines and only evokes minor internalization in shafts. The G/R ratio is coded in rainbow colors and is scaled to encompass 2 standard deviations (2σ) of the average dendritic ratio before NMDA application to allow direct comparison with Fig. 6A. Similar to GB1b (14), GB1bS867A is effectively excluded from axons (arrowheads). Scale bar = 5 μm . (B) Time course of red and green fluorescence in dendritic spines and shafts before and after NMDA application. 7 cells were analyzed; data are means \pm SEM, spines: n = 34, dendrites: n = 7.

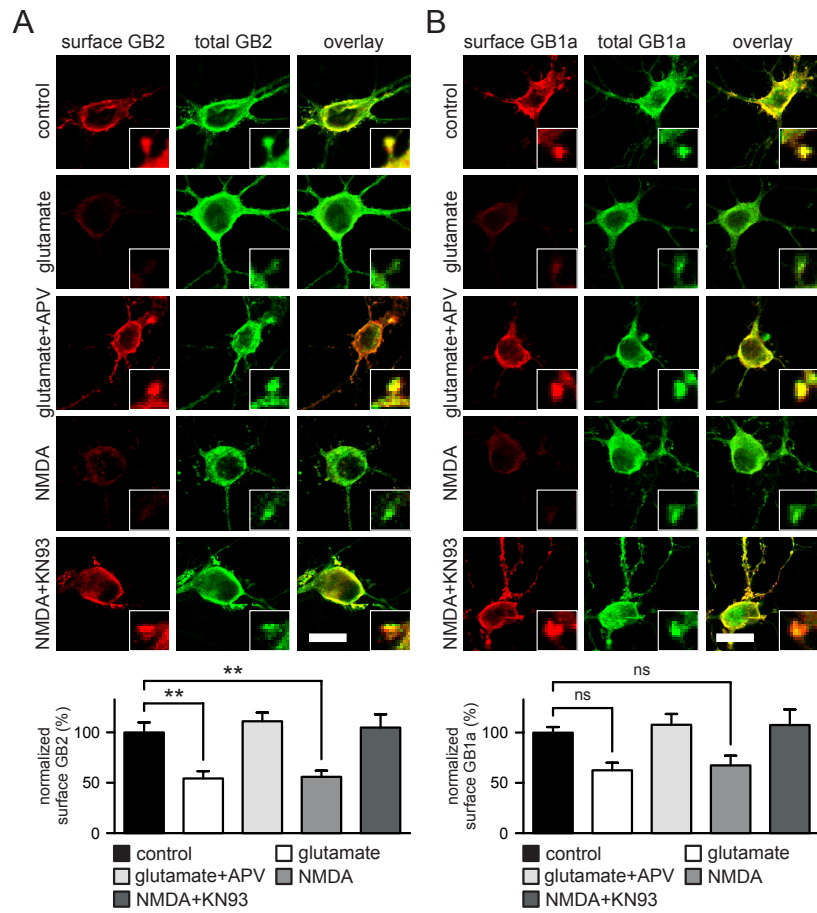


Figure S1
Guetg et al.

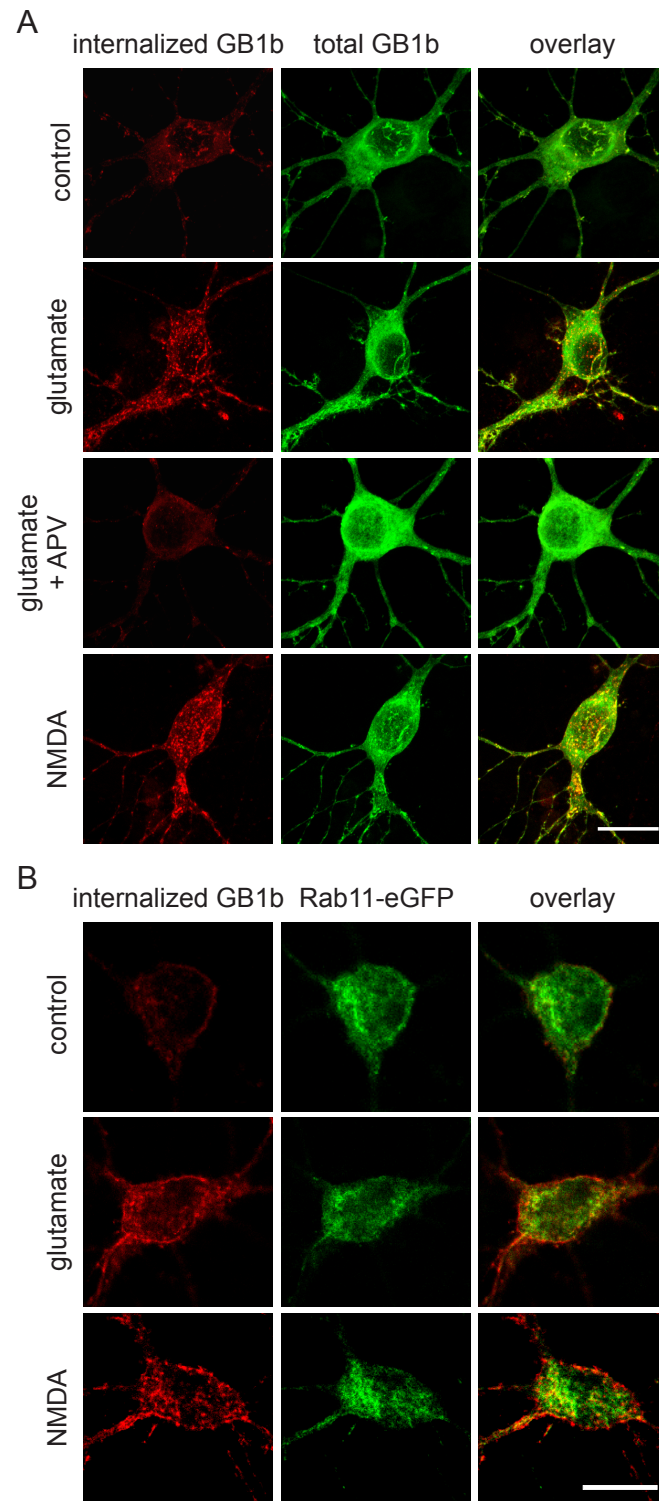


Figure S2
Guetg et al.

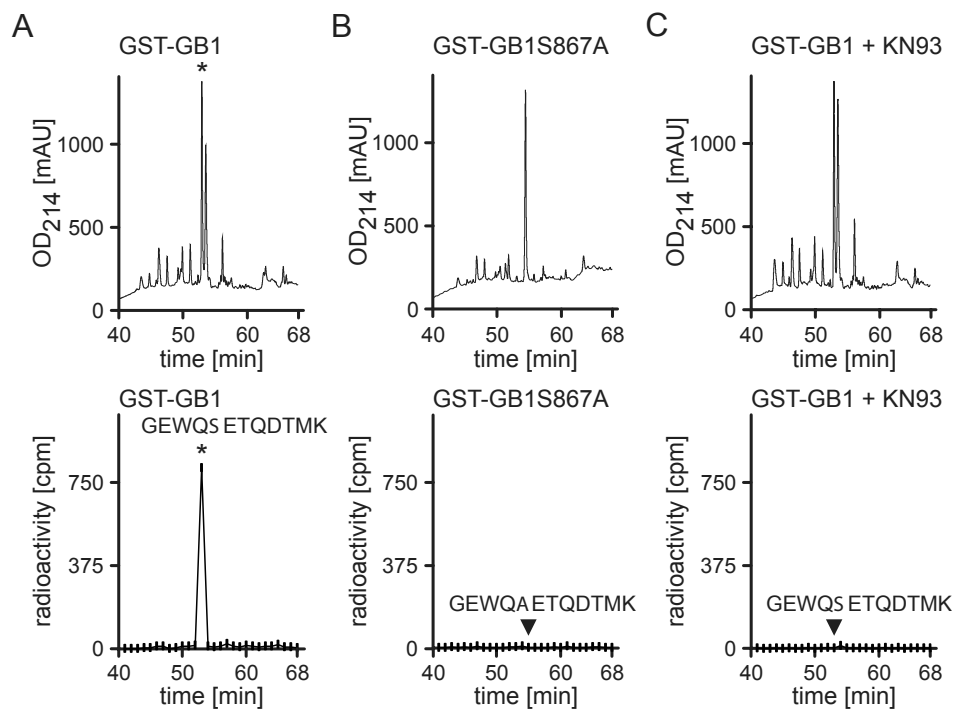


Figure S3
Guettg et al.

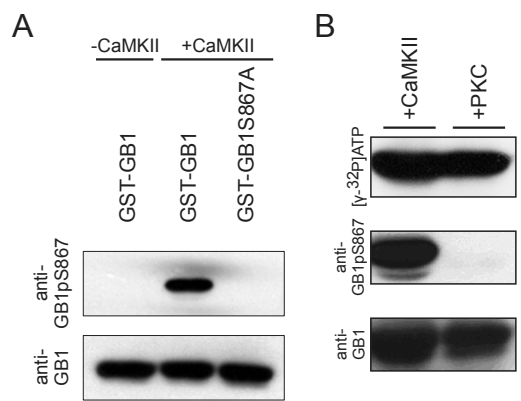


Figure S4
Guetg et al.

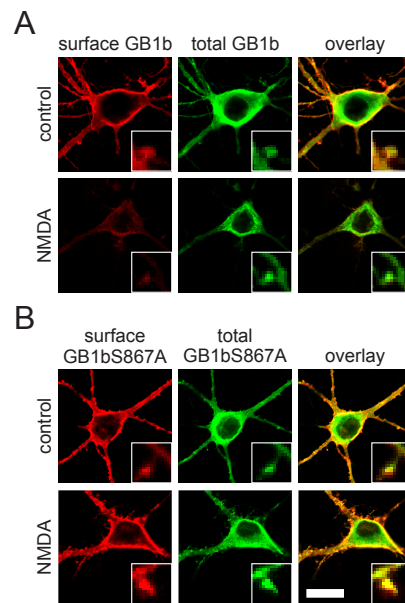


Figure S5
Guetg et al.

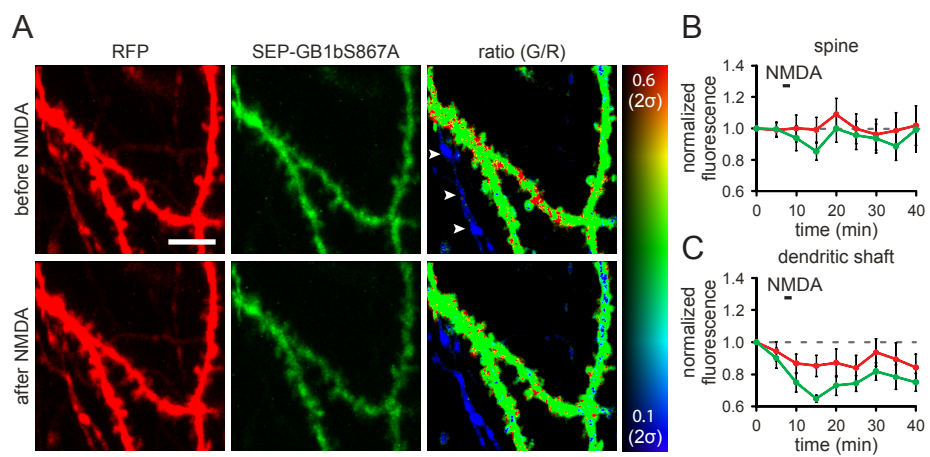


Figure S6
Guetg et al.

Table S1. Putative phosphorylation sites in the C-terminal domain of GABA_{B1}.

Residue	Position	Consensus Sequence	Experimental Evidence	Kinase		
Serine	867		this paper	CaMKII		
	877					
	878	CK1				
	887					
	909					
	917				(1)	AMPK
	923	PKC				
	934					
	942	CaMKII				
	949					
	953					
Threonine	861	CaMKII/CK2				
	869	GRK				
	872	CK1/GRK/PKC				
	875	CK1				
	879	CK1				
	929	CK2/MAPK	(2-5)	not specified		
Tyrosine	959					

Prediction of phosphorylation sites in the C-terminal domain of GABA_{B1} with PredPhospho available at <http://www.nih.go.kr/phosphovariant/html/predphospho.htm>. Kinase(s) for each predicted phosphorylation site were allocated by consensus sequence. Where available experimental evidence is indicated and the kinase specified.

1. Kuramoto N, et al. (2007) Phospho-dependent functional modulation of GABA_B receptors by the metabolic sensor AMP-dependent protein kinase. *Neuron* 53:233-247.
2. Trinidad JC, et al. (2006) Comprehensive identification of phosphorylation sites in postsynaptic density preparations. *Mol Cell Proteomics* 5:914-922.
3. Munton RP, et al. (2007) Qualitative and quantitative analyses of protein phosphorylation in naive and stimulated mouse synaptosomal preparations. *Mol Cell Proteomics* 5:283-293.
4. Trinidad JC, et al. (2008) Quantitative analysis of synaptic phosphorylation and protein expression. *Mol Cell Proteomics* 7:684-696.
5. Schwenk J, et al. (2010) Native GABA_B receptors are heteromultimers with a family of auxiliary subunits. *Nature* in press.

7. Acknowledgements

Especially I would like to thank Prof. Bernhard Bettler for giving me the opportunity to do my PhD thesis in his lab and in a great scientific environment, giving me such exciting projects and for his guidance and support.

Further, I would like to thank the Neurex network for financial support during part of my PhD thesis.

Thanks to Prof. Michael Frotscher for providing me with the opportunity to perform parts of my work in his lab.

My special and deep thanks go to Dr. Martin Gassmann who supported me scientifically and also in private matters. I would like to thank you, Martin, to take my moods always with patience and to always believe in me. I enjoyed the time working “bench-to-bench” and the coffee breaks a lot. It is nice to have you as a friend.

Special thanks to Dr. Àkos Kulik for introducing me to the world of electron microscopy, the support and the stimulating discussions. I enjoyed the time in Freiburg im Breisgau very much and marvel your enthusiasm with which you encounter science everyday.

I would like to thank all present and past members of the Bettler lab for advices, helpful comments and the good time. Especially to Dr. Emilio Casanova for starting off my fascination for DNA manipulation; Michaela Metz for always taking time for a chat in and outside of the lab and Dr. Jim Tiao for suggestions, comments and all the beers in the Cargo Bar, I enjoyed the time, while you were in Basel, a lot.

I thank Susanne Blank for always having had everything under control and the nice time we had together in the office.

Special thank to Francois Grenier, Audree Pinard, Franziska Schatzmann and Martin Gassmann for proofreading this thesis.

I thank Andreas Galli, Emiliano Bello, Constanze Baranek and Dalma Seboek to make my time in Basel and on our balcony unforgettable.

I thank Franziska Schatzmann for the nice holidays spent together and everlasting support. I’m proud and happy to be your bridesmaid. I thank Susanne Strickler for the nice climbs and happy hours spent together. I’m happy to have all of you as my friends.

I would like to specially thank my parents, my sister and my brother for their invaluable support throughout my life.

Last but not least, thanks to Claudio for enormous support.

CURRICULUM VITAE

Personal Details

Name: Nicole Guetg
Date of birth: November, 26 1976
Gender: Female
Nationality: Swiss

Education History

2009 – 2010: Postdoc position
Prof. Bernhard Bettler
Institute of Physiology
Pharmacenter/University of Basel

2004 – 2009: PhD thesis in neurobiology:
“GABA_B Receptor Localization and Regulation”
Prof. Bernhard Bettler
Institute of Physiology
Pharmacenter/University of Basel

2003 – 2004: Diploma thesis:
“*N.caninum* Bradyzoite *in vitro* Culture: Development and Applications”
Prof. Andrew Hemphill
Institute of Parasitology
University of Bern

1999 – 2003: Master in Cell Biology
University of Bern
Switzerland

1997-1999: Faculty of Veterinary Medicine
University of Bern
Switzerland

1996: Matura Typus E, Gymnasium Sursee, Luzern

Publications

Journal articles

Guetg N, Abdel Aziz S, Holbro N, Turecek R, Rose T, Seddik R, Gassmann M, Moes S, Jenoe P, Oertner TG, Casanova E, Bettler B. NMDA Receptor-Dependent GABA_B Receptor Internalization via CaMKII Phosphorylation of Serine 867 in GABA_{B1}. *submitted*

Casanova E, **Guetg N**, Vigot R, Julio-Pieper M, Hyland NP, Cryan JF, Gassmann M, Bettler B. A Mouse Model for Visualization of GABAB Receptors. *Genesis* (2009)

Guetg N, Seddik R, Vigot R, Turecek R, Gassmann M, Vogt KE, Bräuner-Osborne H, Shigemoto R, Kretz O, Frotscher M, Kulik A and Bettler B. The GABA_{B1a} Isoform Mediates Heterosynaptic Depression at Hippocampal Mossy Fiber Synapses. *Journal of Neuroscience* (2009)

Vigot R, Barbieri S, Bräuner-Osborne H, Turecek R, Shigemoto R, Zhang YP, Luján R, Jacobson LH, Biermann B, Fritschy JM, Vacher CM, Müller M, Sansig G, **Guetg N**, Cryan JF, Kaupmann K, Gassmann M, Oertner TG and Bettler B. Differential compartmentalization and distinct functions of GABA_B receptor variants. *Neuron* (2006)

Kulik A, Vida I, Fukazawa Y, **Guetg N**, Kasugai Y, Marker CL, Rigato F, Bettler B, Wickman K, Frotscher M, Shigemoto R. Compartment-dependent colocalization of Kir3.2-containing K⁺ channels and GABA_B receptors in hippocampal pyramidal cells. *Journal of Neuroscience* (2006)

Hemphill A, Vonlaufen N, Naguleswaran A, Keller N, Riesen M, **Guetg N**, Srinivasan S, Alaeddine F. Tissue culture and explant approaches to studying and visualizing *Neospora caninum* and its interactions with the host cell. *Microscopy and Microanalysis* (2004)

Vonlaufen N, **Guetg N**, Naguleswaran A, Muller N, Bjorkman C, Schares G, von Blumroeder D, Ellis J, Hemphill A. In vitro induction of *Neospora caninum* bradyzoites in vero cells reveals differential antigen expression, localization, and host-cell recognition of tachyzoites and bradyzoites. *Infection and Immunity* (2004)

Conference abstracts (poster presentations)

Guetg N, Vigot R, Gassmann M, Shigemoto S, Frotscher M, Kulik A, Bettler B. Differential compartmentalization of GABA_B receptor subtypes at mossy-fiber CA3 pyramidal neuron synapse. *Society for Neuroscience (SfN) Annual Meeting, San Diego (USA) 2007*

Guetg N, Vigot R, Gassmann M, Shigemoto S, Frotscher M, Bettler B, Kulik À. Pre- and postsynaptic localization of GABA_{B1a} and GABA_{B1b} subunit isoforms in the CA3 area of the hippocampus. *5th Forum of European Neuroscience, Vienna (Austria) 2006*

Guetg N, Vigot R, Gassmann M, Shigemoto S, Frotscher M, Bettler B, Kulik À. Pre- and postsynaptic segregation of two isoforms, GABA_{B1a} and GABA_{B1b}, of the metabotropic GABA_B receptor in the hippocampus. *Anatomische Gesellschaft – 101st annual meeting, Freiburg i. B. (Germany) 2006*

Guetg N, Vigot R, Gassmann M, Shigemoto S, Frotscher M, Bettler B, Kulik À. Pre- and postsynaptic localization of GABA_{B1a} and GABA_{B1b} subunit isoforms in the CA3 area of the hippocampus. *Swiss Society of Neuroscience Meeting, Basel (Switzerland) 2006*

Guetg N, Vigot R, Gassmann M, Shigemoto S, Frotscher M, Bettler B, Kulik À. Pre- and postsynaptic localization of GABA_{B1a} and GABA_{B1b} subunit isoforms in the CA3 area of the hippocampus. *Neurex Annual Meeting, Basel (Switzerland) 2006*